Molecular and spatial characterisation of *Arabidopsis* EDS1 defence regulatory complexes

Inaugural-Dissertation
zur
Erlangung des Doktorgrades
der Mathematisch-Naturwissenschaftlichen Fakultät
der Universität zu Köln

vorgelegt von

Marcel Wiermer

aus Greven

Köln, Mai 2005

Die vorliegende Arbeit wurde am Max-Planck-Institut für Züchtungsforschung in Köln in der Abteilung für Molekulare Phytopathologie (Direktor: Prof. Dr. P. Schulze-Lefert) angefertigt.

MAX-PLANCK-GESELLSCHAFT

Max-Planck-Institut
für Züchtungsforschung

Berichterstatter:	Prof. Dr. Paul Schulze-Lefert
	Prof. Dr. Martin Hülskamp
Prüfungsvorsitzender:	Prof. Dr. Ulf-Ingo Flügge
Tag der Disputation:	04. Juli 2005

Publications

Feys, B.J.*, Wiermer, M.*, Bhat, R.A., Moisan, L.J., Medina-Escobar, N., Neu, C., Cabral, A. and Parker, J.E. (2005). *Arabidopsis* SENESCENCE-ASSOCIATED GENE101 Stabilizes and Signals within an ENHANCED DISEASE SUSCEPTIBILITY1 Complex in Plant Innate Immunity. (submitted) *co-first authors

Wiermer, M., Feys, B.J. and Parker, J.E. (2005). Plant immunity: the EDS1 regulatory node. Curr Opin Plant Biol **8,** (in press).

Abstract

In plants, cellular innate immune responses are indispensable for defence against pathogens. *Arabidopsis* EDS1 (Enhanced Disease Susceptibility 1) and PAD4 (Phytoalexin Deficient 4) are essential regulators of basal resistance to virulent pathogens, controlling defence amplification and accumulation of the signalling molecule salicylic acid (SA). Also, EDS1 is necessary for Resistance (R) protein-triggered programmed cell death to avirulent pathogen isolates conditioned by the TIR (Toll-Interleukin-1 Receptor) class of nucleotide-binding/leucine-rich-repeat (NB-LRR) immune receptor. Complete loss of TIR-NB-LRR mediated resistance and its associated cell death programme in *Arabidopsis eds1* mutants and partial disabling of the same resistances in *pad4* suggested a mechanism in which TIR-type NB-LRR proteins engage EDS1 early in the defence cascade that connects the recognition process to basal defences, requiring both EDS1 and PAD4. Consistent with such a cooperative role, EDS1 and PAD4 interact in *Arabidopsis* soluble leaf extracts. EDS1 and PAD4 have homology to eukaryotic lipases in their N-terminal halves and share a domain of high sequence homology (the EP domain) in their C-termini with one other plant lipase-like protein, SAG101 (Senescence Associated Gene 101) that was recently identified as part of an EDS1 complex in leaf soluble extracts. However, the nature of this association and whether SAG101 signals in plant innate immunity was not known.

The work presented here shows that SAG101 interacts directly with EDS1 inside the nucleus of *Arabidopsis* cells and, together with PAD4, contributes intrinsic and indispensable signalling activity to the EDS1 defence pathway in resistance and programmed cell death triggered by TIR-type R proteins and in expression of basal defences. The EDS1-SAG101 complex is molecularly and spatially distinct from EDS1-EDS1 homomeric interactions that occur in the cytosol but not in the nucleus. *SAG101* possesses a defence regulatory function that is partially redundant with *PAD4*. Loss of *SAG101* can be compensated for by the presence of *PAD4*. Single null *sag101* mutant alleles had no effect on plant disease resistance but combining *sag101* with a null *pad4* mutation disabled resistance as fully as *eds1*. Restriction of SAG101 to the nucleus may account for its inability to fully complement loss of PAD4 that co-localises with EDS1 in the cytosol and the nucleus. These new findings demonstrate that all three proteins are important regulators of innate immunity and point to a complex nucleo-cytoplasmic dynamic between EDS1 and its signalling partners that may be important for plant defence signal relay.

Zusammenfassung

Zelluläre Immunantworten sind bei Pflanzen unabdingbar für eine erfolgreiche Pathogenabwehr. EDS1 (Enhanced Disease Susceptibility 1) und PAD4 (Phytoalexin Deficient 4) spielen hierbei eine essentielle Rolle in der basalen Resistenz gegenüber virulenten Pathogenen in *Arabidopsis*, indem sie Verteidigungssignale potenzieren sowie die Akkumulation des Signalmoleküls Salizylsäure fördern. EDS1 ist zudem unerlässlich für die Etablierung des programmierten Zelltods, der nach der Erkennung von avirulenten Pathogenen durch intrazelluläre TIR-NB-LRR (Toll-Interleukin-1 Receptor/ nucleotide-binding / leucine-rich-repeat) Resistenzproteine (R) ausgelöst wird. Der Verlust von TIR-NB-LRR-vermittelter Krankheitsresistenz und des damit assoziierten Zelltod Programms in *eds1*- sowie der partielle Resistenzverlust in *pad4*-Mutanten, lassen auf einen Verteidigungsmechanismus schließen, bei dem EDS1 eine „frühe" Signalfunktion übernimmt und dabei den Erkennungsprozess mit basalen Abwehrmechanismen verknüpft, die ihrerseits sowohl EDS1 als auch PAD4 benötigen. In Übereinstimmung mit einer solch kooperativen Rolle von EDS1 und PAD4 hat sich gezeigt, dass EDS1 und PAD4 in löslichen Proteinextrakten miteinander interagieren. Aminosäuresequenzanalysen haben ferner ergeben, dass sowohl EDS1 als auch PAD4 in ihrer N-terminalen Hälfte Sequenzhomologie zu eukaryotischen Lipasen aufweisen. Zudem besitzen beide Proteine im C-terminalen Bereich eine Domäne hoher Sequenzhomologie, die sie mit SAG101 (Senescence Associated Gene 101), einem weiteren Lipase-ähnlichen Protein, teilen. Letzteres wurde kürzlich als Komponente eines EDS1-Komplexes in löslichen Proteinextrakten identifiziert. Bis zum jetzigen Zeitpunkt war jedoch weder etwas über die molekulare Beschaffenheit dieses Komplexes noch über eine mögliche Rolle von SAG101 in der pflanzlichen Pathogenabwehr bekannt.

Im Rahmen dieser Arbeit konnte mittels *in planta* FRET (Fluorescence Resonance Energy Transfer)-Studien und Immunoblot-Analysen gezeigt werden, dass es sich bei der EDS1-SAG101 Assoziation um eine direkte Interaktion zwischen diesen beiden Proteinen im Zellkern handelt. Zusammen mit PAD4 steuert SAG101 eine Signalfunktion bei, die sowohl für den TIR-NB-LRR Immunrezeptor-vermittelten Zelltod und die daraus resultierende Resistenz gegenüber avirulenten Pathogenen als auch für basale Resistenzmechanismen gegenüber virulenten Pathogenen unentbehrlich ist. Die Funktion von *SAG101* ist partiell redundant zu der von *PAD4*. Der Verlust von *SAG101* führt zu keiner erhöhten

Krankheitsanfälligkeit, *pad4/sag101*-Doppelmutanten sind jedoch genauso anfällig gegenüber virulenten und avirulenten Pathogenen wie *eds1*-Mutanten. Während PAD4 den Verlust von SAG101 kompensieren kann, ist SAG101 umgekehrt dazu nicht in der Lage, was möglicherweise auf die unterschiedliche subzelluläre Lokalisation dieser beiden Proteine zurückzuführen ist. SAG101 ist ausschließlich im Zellkern lokalisiert, hingegen zeigen PAD4 und EDS1 eine Co-Lokalisation sowohl im Zellkern als auch im Cytosol. Im Rahmen dieser Arbeit konnte außerdem gezeigt werden, dass EDS1-Homodimere zwar im Cytosol, im Gegensatz zur EDS1-SAG101 Interaktion jedoch nicht im Zellkern nachweisbar sind. Die dargestellten Ergebnisse zeigen, dass EDS1, PAD4 und SAG101 unerläßliche Komponenten der zellulären Immunantwort bei Pflanzen sind. Die Ergebnisse deuten des weiteren auf eine komplexe nukleo-cytoplasmatische Dynamik zwischen EDS1 und dessen Interaktionspartnern hin, die essentiell für pflanzliche Verteidigungsmachanismen gegenüber Pathogenen sein könnte.

Publications .... **I**

Abstract .... **III**

Zusammenfassung .... **V**

Table of contents .... **VII**

Table of abbreviations .... **XIII**

1 Introduction **1**

1.1 Layers of innate immunity in plants **1**

1.2 The disease resistance signalling proteins EDS1 and PAD4 .... **6**

1.3 SAG101 shows sequence homology to EDS1 and PAD4 .... **12**

1.4 Thesis aims **14**

2 Materials and Methods **15**

2.1 Materials **15**

2.1.1 Plant Materials 15

2.1.1.1 *Arabidopsis thaliana* 15

2.1.1.2 *Nicothiana benthamiana* 16

2.1.2 Pathogens 16

2.1.2.1 *Peronospora parasitica* 17

2.1.2.2 *Pseudomonas syringae* pv. *tomato* (*Pst*) 17

2.1.3 Bacterial strains 18

2.1.3.1 *Escherichia coli* strains 18

2.1.3.2 *Agrobacterium tumefaciens* strains 18

2.1.4 Vectors 19

2.1.5 Oligonucleotides 20

2.1.6 Enzymes 21

2.1.6.1 Restriction endonucleases 21

2.1.6.2 Nucleic acid modifying enzymes 22

2.1.7 Chemicals 22

2.1.8 Antibiotics 22

2.1.9 Media 23

2.1.10 Antibodies 24

2.1.11 Buffers and solutions 25

2.2 Methods 29
2.2.1 Maintenance and cultivation of *Arabidopsis* plant material 29
2.2.2 Generation of *Arabidopsis* F_1 and F_2 progeny 29
2.2.3 *Arabidopsis* seed sterilisation 30
2.2.4 *Agrobacterium*-mediated stable transformation of *Arabidopsis* (floral dip) ... 30
2.2.5 Glufosinate selection of *Arabidopsis* transformants on soil 31
2.2.6 Generation of *Arabidopsis* protoplasts 31
2.2.7 Inoculation and maintenance of *Peronospora parasitica* 32
2.2.8 Quantification of *P. parasitica* sporulation 32
2.2.9 Histochemical analysis of *P. parasitica* development and necrotic plant tissues 33
2.2.10 Maintenance of *P. syringae* pv. *tomato* (*Pst*) cultures 33
2.2.11 *P. syringae* pv. *tomato* (*Pst*) growth assay 33
2.2.12 Biochemical methods 34
2.2.12.1 *Arabidopsis* total protein extraction for immunoblot analysis 34
2.2.12.2 Nuclear fractionation for immunoblot analysis 35
2.2.12.3 Isolation of microsomal membranes 35
2.2.12.4 Co-immunoprecipitation 36
2.2.12.5 Denaturing SDS-polyacrylamide gel electrophoresis (SDS-PAGE) 37
2.2.12.6 Immunoblot analysis 38
2.2.12.7 Histochemical staining for β-glucuronidase (GUS) activity 39
2.2.13 Molecular biological methods 39
2.2.13.1 Isolation of genomic DNA from *Arabidopsis* (Quick prep for PCR) 39
2.2.13.2 Isolation of total RNA from *Arabidopsis* 40
2.2.13.3 Polymerase chain reaction (PCR) 40
2.2.13.4 Site directed mutagenesis 41
2.2.13.5 Reverse transcription-polymerase chain reaction (RT-PCR) 42
2.2.13.6 Plasmid DNA isolation from bacteria 43
2.2.13.7 Restriction endonuclease digestion of DNA 43
2.2.13.8 DNA ligations 43
2.2.13.9 Agarose gel electrophoresis of DNA 43
2.2.13.10 Isolation of DNA fragments from agarose gel 44

2.2.13.11 Generation of Gateway-compatible vectors for protein-localisation and fluorescence resonance energy transfer (FRET) studies 44

2.2.13.12 Site specific recombination of DNA in Gateway-compatible vectors 45

2.2.13.13 DNA sequencing 45

2.2.13.14 DNA sequence analysis 46

2.2.13.15 Preparation of chemically competent *E. coli* cells 46

2.2.13.16 Transformation of chemically competent *E. coli* cells 46

2.2.13.17 Preparation of electro-competent *A. tumefaciens* cells 47

2.2.13.18 Transformation of electro-competent *A. tumefaciens* cells 47

2.2.14 Transient plant transformations 48

2.2.14.1 *Agrobacterium*-mediated transient transformation of *N. benthamiana* leaves 48

2.2.14.2 Single cell transient gene expression in *Arabidopsis* epidermal cells using particle bombardment 49

2.2.14.2.1 Preparation of *Arabidopsis* leaves for transfection 49

2.2.14.2.2 Preparation of microcarriers 49

2.2.14.2.3 Coating of microcarriers with DNA 49

2.2.14.2.4 The particle bombardment 50

2.2.15 Localisation studies using confocal laser scanning microscopy (CLSM) 50

2.2.16 Fluorescence resonance energy transfer-acceptor photobleaching (FRET-APB) 51

3 Results 53

3.1 EDS1, PAD4 and SAG101 expression in different plant tissues 53

3.1.1 Immunoblot analysis of EDS1, PAD4 and SAG101 protein abundance 54

3.1.2 Gene expression analysis of *EDS1*, *PAD4* and *SAG101* 55

3.1.3 Transcriptional activity of the EDS1 promoter in different plant tissues using P_{EDS1}::*GUS* stable transgenic plants 57

3.1.4 Summary of EDS1, PAD4 and SAG101 expression patterns 59

3.2 Subcellular localisation of EDS1, PAD4 and SAG101 and analysis of their *in vivo* interactions via fluorescence resonance energy transfer (FRET)............. 60
3.2.1 Subcellular localisation of EDS1, PAD4 and SAG101.................................. 63
3.2.2 EDS1 dimerises in the cytosol and interacts with SAG101 inside the nucleus 70
3.2.3 Summary of EDS1, PAD4 and SAG101 localisation and protein-protein interaction studies... 76
3.3 Investigating the role of SAG101 in *Arabidopsis* innate immunity....................... 77
3.3.1 *SAG101* expression is induced upon infection with compatible and incompatible *P. parasitica* isolates... 77
3.3.2 SAG101 signals in plant innate immunity 81
3.3.2.1 Loss of *RPP2* resistance in *pad4-1/sag101* double mutants........... 81
3.3.2.2 Loss of basal resistance in *pad4-1/sag101* double mutants............ 84
3.3.2.3 EDS1 protein is stabilised by its interacting partners PAD4 and SAG101.. 86
3.3.2.4 SAG101 and PAD4 have defence regulatory functions beyond stabilising EDS1 87
3.3.2.5 The combined activities of PAD4 and SAG101 are required for TIR-NB-LRR type *R* gene-mediated and basal resistance against bacterial pathogens 92
3.3.3 Summary of the role of SAG101 in plant innate immunity 96

4 Discussion 99
4.1 *EDS1*, *PAD4* and *SAG101* are expressed in all major plant organs..................... 99
4.2 Subcellular localisation of EDS1, PAD4 and SAG101 and analysis of their *in vivo* interactions via fluorescence resonance energy transfer (FRET)........... 104
4.2.1 EDS1 and PAD4 co-localise in the cytosol and the nucleus whereas SAG101 is exclusively nuclear 105
4.2.2 EDS1 forms molecularly and spatially distinct associations 110
4.3 Investigating the role of SAG101 in *Arabidopsis* innate immunity..................... 114
4.3.1 EDS1, PAD4 and SAG101 accumulate upon pathogen infection 114
4.3.2 SAG101 contributes to the EDS1 defence signalling pathway..................... 115
4.4 Perspectives... 120

5 Literature 121

Danksagung 129

Erklärung 131

Lebenslauf 133

Table of abbreviations

::	fused to (in the context of gene fusion constructs)
° C	degree Celsius
APB	acceptor photobleaching
avr	avirulence
bp	base pair(s)
C	carboxy-terminal
Cala2	*Peronospora parasitica* isolate Cala2
CaMV	cauliflower mosaic virus
CC	coiled-coil
cDNA	complementary DNA
CFP	cyan fluorescent protein
cfu	colony forming unit
CLSM	confocal laser scanning microscopy
d	day(s)
dATP	deoxyadenosinetriphosphate
dCTP	deoxycytidinetriphosphate
DEPC	diethylpyrocarbonate
dGTP	deoxyguanosinetriphosphate
dH_2O	deionised water
DMF	dimethylformamide
DMSO	dimethylsulfoxide
DNA	deoxyribonucleic acid
DNase	deoxyribonuclease
dNTP	deoxynucleosidetriphosphate
dsRNAi	double-stranded RNA interference
DTT	dithiothreitol
dTTP	deoxythymidinetriphosphate
EDS1	Enhanced Disease Susceptibility 1
EDTA	ethylenediaminetetraacetic acid
Emwa1	*Peronospora parasitica* isolate Emwa1
ET	ethylene

EtOH	ethanol
Fig.	Figure
fp	fluorescent protein
FRET	Fluorescence Resonance Energy Transfer
f. sp.	forma specialis
g	gram
g	gravity constant (9.81 ms^{-1})
GFP	green fluorescent protein
GUS	β-glucuronidase
h	hour(s)
HR	hypersensitive response
HRP	horseradish peroxidase
kb	kilobase(s)
kDa	kiloDalton(s)
l	litre
LRR	leucine-rich repeats
m	milli
M	molar (mol/l)
µ	micro
min	minute(s)
mM	millimolar
mRNA	messenger ribonucleic acid
N	amino-terminal
NB	nucleotide binding site
ng	nanogram
nm	nanometer
Noco2	*Peronospora parasitica* isolate Noco2
OD	optical density
ORF	open reading frame
P_{35SS}	double 35S promoter of CaMV
PAA	polyacrylamide
PAD4	Phytoalexin Deficient 4
PAMP	pathogen-associated molecular pattern
PCR	polymerase chain reaction

PAGE	polyacrylamide gel-electrophoresis
pH	negative decimal logarithm of the H^+ concentration
PR	pathogenesis related
Pst	*Pseudomonas syringae* pv. *tomato*
pv.	pathovar
R	resistance
RNA	ribonucleic acid
ROI	reactive oxygen intermediates
rpm	rounds per minute
RPM	resistance to *Pseudomonas syringae* pv. *maculicola*
RPP	resistance to *Peronospora parasitica*
RPS	resistance to *Pseudomonas syringae*
RT	room temperature
RT-PCR	reverse transcription-polymerase chain reaction
SA	salicylic acid
SAG101	Senescence Associated Gene 101
SAR	systemic acquired resistance
SDS	sodium dodecyl sulphate
sec	second(s)
TBS	Tris buffered saline
T-DNA	transfer DNA
TIR	*Drosophila* Toll and mammalian interleukin-1 receptor
TLR	Toll-like receptor
Tris	Tris-(hydroxymethyl)-aminomethane
U	unit
UV	ultraviolet
V	Volt
VIGS	virus induced gene silencing
vir	virulence
v/v	volume per volume
WT	wild-type
w/v	weight per volume
X-Gluc	5-bromo-4-chloro-3-indolyl-β-D-glucuronic acid
YFP	yellow fluorescent protein

1 Introduction

Plants represent a valuable nutrient resource for a multitude of potential pathogens and rarely grow without attempted pathogen colonisation. Fungi, oomycetes, bacteria, as well as nematodes and insects utilise the photosynthate produced by plants and viruses exploit replication machinery (Dangl and Jones, 2001). Individual plant cells perceive an enormous range of external cues and have to integrate this information into the appropriate defence responses to ensure survival of the plant. Despite the large number of genetically diverse pathogens, disease is the exceptional case as plants routinely combat pathogenic microbes and survive (Hammond-Kosack and Parker, 2003). Plants have evolved an elaborate, multi-layered system of innate immunity that is able to perceive non-self and is indispensable for defence mechanisms against attempted pathogen attack. Unravelling these layers and comprehending how pathogen recognition is transduced to downstream signalling components and converted into adequate resistance responses is of major current interest.

1.1 Layers of innate immunity in plants

Immunity of an entire plant species towards most phytopathogenic microbes is the predominant form of disease resistance and termed “non-host” or “species level resistance” (Heath, 2000). A pathogen that cannot cause disease on a non-host plant is referred to as non-host pathogen. The underlying mechanisms of non-host resistance are poorly understood. Emerging evidence suggests that non-host resistance is the composite of multiple overlapping mechanisms that include both constitutive barriers such as wax layers, toxic secondary metabolites and antimicrobial peptides as well as inducible reactions (Heath, 2000; Kamoun, 2001; Hammond-Kosack and Parker, 2003; Thordal-Christensen, 2003). The importance of the plant cell wall for non-host resistance as a preformed barrier against pathogen penetration is reinforced by recent findings that demonstrate a complex process of pathogen-triggered cell polarisation and cell wall remodelling. These findings further suggest involvement of a surveillance system for cell wall integrity that apparently has the capability to sense perturbation of the cell wall structure (Kobayashi *et al.*, 1997; McLusky *et al.*, 1999; Schmelzer, 2002; Collins *et al.*, 2003; Schulze-Lefert, 2004). This surveillance system is likely to be interconnected with known plant defence signalling pathways (Peart *et al.*, 2002b; Mysore and Ryu, 2004; Schulze-Lefert, 2004).

Pathogens, able to overcome constitutive barriers are subject to a layer of plant innate immunity that presumably also contributes to the rejection of non-host pathogens and displays some striking similarities to induction of innate immune response of animals (Felix *et al.*, 1999; Holt *et al.*, 2003; Nürnberger *et al.*, 2004). In animals, the first line of rapid defence upon microbial infection is mediated via activation of innate immune responses with a capacity to respond to a broad range of pathogens by utilising a family of host pattern recognition receptors (PRR) that respond to the presence of invariant, pathogen-derived molecules. Such "pathogen-associated molecular patterns" (PAMPs) or "general elicitors" are absent in the host and usually indispensable for microbial lifestyle (Nürnberger *et al.*, 2004). Lipopolysaccharides of Gram-negative bacteria, peptidoglycans of Gram-positive bacteria and the bacterial flagellin are some examples of PAMPs that cause innate immune responses in animals (Underhill and Ozinsky, 2002; Chamaillard *et al.*, 2003b). PRRs that recognise PAMPs include transmembrane Toll-like receptors (TLRs) and cytoplasmic nucleotide-binding oligomerisation domain (NOD) proteins (Girardin *et al.*, 2002). Toll-like receptors reside within the plasma membrane and mediate PAMP recognition via extracellular leucine-rich repeats (LRRs) and transduce signals into intracellular resistance responses through their intra-cytoplasmic domain (- homologous to the mammalian interleukin-1 (IL-1) receptor, referred to as Toll/IL-1 receptor- or TIR-domain) (Akira and Takeda, 2004).

An excellent example of an *Arabidopsis* transmembrane receptor that shows structural similarities to TLRs and is essential for perception of bacterial flagellin is encoded by the receptor-like kinase *FLS2* (*Flagellin Sensing 2*) that also possesses extracellular LRRs (Gómez-Gómez and Boller, 2002; Zipfel *et al.*, 2004). This example shows that plants, like animals, possess broad perception systems for "general elicitors" characteristic for entire classes of microbes.

NOD proteins, that in contrast to TLRs are cytoplasmic, also contribute to innate immune responses as some of the members were shown to have the capability to sense PAMPs (Chamaillard *et al.*, 2003a; Chamaillard *et al.*, 2003b; Viala *et al.*, 2004). NOD proteins are characterised by a central nucleotide binding site (NB) and carboxy-terminal LRRs (Athman and Philpott, 2004) and thus are structurally related to plant Resistance (R) proteins, referred to later.

Despite the similarities between the innate immune systems of animals and plants, the latter lack the adaptive (acquired) arm of the immune system found in animals that acts in concert with innate immunity and depends on somatic gene rearrangements for generation of antigen-specific receptors expressed on B and T lymphocytes (Girardin *et al.*, 2002; Nürnberger *et al.*, 2004). Moreover, plants lack specialised cell types such as macrophages as part of the circulatory blood system. In consequence, every plant cell autonomously has the capability to perceive biotic stresses and to transduce this perception into resistance responses.

Although non-host resistance in plants generally exerts a robust and durable barrier to a broad range of pathogens, individual pathogen races have evolved mechanisms to evade surface detection or disrupt/suppress internal host defences by acquisition of "pathogenicity factors" (also called "virulence factors" or "effectors") (Abramovitch and Martin, 2004). In this case the plant becomes host to the respective pathogen and disease occurs. Interaction between such a susceptible host cultivar and a virulent pathogen isolate is called a "compatible interaction". According to their lifestyles plant pathogens can be subdivided into biotrophs that derive nutrients from living host tissues and require a living host to complete their life cycle and necrotrophs that feed from dead or dying cells. Necrotrophy is often accompanied by production of toxins. While some pathogens can be clearly assigned as biotrophs or necrotrophs, others behave as both, depending on the stages of their life cycles or environmental influences. Such pathogens are called hemi-biotrophs.

While pathogen effectors permit a certain degree of host tissue colonisation, plants exert additional layers of so-called "basal resistance" or "basal defences" that impede pathogen growth. Mutations in basal defence components characteristically cause hypersusceptibility to virulent pathogen strains (Glazebrook *et al.*, 1996; Parker *et al.*, 1996; Reuber *et al.*, 1998). Expression of basal resistance to invasive pathogens is a crucial protective layer. Without it plants become hyper-susceptible to even mild infections and are less likely to survive in a competitive environment. A large catalogue of *Arabidopsis* mutants compromised in basal defences to virulent pathogen strains points to involvement of many genes in maintenance of this resistance layer and numerous potential targets for the pathogen to disable in promoting disease (Cao *et al.*, 1994; Glazebrook *et al.*, 1996; Parker *et al.*, 1996; Menke *et al.*, 2004; Zhang and Li, 2005).

What further emerges from genetic analysis is a complex circuitry, balancing the activation of basal defences involving the hormones jasmonic acid (JA) and related oxygenated lipids and ethylene (ET) principally against necrotrophic pathogens or feeding insects, and salicylic acid (SA) against biotrophs (Kunkel and Brooks, 2002; Glazebrook, 2004). For example the *Arabidopsis* mutant, *npr1* (*non-expresser of PR genes 1*), which blocks SA signalling shows enhanced susceptibility to the biotrophic oomycete *P. parasitica* but is unaffected in resistance to the necrotrophic pathogen *Alternaria brassicicola*. The converse phenotype is observed in *coi1* (*coronatine insensitive 1*) mutants that are affected in the JA-response pathway (Thomma *et al.*, 1998). Mutual antagonism between the SA and JA signalling pathways might allow plants to fine tune their defence responses and ensure that inappropriate defences are not activated in response to certain pathogens (Feys and Parker, 2000; Kunkel and Brooks, 2002; Glazebrook, 2004). The JA/ET pathway may thereby be part of a basal defence layer that biotrophic host pathogens either fail to elicit or actively suppress (Zimmerli *et al.*, 2004). Activation of the JA/ET pathway in response to non-host pathogens has also been described recently (Huitema *et al.*, 2003; Zimmerli *et al.*, 2004).

Superimposed on basal defences is a further layer of plant resistance, executed by Resistance (*R*) genes that have co-evolved in individual cultivars of otherwise susceptible host plants to recognise the presence of specific pathogen virulence factors, resulting in defence of the pathogen. Hence, recognition of the pathogen virulence (*Vir*) gene product by the host plant´s R protein alters a *Vir* into an Avirulence (*Avr*) determinant. This "race-specific", "cultivar-specific" or "*R* gene-mediated" resistance is described in the "gene-for-gene hypothesis" (Flor, 1971) and is genetically determined by complementary pairs of pathogen-encoded avirulence *Avr* genes and plant *R* genes. The lack of either determinant leads to breakdown of resistance (Flor, 1971; Dangl and Jones, 2001). Most Avr proteins are considered to be effectors that are required for colonisation of the host and provide a selective advantage to pathogens in the absence of specific host recognition by a corresponding R protein (Kearney and Staskawicz, 1990; Ritter and Dangl, 1995; Chen *et al.*, 2000; Chen *et al.*, 2004).

One possible interpretation of the gene-for-gene hypothesis is a receptor-ligand model in which R and Avr proteins physically interact and trigger downstream signalling to restrict pathogen growth. However, studies carried out for many R-Avr pairs so far revealed only two examples demonstrating such direct interaction (Jia *et al.*, 2000; Deslandes *et al.*, 2003). Thus it is conceivable that at least some R proteins mediate indirect pathogen recognition involving further host proteins. This, together with the fact that *R* genes, despite the wide range of pathogen taxa and their presumed effector molecules, only encode five different classes of proteins (Dangl and Jones, 2001) and that the annotation of the complete *Arabidopsis* genome revealed only about 150 potential *R* genes with homology to the largest class of R proteins (see below) (Meyers *et al.*, 2003), led to the postulation of the "guard-hypothesis". The guard-hypothesis proposes that R proteins function in the surveillance of a host factor (the "guardee") that is targeted by an Avr protein for modifications, favouring pathogen growth if the R protein is absent (Van der Biezen and Jones, 1998; Dangl and Jones, 2001). Detection of this modification by the R protein activates plant defences.

Recent studies on RIN4 (RPM1-interacting protein), which is a target by the three unrelated Avr proteins AvrRpm1, AvrB and AvrRpt2 and guarded by the R proteins RPM1 and RPS2 (Mackey *et al.*, 2002; Axtell and Staskawicz, 2003; Mackey *et al.*, 2003) as well as on PBS1, a protein kinase, which is a target of AvrPphB and guarded by RPS5 (Shao *et al.*, 2003) strongly support this hypothesis.

R protein triggered resistance often involves a localised burst of reactive oxygen intermediates (ROI) such as superoxide (O_2^-) and hydrogen peroxide (H_2O_2) and is usually associated with strictly delimited programmed plant cell death, known as the hypersensitive response (HR) at the site of attempted invasion to restrict pathogen growth. The HR is thought to act against biotrophic pathogens and activates SA-dependent signalling. ROI may thereby have a direct antimicrobial effect and contribute to structural reinforcement of the plant cell wall, as well as serving as a signal for the activation of other defence responses (Rustérucci *et al.*, 2001; Nimchuk *et al.*, 2003). A positive feedback loop involving production of ROI, NO (nitric oxide) and SA appears to be central for the activation of defence responses including triggering of the HR (Nimchuk *et al.*, 2003).

Triggering of local resistance responses serves also to prime uninfected tissues against subsequent attack in a process called systemic acquired resistance (SAR) that is effective to a broad spectrum of pathogens (Durrant and Dong, 2004). The establishment of SAR is associated with elevated levels of SA both at the site of infection and in systemic tissues. SA is a necessary and sufficient signal molecule for SAR induction. A recent study demonstrated that SA mediated changes in the cellular redox state reduces a key regulator of SAR, the ankyrin-repeat protein NPR1. In the absence of SA, NPR1 accumulates in an oligomeric complex in the cytosol through intermolecular disulfide bridges. Redox changes cause NPR1 to form monomers that can translocate to the nucleus and thus activate defence gene expression (Mou *et al.*, 2003).

The most prevalent class of functionally defined *R* genes within the 5 different classes encodes putative cytosolic proteins containing a central NB and carboxyterminal LRRs (Dangl and Jones, 2001; Meyers *et al.*, 2003; Belkhadir *et al.*, 2004) and thus resembles structurally mammalian NOD immune receptors. The NB-LRR class of R proteins can be further subdivided into members that possess an amino-terminal coiled-coil (CC) domain (CC-NB-LRR) and those that have amino-terminal homology to the intracellular signalling domains of the *Drosophila* Toll and mammalian interleukin-1 receptors (TIR-NB-LRR).

The limited number of common structural motifs in the R proteins identified so far, together with the fact that pathogens, as diverse as they are, trigger remarkably similar R protein-mediated defence responses, suggests that plant resistance to a wide range of pathogens may operate by similar mechanisms and that additional conserved host components participate within these signalling pathways (Aarts *et al.*, 1998; Xiao *et al.*, 2005).

1.2 The disease resistance signalling proteins EDS1 and PAD4

Arabidopsis EDS1 and PAD4 constitute a central regulatory node in innate immunity. The *eds1* (*enhanced disease susceptibility 1*) mutation was originally identified in a mutational screen for defects in *RPP1*- and *RPP5*-specified resistance to isolates of the obligate biotrophic oomycete pathogen *Peronospora parasitica* (Parker *et al.*, 1996), whereas *pad4* (*phytoalexin deficient 4*) was first discovered among several mutants in a screen for enhanced disease susceptibility to virulent *Pseudomonas syringae* pv. *maculicola* (*Psm*) ES4326 (Glazebrook *et al.*, 1996). *EDS1* and *PAD4* were cloned in 1999 (Falk *et al.*, 1999; Jirage *et al.*, 1999) and pathology assays of *eds1* and *pad4* null mutants showed that both *EDS1* and *PAD4* are required genetically by the same spectrum of *Arabidopsis R* genes belonging to the intracellular TIR-NB-LRR class (Parker *et al.*, 1996; Aarts *et al.*, 1998; Feys *et al.*, 2001). NB-LRR genes possessing, instead, an amino-terminal CC domain triggered resistance independently of *EDS1* and *PAD4*, suggesting that these defence regulators may constitute a point of signal discrimination between the two classes of intracellular immune receptors (Aarts *et al.*, 1998; Feys *et al.*, 2001). As discussed below, such absolute discrimination is an over simplification, although recruitment of EDS1 in TIR-NB-LRR-conditioned resistance is conserved in other plant species tested so far such as tobacco and tomato (Liu *et al.*, 2002; Peart *et al.*, 2002a; Hu *et al.*, 2005).

Close inspection of *eds1* and *pad4* null mutant phenotypes in *Arabidopsis* has shown that EDS1 exerts an early activity in TIR-NB-LRR type *R* gene-mediated resistance that is necessary for the oxidative burst and expression of the HR whereas EDS1 and PAD4, together, are required for defence potentiation around infection sites through the accumulation of SA (Feys *et al.*, 2001; Rustérucci *et al.*, 2001). Phenotypically *eds1* mutant plants show a complete loss of TIR-NB-LRR gene-mediated resistance after infection with certain incompatible *P. parasitica* isolates and support unimpeded hyphal growth, whereas *pad4* plants still retain a delayed HR but fail to fully restrict pathogen growth, resulting in a trail of dead plant cells concomitant with pathogen growth, described as a trailing necrosis phenotype (Feys *et al.*, 2001). This demonstrates that EDS1 has a wider function as PAD4 in TIR-NB-LRR resistance.

Evidence for cooperative activities of EDS1 and PAD4 in defence signalling was strengthened by the finding that EDS1 and PAD4 interacted in a yeast two-hybrid assay and co-immunoprecipitated in soluble plant extracts, both in unchallenged and pathogen-infected leaf tissues (Feys *et al.*, 2001), suggesting that direct interaction might be important for defence signal relay. Moreover, EDS1 was able to form dimers in a yeast two hybrid assay (Feys *et al.*, 2001) although EDS1 homodimerisation has not been demonstrated *in planta* so far.

The defence-related *PR-1* gene expression phenotypes of *eds1* and *pad4* mutant plants position EDS1 and PAD4 upstream of SA accumulation. Pathogen induced *PR-1* expression is abolished in *eds1* and strongly suppressed in *pad4* but is fully rescued after treatment of both mutants with SA or its active analog benzo-1,2,3-thiadiazole-7-carbothioic acid S-methyl ester (BTH) (Parker *et al.*, 1996; Zhou *et al.*, 1998; Falk *et al.*, 1999; Jirage *et al.*, 1999; Feys *et al.*, 2001). Moreover, treatment of *eds1* and *pad4* plants with SA also restores resistance to *P. parasitica* (Parker *et al.*, 1996; Feys *et al.*, 2001). Pathogen induction of *PAD4* expression depends on EDS1 function, whereas mutations in *PAD4* have a negligible effect on *EDS1* expression (Feys *et al.*, 2001). Additionally, SA contributes to the expression of both genes as part of a positive feedback loop that appears to be important for defence signal amplification (Falk *et al.*, 1999; Jirage *et al.*, 1999; Feys *et al.*, 2001).

Consistent with the combined role of EDS1 and PAD4 in defence signal amplification it was found that both proteins are indispensable components of basal resistance in restricting growth of virulent pathogens (Aarts *et al.*, 1998; Reuber *et al.*, 1998; Feys *et al.*, 2001; Xiao *et al.*, 2005). Both, *eds1* and *pad4* were shown to equally promote growth of virulent *P. parasitica* and *Pst* DC3000 above levels seen on corresponding susceptible wild-type plants (Feys *et al.*, 2001). Accordingly, both *EDS1* and *PAD4* expression is upregulated upon challenge with virulent *Pst* (Feys *et al.*, 2001).

From an evolutionary perspective, involvement of EDS1 and PAD4 in basal resistance is likely to represent their ancestral functions, since rice and other monocotyledonous species so far tested appear to lack TIR-NB-LRR type *R* genes (Meyers *et al.*, 2003) but contain orthologs of *EDS1* and *PAD4* (http://www.tigr.org/tdb/e2k1/osa1/). Functional engagement of EDS1 and PAD4 signalling properties by TIR-NB-LRR type R proteins in dicotyledonous plants is therefore likely to have occurred after the two plant lineages diverged 150 million years ago.

A simplified model for the roles of EDS1 and PAD4 in R protein-mediated and basal plant disease resistance is shown in Figure 1.1.

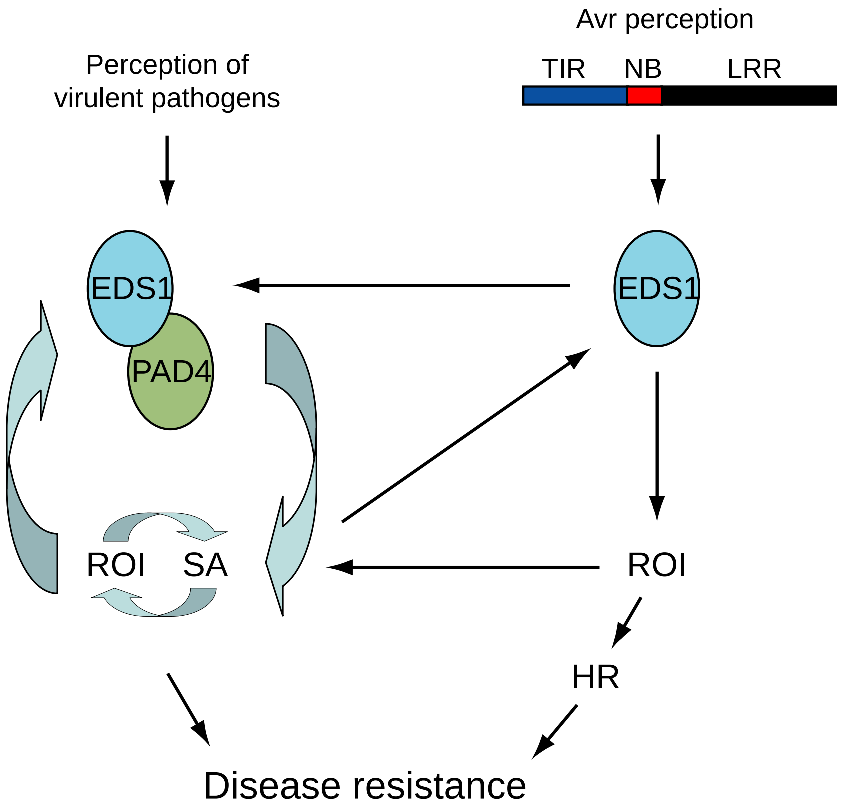

Fig. 1.1. Simplified model for the roles of EDS1 and PAD4 in R protein-mediated and basal plant disease resistance. Two functions are proposed for EDS1. One is an early activity in TIR-NB-LRR type R protein-mediated resistance that is necessary for the oxidative burst upstream of the local HR. The second function recruits PAD4, possibly through direct EDS1-PAD4 interaction, and drives amplification of R protein-mediated and basal defences in a positive feedback loop involving SA and ROI. Negative regulatory elements of the feedback loop are not displayed in the model. Curved arrows typify positive feedback. For further details see text.

A broader relevance of EDS1 and PAD4, apart from their known functions as positive regulators in TIR-NB-LRR type *R* gene-mediated and basal defences, was accentuated by a number of recent genetic epistasis analyses that point to fundamental activities of EDS1 and PAD4 in controlling redox-related processes. These studies further suggest a placement of EDS1 and PAD4 as important activators of SA signalling and mediators of antagonism towards the JA/ET defence pathway. Moreover these experiments revealed that EDS1 and

PAD4 are involved in the interplay between biotic and abiotic stress signalling pathways, are recruited for defence signalling by certain CC-immune receptors as well as being important signalling components of SAR and resistance against certain non-host pathogens. For example, Rustérucci *et al.* (2001) demonstrated the existence of an ROI- and SA-stimulated propagative loop requiring EDS1 and PAD4 in *lsd1* (*lesion simulating disease 1*)-conditioned runaway cell death (rcd) that is separable from processes associated with the localised *R* gene-mediated HR and disease resistance. Neither EDS1 nor PAD4 is required for an oxidative burst and HR conditioned by the CC-NB-LRR type R protein RPM1 yet both are required for rcd in *lsd1* after triggering the RPM1 pathway. *LSD1*, encoding a zinc finger protein, negatively regulates this cell death pathway (Dietrich *et al.*, 1997). Further work by Karpinski and colleagues established that *lsd1* mutants fail to acclimate to excess excitation energy generated by photosynthesis in high light, causing ROI overload and ultimately cell death due to photooxidative stress (Mateo *et al.*, 2004). Coupled with this, *lsd1* mutant plants show a reduced stomatal conductance which results in a rapid fall in internal CO_2 concentrations and impaires the consumption of electrons by CO_2 fixation. This is accompanied by a lower catalase activity in *lsd1*. Importantly, all of the described traits depend on *EDS1* and *PAD4*, as stomatal conductance, catalase activity and ROI accumulation are restored to wild-type levels in *pad4-5/lsd1* and *eds1-1/lsd1*. Interestingly, rapid closure of stomata and an increase in foliar H_2O_2 occurs upon SA treatment (Mateo *et al.*, 2004). These results, taken together with those of Rustérucci *et al.* (2001), who propose a negative regulatory function of LSD1 on the SA-dependent feedback loop controlled by EDS1 and PAD4, make it conceivable that ROI, SA, EDS1 and PAD4 all operate within the same feedback loop to mediate defence responses including the HR. This loop might be negatively regulated by LSD1 through diminishing the cellular content of ROS in controlling EDS1- and PAD4-dependent stomatal closure.

Related to the results of Mateo *et al.* (2004) are findings from Shirano *et al.* (2002) and Zhou *et al.* (2004). The phenotype of *ssi4*, a gain-of-function mutation in a TIR-NB-LRR *R* gene, that develops spontaneous lesions, exhibits a stunted morphology, induces SA and H_2O_2 accumulation and shows enhanced resistance to virulent bacterial and oomycete pathogens, is suppressed by *eds1*. Intriguingly, all of the *ssi4*-induced responses are also suppressed when plants are grown at high humidity suggesting that high humidity suppresses the *ssi4*-induced phenotypes by blocking *EDS1*-dependent SA accumulation and prompted Zhou and colleagues to postulate the presence of a “humidity sensing factor” (Zhou *et al.*, 2004). These results correlate with a role of stomatal gas exchange in promoting photorespiration as suggested by Mateo *et al.* (2004). Failure to close stomata due to high humidity would slow down ROS accumulation. Mateo *et al.* (2004) propose that a humidity sensitive factor is a manifestation of EDS1-dependent stomatal guard cell function.

A further example for the interplay between defence and abiotic responses is given by the growth regulator *BON1* (=*CPN1*). *BON1* shows homology to the copine gene family which are thought to encode Ca^{2+}-dependent phospholipid-binding proteins and was found to be a negative regulator of the TIR-NB-LRR type *R* gene, *SNC1* (Hua *et al.*, 2001; Yang and Hua, 2004). Loss of *BON1* function in *bon1-1* results in constitutive defence activation and, consequently, reduced cell growth that is dependent on the presence of *SNC1*. *SNC1* is under positive feedback regulation of expression involving *EDS1*, *PAD4* and SA. Mutations in EDS1 and PAD4 as well as depletion of SA by the *sid2-1* mutation suppress the growth defects and the enhanced disease resistance phenotype of *bon1-1*. In addition, the feedback amplification of *SNC1* is subject to temperature control as indicated by the fact that at heigh temperature (28° C) the growth defects of *bon1-1*, normally seen at 22° C, are not observed. Consistent with this conditionality all components of the feedback loop, including *EDS1*, *PAD4*, *SNC1* and SA, are strongly reduced at higher temperature in *bon1-1*. Notably, Jambunathan *et al.* (2001) demonstrated that the lesion-mimic and stunted phenotype, as well as increased resistance to virulent *P. syringae* and *P. parasitica* isolates of a *bon1* mutant allele *cpn1-1* (=*bon1-4*) is also suppressed when plants are grown under high humidity conditions, providing a possible link back to the effect of closed stomata in promoting photorespiration and consequently ROS accumulation, as suggested by Mateo *et al.* (2004). Constitutive disease resistance conferred by a deregulated variant of *SNC1* itself is also dependent on *EDS1* and *PAD4* (Li *et al.*, 2001; Zhang *et al.*, 2003). A single point mutation between the NB and LRR in *snc1* (*suppressor of npr1-1, constitutive 1*) renders the R protein constitutively active and results in a stunted morphology and elevated levels of *PR* gene expression and SA. Suppression of the *snc1* mutant phenotype by *eds1* and *pad4* is consistent with their involvement in TIR-NB-LRR type R protein signalling. However, it is surprising that the *pad4* mutation completely suppresses the *snc1* phenotype since resistance conferred by TIR-NB-LRR class of *R* genes so far tested often is only partially dependent on *PAD4* (Zhang *et al.*, 2003).

The idea, that EDS1 represents a point of signal discrimination in disease resistance between CC- and TIR-NB-LRR type immune receptors is also not absolute, since at least one *Arabidopsis* CC-NB-LRR protein, HRT, that mediates viral resistance, and two small CC-proteins with a predicted transmembrane domain, RPW8.1 and RPW8.2, that confer powdery mildew resistance, are dependent on EDS1 and PAD4, suggesting that defence signal regulation via EDS1 is wider than previously thought (Xiao *et al.*, 2001; Chandra-Shekara *et al.*, 2004). *HRT*, a member of the *RPP8* locus that confers resistance to turnip crinkle virus (TCV) displays particularities in two respects. First, resistance mediated by this CC-NB-LRR type *R* gene is dependent on *EDS1* and *PAD4* but independent of *NDR1* (*nonrace-specific disease resistance 1*) (Chandra-Shekara *et al.*, 2004). Second, *HRT* shows a stronger requirement for *PAD4* than for *EDS1*. Whereas resistance to TCV was restorable in *HRT/eds1-1* plants by exogenous application of SA, SA treatment of *HRT/pad4-1* plants failed to enhance resistance, thus PAD4 is required for SA induced resistance, implicating a function of PAD4 that is separable from that exerted in combination with EDS1. The two *RPW8* genes each mediate broad spectrum resistance to a range of powdery mildew pathogens that is associated with an EDS1-, PAD4- and SA-dependent HR and H_2O_2 accumulation, similar to defence responses triggered by TIR-NB-LRR type *R* genes (Xiao *et al.*, 2001). *RPW8*-mediated broad spectrum resistance engages the same components and mechanisms used by TIR-NB-LRR mediated race-specific resistance (Xiao *et al.*, 2005).

A role for EDS1 in non-host resistance has also been demonstrated. *Eds1* mutant plants displayed loss of non-host resistance towards *Albugo candida* or *P. parasitica* isolate P-005, that naturally infect *Brassica oleracea* (Parker *et al.*, 1996) and supported an increase in penetration success by the barley powdery mildew (Zimmerli *et al.*, 2004). When the *eds1* mutation was further accompanied with pharmacological disruption of the actin cytoskeleton non-host resistance against wheat powdery mildew was abolished (Yun *et al.*, 2003). Together, these data provide evidence that resistance mechanisms against both host-adapted and non-host pathogens may share certain signalling components, as suggested before (Peart *et al.*, 2002b).

EDS1 and PAD4 are also necessary for establishment of SAR. *Eds1* and *pad4* single mutants exhibit a dramatic loss of systemic resistance similar to *dir1* (*defective in induced resistance 1*) plants (L. Jorda and A. Maldonado, unpublished data). DIR1, a putative lipid transfer protein (Maldonado *et al.*, 2002), contributes to transmission of long-distance signals in systemic resistance. This defect, coupled with a failure of *eds1* and *pad4* in both signal emission and distal signal perception (L. Jorda and A. Maldonado, unpublished data), is consistent with the known roles of EDS1 and PAD4 as defence potentiators. It remains to be established whether DIR1 is a systemic component of an EDS1 and PAD4 driven amplification system.

SAR is constitutively activated in *mpk4* (*map kinase 4*) mutant plants that display elevated SA levels and increased resistance to virulent biotrophic pathogens (Petersen *et al.*, 2000). MPK4 functions as a repressor of the SA-defence pathway but stimulates JA and ET signalling in resistance to a necrotrophic pathogen, *Alternaria brassicicola* (P. Brodersen and J. Mundy, personal communication). Both of those functions involve EDS1 and PAD4 and led J. Mundy and colleagues to propose that EDS1 and PAD4 are central to the control of antagonism between SA and JA/ET defence pathways as activators of SA but repressors of JA/ET defences. MPK4 negatively regulates both of these functions such that in *mpk4* mutant plants EDS1 and PAD4 are constitutively activated as SAR inducers in SA amplification and as repressors of JA/ET signalling. The results show that EDS1 and PAD4 are also involved in controlling signal antagonism between SA and JA/ET defences, as was hinted at in earlier studies (Gupta *et al.*, 2000; Clarke *et al.*, 2001).

1.3 SAG101 shows sequence homology to EDS1 and PAD4

EDS1 and PAD4 have homology to eukaryotic class 3 lipases (http://www.sanger.ac.uk/Software/Pfam/). Both proteins possess a central lipase domain and embedded in the conserved domains are three predicted catalytic residues: a serine, an aspartic acid and a histidine that comprise an α/β hydrolase catalytic triad (Falk *et al.*, 1999; Jirage *et al.*, 1999). In most known esterases and lipases the motif GXSXG that contains the active site serine is conserved and was also found in EDS1 and PAD4. Nevertheless, no esterase activities have so far been demonstrated for these proteins, suggesting that EDS1 and PAD4 signalling properties do not depend on enzymatic hydrolysis. This is supported by the finding that stable transgenic *Arabidopsis* lines expressing EDS1 and PAD4 variants with exchanges of the predicted lipase catalytic residues are not compromised in resistance (B. Feys and J. Parker, unpublished data). The apparent dispensability of these catalytic amino acids in EDS1 and PAD4 indicates that they may fulfil a structural rather than enzymatic role as discovered in some other signalling proteins (Llompart *et al.*, 2003; Lu *et al.*, 2004) or that their signalling properties are based on binding a lipid or lipid derived molecule.

EDS1 and PAD4 are soluble proteins of ~72 and ~61 kDa, respectively (Falk *et al.*, 1999; Jirage *et al.*, 1999; Feys *et al.*, 2001). Inspection of the EDS1 amino acid sequence revealed no obvious signal peptide or transmembrane regions suggesting that the protein is cytoplasmic. However, two possible bipartite nuclear localisation signals (NLS) were predicted for EDS1 (Falk *et al.*, 1999). As PAD4 was shown to interact with EDS1 *in vivo*

(Feys *et al.*, 2001), one prediction would be that at least certain pools of these proteins co-localise within the plant cell. Recent size exclusion chromatography studies on healthy (pathogen-unchallenged) leaf material revealed that the entire cellular pool of PAD4 associates with only a small proportion of total EDS1 in a ~200 kDa complex that can be distinguished from the majority of EDS1 present in a ~120 kDa fraction (Feys *et al.*, submitted). This suggests that EDS1 is able to form molecularly distinct complexes *in planta*. One possible complex could contain EDS1 homodimers, as EDS1 was capable to dimerise in a yeast two-hybrid assay (Feys *et al.*, 2001).

EDS1 and PAD4 possess a further domain of high sequence homology apart from the lipase-domain in their carboxy-terminal portions. This so called EP-domain (for EDS1 and PAD4 defined) was found in only one other plant lipase-like sequence, *SAG101*, identified previously as a *S*enescence-*A*ssociated *G*ene in *Arabidopsis* accession Columbia *glabrous1* (Feys *et al.*, 2001; He and Gan, 2002). The domain structures of EDS1, PAD4 and SAG101 are shown in Figure 1.2.

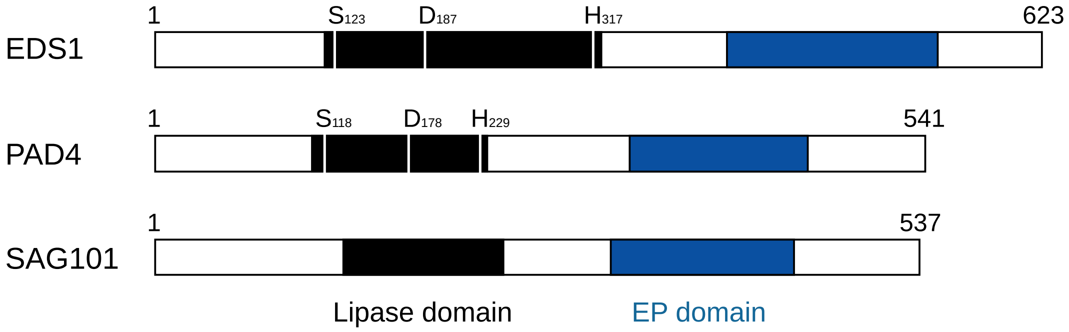

Fig. 1.2. Schematic representation of the domain structure of *Arabidopsis* ecotype L*er* EDS1, PAD4 and SAG101 proteins. The lipase domain (filled black box) and EP (EDS1 and PAD4 defined) domain (filled blue box) are shown. The putative lipase catalytic triade consisting of a Serine (S), an Aspartic acid (D) and a Histidine (H) in EDS1 and PAD4 is indicated with white vertical bars and the corresponding amino acid letters above each diagram. Clear catalytic residues in SAG101 are absent. Numbers indicate amino acid positions within the protein sequence.

Recent analysis carried out by B. Feys using an affinity purification approach with hemagglutinin (HA)-tagged EDS1 combined with MALDI- and Q-TOF mass spectrometry identified SAG101 as part of an EDS1 complex in soluble protein extracts derived from pathogen-unchallenged leaves. Whether EDS1 associates directly or indirectly with SAG101 and in which cellular compartment the association takes place is not known.

SAG101 encodes a protein with apparent acyl hydrolase activity on triolein after expression in *E. coli*, although the predicted SAG101 protein lacks the catalytic triad found in EDS1 and PAD4 (He and Gan, 2002). However, neither the senescence phenotype nor an enzymatic activity of SAG101 using a wide range of putative substrates was reproducible when tested in our laboratory (S. Rietz, B. Feys and J. Parker, unpublished data) and raises questions about the intrinsic functions of SAG101, EDS1 and PAD4.

1.4 Thesis aims

A key objective in plant pathology is to unravel the molecular mechanisms underlying recognition specificity and the associated signal transduction events leading to disease resistance.

Arabidopsis EDS1 and PAD4 have been shown to be central regulators of *R* gene-mediated and basal plant resistance (Falk *et al.*, 1999; Jirage *et al.*, 1999; Feys *et al.*, 2001; Rustérucci *et al.*, 2001). EDS1 and PAD4 interact in soluble plant extracts both in healthy and pathogen challenged leaf tissues (Feys *et al.*, 2001) although only a small portion of the total EDS1 pool is associated with PAD4 (Feys *et al.*, submitted). The capability of EDS1 to form homomeric dimers in a yeast two-hybrid assay (Feys *et al.*, 2001) further suggested that EDS1 may form molecularly distinct complexes *in planta*. This idea was supported by the finding at the start of this study that SAG101 is part of an EDS1 complex in soluble protein extracts of healthy (pathogen-unchallenged) leaf tissues. However, the molecular and spatial character of this association and its biological relevance was not known. In order to unravel the signalling functions of EDS1, SAG101 and PAD4, a key aim of this study was to determine their subcellular localisations and the nature of EDS1 associations within the cell. Another important aspect was to establish whether SAG101 signals in plant innate immunity and whether this function is related to EDS1 and PAD4 signalling. A further aim was to analyse the tissue expression profiles of EDS1, PAD4 and SAG101 which might point to further local and/or systemic signalling properties of these proteins in resistance to pathogens with distinct infection habits.

2 Materials and Methods

The Materials and Methods section is subdivided into two parts. In the first part **(2.1)** Materials used throughout this study, including plant lines, pathogens, bacterial strains, chemicals, enzymes, media, buffers and solutions are listed, Methods applied in this work are described in the second part **(2.2)**.

2.1 Materials

2.1.1 Plant materials

2.1.1.1 *Arabidopsis thaliana*

Arabidopsis wild-type and mutant lines use in this study are listed in Table 2.1 and 2.2, respectively.

Table 2.1. Wild-type *Arabidopsis* accessions used in this study

Accession	**Abbreviation**	**Original source**
Columbia	Col-0	J. Dangl[a]
Landsberg-*erecta*	L*er*	Nottingham *Arabidopsis* Stock Centre[b]
Wassilewskija	Ws-0	K. Feldmann[c]

[a] University of North Carolina, Chapel Hill, NC, USA
[b] Nottingham, UK
[c] University of Arizona, Tucson, AZ, USA

Table 2.2. Mutant *Arabidopsis* lines used in this study

Gene	Accession	Mutagen	Reference/Source
eds1-1	Ws-0	EMS	(Parker *et al.*, 1996)
eds1-2	L*er*	FN	(Falk *et al.*, 1999)
pad4-1	Col-0	EMS	(Glazebrook *et al.*, 1997)
pad4-2	L*er*	FN	(Jirage *et al.*, 1999)
pad4-5	Ws-0	T-DNA	(Feys *et al.*, 2001)
eds1-1/pad4-5	Ws-0	EMS/T-DNA	J. Parker[a], unpublished
sag101-1	Col-0	d*Spm*	(Feys *et al.*, submitted)
sag101-2	Col-0	d*Spm*	(Feys *et al.*, submitted)
pad4-1/sag101-1	Col-0	EMS/d*Spm*	(Feys *et al.*, submitted)
pad4-1/sag101-2	Col-0	EMS/d*Spm*	(Feys *et al.*, submitted)
EDS1 A+B dsRNAi	Col-0	dsRNAi	(Feys *et al.*, submitted)
EDS1A k.o.	Col-0	T-DNA	(Alonso *et al.*, 2003)
EDS1B k.o.	Col-0	T-DNA	(Alonso *et al.*, 2003)
snc1/npr1-1/eds1-2	Col-0/L*er*	EMS/EMS/FN	(Li *et al.*, 2001)

[a] Max-Planck-Institute for Plant Breeding Research, Carl-von-Linné-Weg 10, 50829 Cologne, Germany

EMS: ethylmathane sulfonate; FN: fast neutron; d*Spm*: defectice *Suppressor-mutator*; T-DNA: transfer-DNA; dsRNAi: double-stranded RNA interference

2.1.1.2 *Nicotiana benthamiana*

Nicotiana benthamiana plants were obtained from T. Romeis (MPIZ, Cologne) and used for transient *Agrobacterium*-mediated transformation of leaf tissues.

2.1.2 Pathogens

Different isolates of the oomycete pathogen *Peronospora parasitica*, listed in Table 2.3, and the bacterial pathogen *Pseudomonas syringae* pv. *tomato* strain DC3000 (see 2.1.2.2) were used for infections of *Arabidopsis* plants.

2.1.2.1 *Peronospora parasitica*

Table 2.3. *Peronospora parasitica* isolates used in this study

Isolate	**Original source**	**Reference**
Cala2	Oospore infection of a single seedling	(Holub *et al.*, 1994)
Emwa1	Oospore infection of a single seedling	(Holub *et al.*, 1994)
Noco2	Conidia isolated from a single seedling	(Parker *et al.*, 1993)

***Peronospora parasitica* isolates and their interaction with *Arabidopsis* ecotypes**

***Arabidopsis* ecotype**	***Peronospora parasitica* isolate**		
	Cala2	Emwa1	Noco2
Col-0	incompatible (*RPP2*)*	incompatible (*RPP4*)	compatible
L*er*	compatible	incompatible (*RPP5* and *RPP8*)	incompatible (*RPP5*)
Ws-0	incompatible (*RPP1A*)	compatible	incompatible (*RPP1*)

* Genetic analysis of *Arabidopsis* segregating populations and cloning has established isolate specific *R*esistance to *P*eronospora *P*arasitica (*RPP*) genes.

2.1.2.2 *Pseudomonas syringae* pv. *tomato* (*Pst*)

Pseudomonas syringae pv. *tomato* (*Pst*) strain DC3000 expressing the avirulence determinants *avrRps4* (Hinsch and Staskawicz, 1996) or *avrRpm1* (Grant *et al.*, 1995) from the broad host range plasmid pVSP61 (Innes *et al.*, 1993) or DC3000 containing empty pVSP61 were used throughout this study. The *Pst* isolates were originally obtained from R. Innes (Indiana University, Bloomington Indiana, USA).

2.1.3 Bacterial strains

2.1.3.1 *Escherichia coli* strains

All *E. coli* strains were obtained from Invitrogen™ (Karlsruhe, Germany).

DH5α

Genotype: F$^-$ Φ80d*lac*ZΔM15 Δ(*lac*ZYA-*arg*F) U169 *deo*R *rec*A1 *end*A1 *hsd*R17(r$_k^-$, m$_k^+$) *pho*A *sup*E44 λ^- *thi*-1 *gyr*A96 *rel*A1

DH10B

Genotype: F$^-$ *mcr*A Δ(*mrr*-*hsd*RMS-*mcr*BC) Φ80*lac*ZΔM15 Δ*lac*X74 *deo*R *rec*A1 *end*A1 *ara*Δ139 Δ(*ara*, *leu*)7697 *gal*U *gal*K λ^- *rps*L (Str^R) *nup*G

TOP10

Genotype: F$^-$ *mcr*A Δ(*mrr*-*hsd*RMS-*mcr*BC) Φ80*lac*ZΔM15 Δ*lac*X74 *deo*R *rec*A1 *ara*D139 Δ(*ara*-*leu*)7697 *gal*U *gal*K *rps*L (Str^R) *end*A1 *nup*G

DB3.1

Genotype: F$^-$ *gyr*A462 *end*A Δ(*sr*1-*rec*A) *mcr*B *mrr* *hsd*S20 (r$_B^-$ m$_B^-$) *sup*E44 *ara*14 *gal*K2 *lac*Y1 *pro*A2 *rps*L20 (Str^R) *xyl*5 λ^- *leu* *mtl*1

2.1.3.2 *Agrobacterium tumefaciens* strains

For stable transformation of *Arabidopsis thaliana* plants and transient expression of constructs in *Nicotiana benthamiana*, *Agrobacterium tumefaciens* strain GV3101 containing the helper plasmid pMP90RK was used (Koncz and Schell, 1986). This strain carries resistances for gentamycin, kanamycin and rifampicin.

2.1.4 Vectors

Following vectors have been used or were generated in this study:

pENTR™/D-TOPO®	Entry vector for the Gateway® system that allows directional TOPO® cloning of blunt-end PCR products (Invitrogen™)
pMon999-$^{CFP}/_{YFP}$	(Shah *et al.*, 2001); *CFP* and *YFP* were PCR amplified for generation of pXCSG $^{CFP}/_{YFP}$ and pXCG $^{CFP}/_{YFP}$ (see below and 2.2.13.11)
pXCS-HisHA	(Witte *et al.*, 2004); Vector-backbone used to generate pXCSG and pXCG vectors (see below and 2.2.13.11)
pXCSG-$^{CFP}/_{YFP}$	Binary Gateway® destination vectors for expression of fusion proteins under control of P_{35SS} with a C-terminal $^{CFP}/_{YFP}$ tag (see 2.2.13.11 and Figure 3.5)
pXCG-$^{CFP}/_{YFP}$	Binary Gateway® destination vector for expression of fusion proteins under control of their native promoter with a C-terminal $^{CFP}/_{YFP}$ tag (see 2.2.13.11 and Figure 3.5)
pXCSG-StrepII	Binary Gateway® destination vector for expression of fusion proteins under control of P_{35SS} with a C-terminal StrepII tag
pXCG-StrepII	Binary Gateway® destination vector for expression of fusion proteins under control of their native promoter with a C-terminal StrepII tag

2.1.5 Oligonucleotides

Listed below are primers used in this study that were synthesised by Operon or Metabion. Start and Stop codons are accentuated in red, recognition sited for restriction endonucleases are underlined and CACC sequences for pENTR™/D-TOPO® cloning purpose are in blue. Lyophilised primers were resuspended in nuclease-free water to a final concentration of 100 pmol/µl (= 100 µM). Working stocks were diluted to 10 pmol/µl (=10 µM).

Primer	**Sequence (5´ → 3´)**	**Characteristics**
MW3	CTTAGCTCATTAAACTCCAGAAACC	*Pnos* upstream rev.
MW4	GCTTTTTTGTACAAACTTGTGATCC	*attR1/B1* rev.
MW6	CGACGGCCTGTGGGCATTCAGTCTGG	*GUS* fwd.
MW7	ATCACCACGATGCCATGTTCATCTGCC	*GUS* rev.
MW8	AACCTCCTCGGATTCCATTGCCCAGC	P_{35S} upstream fwd.
MW9	TTGTACAAAAAAGCAGGC	*attL1/B1* fwd.
MW10	TTTGTACAAGAAAGCTGG	*attL2/B2* rev.
MW12	CACCAGATCTGAGTTTATCAG	L*er* *EDS1*-promoter fwd. D-TOPO
MW13	GGTATCTGTTATTTCATCCATC	L*er* *gEDS1* rev. without Stop for C-terminal fusions
MW14	CACCATGGCGTTTGAAGCTCTTACC	L*er* *gEDS1* fwd. D-TOPO
MW15	ATCCCCGGGATGGTGAGCAAGGGCGAGGAGC	*CFP/YFP* fwd. with *Sma*I-site
MW16	AGTCTAGAGCTCTTACTTGTACAGCTCGTCCATGC	*CFP/YFP* rev. incl Stop and *Xba*I-site
MW17	GTTGGAACACTTTACATGGC	L*er* *EDS1*-promoter sequencing fwd.
MW18	TCTGAAAACCCAAGTCAAGC	L*er* *EDS1*-promoter sequencing fwd.
MW19	ATAGCCAAAGAGTCAACTCC	L*er* *EDS1*-promoter sequencing fwd.
MW20	ACTTATCTCGCTGGATTCG	L*er* *EDS1*-promoter sequencing rev.
MW21	ACCTTGAGCCTCGTTGTGTG	L*er* *gEDS1* sequencing fwd.
MW22	GAACTGGTACAGTCGATGG	L*er* *gEDS1* sequencing fwd.
MW23	CAAACGTCAAGAGAGCTGAG	L*er* *gEDS1* sequencing fwd.
MW24	ATCATGCTTTTGGGCTGAGG	L*er* *gEDS1* sequencing fwd.
MW25	CACCATGGAGTCTTCTTCTTCAC	*SAG101* fwd. D-TOPO
MW26	TTGGGACTTACCATAACTC	L*er* *SAG101* rev. without Stop for C-terminal fusions
MW27	TTATTGGGACTTACCATAAC	L*er* *SAG101* rev. with Stop for N-terminal fusions
MW28	CTTCTTGAAACCATCGAACC	*SAG101* Sequencing fwd.
MW29	ATGCAAGGAGGTCAAGATCG	*SAG101* Sequencing fwd.
MW30	GGGCTGAAGTTGAGGATTCG	*SAG101* Sequencing fwd.
MW31	CTTCAATGGCGGTGTTTTC	Detection pointmutation in *snc1* fwd.
MW32	GGCATGCGTAATCTGCAATATCTAA	Detection pointmutation in *snc1* rev.

Primer	**Sequence (5´ → 3´)**	**Characteristics**
MW33	GAGGGGATATACGGTGGTTT	Detection of *NPR1* fwd. (SNP marker)
MW34	GAGGGGATATACGGTGGTTC	Detection of *npr1-1* fwd. (SNP marker)
MW35	CCGACGACGATGAGAGAGTTTACG	Detection *NPR1* and *npr1-1* common rev. Primer
MW42	CACCACCTTTATATGACGATGG	Col-0 *SAG101*-promotor fwd. D-TOPO
MW43	TTGTGACTTACCATAACTCTCG	Col-0 *gSAG101* rev. without stop for C-terminal fusions
MW44	TCTTATGTGCATATGGTCC	Col-0 *SAG101*-promoter Sequencing fwd.
MW45	ATGGTAAGCTTTCAAATGC	Col-0 *SAG101*-promoter Sequencing fwd
MW46	CGATCTGCAGAAGTAGTAGC	Col-0 *gSAG101* Sequencing fwd.
MW47	TGCAATTCAGTCCAATAGC	Col-0 *gSAG101* Sequencing fwd.
MW48	GGTCTACAAGTTTCAAAAAGTAGTAAAGATTCAGG TCTAGAATTTC	Site directed mutagenesis of L*er* *SAG101* fwd. KKKK → KSSK
MW49	GAAATTCTAGACCTGAATCTTTACTACTTTTTGAAA CTTGTAGACC	Site directed mutagenesis of L*er* *SAG101* rev. KKKK → KSSK
MW50	CGCTCACGTGGATACAGC	Col-0 *EDS1B* mRNA rev.
CN60	AAAGAACGAAGACACAGGGC	Col-0 *EDS1A and B* mRNA fwd.
CN61	GTGTTCTAATAGCTTAAATACTCCACC	Col-0 *EDS1A* mRNA rev.
105/E2	ACACAAGGGTGATGCGAGACA	*EDS1* vs. *eds1-2* detection (deletion)
EDS4	GGCTTGTATTCATCTTCTATCC	*EDS1* vs. *eds1-2* detection (deletion)
EDS6	GTGGAAACCAAATTTGACATTAG	*EDS1* vs. *eds1-2* detection (deletion)

fwd.: forward; rev.: reverse

2.1.6 Enzymes

2.1.6.1 Restriction endonucleases

Restriction enzymes were purchased from New England Biolabs (Frankfurt, Germany) unless otherwise stated. Enzymes were supplied with 10x reaction buffer which was used for restriction digests.

2.1.6.2 Nucleic acid modifying enzymes

Standard PCR reactions were performed using home made *Taq* DNA polymerase. To achieve high accuracy, *Pfu* or *Pfx* polymerases were used when PCR products were generated for cloning. Modifying enzymes and their suppliers are listed below:

Taq DNA polymerase	home made
PfuTurbo® DNA polymerase	Stratagene® (Heidelberg, Germany)
Platinum® *Pfx* DNA polymerase	Invitrogen™ (Karlsruhe, Germany)
T4 DNA ligase	Roche (Mannheim, Germany)
Klenow Enzyme	Roche (Mannheim, Germany)
Alkaline Phosphatase, shrimp	Roche (Mannheim, Germany)
DNaseI	Roche (Mannheim, Germany)
SuperScript™ II RNase H^- Reverse Transcriptase	Invitrogen™ (Karlsruhe, Germany)
Gateway™ LR Clonase™ Enzyme mix	Invitrogen™ (Karlsruhe, Germany

2.1.7 Chemicals

Laboratory grade chemicals and reagents were purchased from Sigma-Aldrich (Deisenhofen, Germany), Roth (Karlsruhe, Germany), Merck (Darmstadt, Germany), Invitrogen™ (Karlsruhe, Germany), Serva (Heidelberg, Germany), and Gibco™ BRL® (Neu Isenburg, Germany) unless otherwise stated.

2.1.8 Antibiotics

Ampicillin (Amp)	100 mg/ml in H_2O
Carbenicillin (Carb)	50 mg/ml in H_2O
Gentamycin (Gent)	15 mg/ml in H_2O
Kanamycin (Kan)	50 mg/ml in H_2O
Rifampicin (Rif)	100 mg/ml in DMSO
Tetracycline (Tet)	12.5 mg/ml in 70 % ethanol

Stock solutions (1000x) stored at -20° C. Aqueous solutions were sterile filtrated.

2.1.9 Media

Media were sterilised by autoclaving at 121° C for 20 min. For the addition of antibiotics and other heat labile compounds the solution or media were cooled down to 55° C. Heat labile compounds were sterilised using filter sterilisation units prior to addition.

Escherichia coli media

LB (Luria-Bertani) broth

Tryptone	10.0	g/l
Yeast extract	5.0	g/l
NaCl	5.0	g/l

pH 7.0

For LB agar plates 1.5 % (w/v) agar was added to the above broth.

SOC

Tryptone	20.0	g/l
Yeast extract	5.0	g/l
NaCl	10.0	mM
KCl	2.5	mM
$MgCl_2$	10.0	mM
$MgSO_4$	10.0	mM
Glucose	20.0	mM

pH 7.0

Pseudomonas syringae media

NYG broth

Peptone	5.0	g/l
Yeast extract	3.0	g/l
Glycerol	20	ml/l

pH 7.0

For NYG agar plates 1.5 % (w/v) agar was added to the above broth.

Agrobacterium tumefaciens media

YEB

Beef extract	5.0	g/l
Yeast extract	1.0	g/l
Peptone	5.0	g/l
Sucrose	5.0	g/l
1M $MgSO_4$	2.0	ml/l

pH 7.2

For YEB agar plates 1.5 % (w/v) agar was added to the above broth.

Arabidopsis thaliana media

MS (Murashige and Skoog) agar plates

MS powder including vitamins and MES buffer	4.8	g/l
Sucrose	10.0	g/l
Plant agar	9.0	g/l

For selection of transgenic *Arabidopsis* plants carrying the phosphinothricin acetyltransferase (*PAT*) gene that confers Basta® (glufosinate-ammonium) resistance, DL-Phosphinothricin (PPT) was added to the agar plates:

DL-Phosphinothricin (100 mg/ml)	1:10000

DL-Phosphinothricin, plant agar and MS powder including vitamins and MES buffer was purchased from Duchefa (Haarlem, The Netherlands).

2.1.10 Antibodies

Listed below are primary and secondary antibodies used for immunoblot detection and co-immunorpecipitation.

Primary antibodies

Antibody	**Source**	**Dilution**	**Reference**
α-EDS1	rabbit polyclonal	1:500	S. Rietz[a]
α-SAG101	rabbit polyclonal	1:500	B. Feys[b]
α-c-Myc (9E10)	mouse monoclonal	1:5000	Santa Cruz (Santa Cruz, USA)
α-GFP	mouse monoclonal	1:2500	Roche (Mannheim, Germany)
α-Histone H3 (ab1791)	rabbit polyclonal	1:5000	Abcam (Cambridge, UK)
α-Hsc70 (plant, cytosolic)	mouse monoclonal	1:10000	Stressgen (Victoria, Canada)

[a] Max-Planck-Institute for Plant Breeding Research, Carl-von-Linné-Weg 10, 50829 Cologne, Germany
[b] Imperial College London, Department of Biological Sciences, 506 Sir Alexander Fleming Building, South Kensington Campus, London SW7 2AZ

Secondary antibodies

Antibody	**Feature**	**Dilution**	**Source**
goat anti-rabbit IgG-HRP	horseradish peroxidase conjugated	1:5000	Santa Cruz (Santa Cruz, USA)
goat anti-mouse IgG-HRP	horseradish peroxidase conjugated	1:5000	Santa Cruz (Santa Cruz, USA)

2.1.11 Buffers and solutions

General buffers and solutions are displayed in the following listing. All buffers and solutions were prepared with Milli-Q® water. Buffers and solutions for molecular biological experiments were autoclaved and sterilised using filter sterilisation units, respectively. Buffers and solutions not displayed in this listing are denoted with the corresponding methods.

DEPC-H_2O	Diethylpyrocarbonate	0.1	% in H_2O
	Shake vigorously, let stand O/N and autoclave 30 min.		
DNA extraction buffer (Quick prep)	Tris	200	mM
	NaCl	250	mM
	EDTA	25	mM
	SDS	0.5	%
	pH 7.5 (HCl)		

DNA gel loading dye (6x)	Sucrose	4	g
	EDTA (0.5 M)	2	ml
	Bromphenol blue	25	mg
	H_2O to 10 ml		
Ethidium bromide stock solution	Ethidium bromide	10	mg/ml H_2O
	Dilute 1:40000 in agarose solution		
GUS staining solution	Na_2HPO_4 (1M)	11.54	ml
	NaH_2PO_4 (1M)	8.46	ml
	$K_3Fe(CN)_6$ (0.05 M)	2	ml
	$K_4Fe(CN)_6$ (0.05 M)	2	ml
	EDTA (0.05 M)	4	ml
	Triton X-100 (10 %)	2	ml
	H_2O	90	ml
	pH 7.0		
	Prior to use add 5 ml methanol and 550 µl X-Gluc stock solution (50 mg/ml DMF) to 50 ml staining solution.		
Honda buffer	Ficoll 400	5	g
	Dextran T40	10	g
	Sucrose	27.38	g
	Tris	0.606	g
	$MgCl_2$	0.407	g
	H_2O to 200 ml		
	pH 7.4		
	Before use add 10 mM β-Mercaptoethanol and protease inhibitor cocktail for plant cell and tissue extracts (Sigma).		

Lactophenol trypan blue	Lactic acid	10	ml
	Glycerol	10	ml
	H_2O	10	ml
	Phenol	10	g
	Trypan blue	10	mg
	Before use dilute 1:1 in ethanol.		
PCR reaction buffer (10x)	Tris	100	mM
	KCl	500	mM
	$MgCl_2$	15	mM
	Triton X-100	1	%
	pH 9.0		
	Stock solution was sterilised by autoclaving and used for homemade *Taq* DNA polymerase.		
Ponceau S	Ponceau S working solution was prepared by dilution of ATX Ponceau S concentrate (Fluka) 1:5 in H_2O.		

SDS-PAGE:

Resolving gel buffer (4x)	Tris	1.5	M
	pH 8.8 (HCl)		
Running buffer (10x)	Tris	30.28	g
	Glycine	144.13	g
	SDS	10	g
	H_2O to 1000 ml		
	Do not adjust pH.		
Sample buffer (2x)	Tris	0.125	M
	SDS	4	%
	Glycerol	20	% (v/v)
	Bromphenol blue	0.02	%
	Dithiothreitol (DTT)	0.2	M
	pH 6.8		

Stacking gel buffer (4x)	Tris	0.5	M
	pH 6.8 (HCl)		
Water-saturated n-butanol	N-butanol	40	ml
	H_2O	10	ml
	Combine in a 50 ml Falcon tube and shake. Allow phases to separate. Use the top phase to overlay SDS-polyacrylamide gels.		
TAE buffer (50x)	Tris	242	g
	EDTA	18.6	g
	Glacial acetic acid	57.1	ml
	H_2O to 1000 ml		
	pH 8.5		
TBS-T buffer	Tris	10	mM
	NaCl	150	mM
	Tween®20	0.05	%
	pH 7.5 (HCl)		
TE buffer	Tris	10	mM
	EDTA	1	mM
	pH 8.0 (HCl)		
Western blotting:			
Stripping buffer	Tris	62.5	mM
	SDS	2	%
	β-Mercaptoethanol	100	mM
	pH 6.8 (HCl)		

Transfer buffer (10x)	Tris	58.2	g
	Glycine	29.3	g
	SDS (10 %)	12.5	ml
	H_2O to 1000 ml		
	pH 9.2		
	Before use dilute 80 ml 10 x buffer with 720 ml H_2O and add 200 ml methanol.		

2.2 Methods

2.2.1 Maintenance and cultivation of *Arabidopsis* plant material

Arabidopsis seed was germinated by sowing directly onto moist compost (Stender, Schermbeck, Germany) containing 10 mg l^{-1} Confidor® WG 70 (Bayer, Germany). Seeds were cold treated by placing pots after sowing on a tray with a lid and incubating them in the dark at 4° C for 48 h. Pots were subsequently transferred to a controlled environment growth chamber, covered with a propagator lid and maintained under short day conditions (10 h photoperiod, light intensity of approximately 200 µEinsteins m^{-2} sec^{-1}, 22° C and 65 % humidity). Propagator lids were removed when seeds had germinated. If required for setting seed, plants were transferred to long day conditions (16 h photoperiod) to allow early bolting and setting of seed. To collect seed, aerial tissue was enveloped with a paper bag and sealed with tape at its base until siliques shattered.

2.2.2 Generation of *Arabidopsis* F_1 and F_2 progeny

Fine tweezers and a magnifying-glass were used to emasculate an individual flower. To prevent self-pollination, only flowers that had a well-developed stigma but immature stamen were used for crossing. Fresh pollen from three to four independent donor stamens was dabbed onto each single stigma. Mature siliques containing F_1 seed were harvested and allowed to dry. Approximately five F_1 seeds per cross were grown as described above and allowed to self pollinate. Produced F_2 seeds were collected and stored.

2.2.3 *Arabidopsis* seed sterilisation

For *in vitro* growth of *Arabidopsis*, seed had to be sterilised. Approximately 50 - 100 *Arabidopsis* seeds were put into a 1.5 ml closable microcentrifuge tube. Tubes were labelled with lead pencil on a sticker as a normal lab pencil will bleach out during the procedure. Open microcentrifuge tubes were put in a plastic rack. 100 ml of 12 % Sodium-hypochloride solution (chlorine bleach) were poured into a beaker and put together with the seed into an exsiccator. The exsiccator was connected to a vacuum pump. 10 ml of 37 % HCl was directly added into the hypochloride solution so that yellow-grenish vapours were forming and the solution was bubbling heavily. The lid of the exsiccator was closed immediately and vacuum was generated, just enough to get an air tight seal. This was left for 4 – 8 h. After the sterilisation period, the exsiccator was slightly opened under a fume hood for 5 min to let out the gas. The lid was closed again, brought to a sterile bench and sterilised seeds were taken out of the exsiccator. Seeds were left for 15 min in opened vessel under the sterile workbench. Sterilised seed were stored for several days at 4° C or directly plated out on suitable culture media.

2.2.4 *Agrobacterium*-mediated stable transformation of *Arabidopsis* (floral dip)

This protocol for *Agrobacterium*-mediated stable transformation of *Arabidopsis* is based on the floral dip protocol described by Clough and Bent (1998). Approximately 10 - 15 *Arabidopsis* plants were grown in 9 cm square pots (3 pots for each transformation) under short day conditions for 5 - 6 weeks before being transferred to the greenhouse to induce flowering. First influorescence shoots were removed as soon as they emerged to encourage the growth of more influorescences. Plants were used for transformation when they did not have pods but maximum number of young flowerheads. *Agrobacterium* was streaked out onto selective YEB plates containing antibiotics for both the Ti and the T-DNA plasmids and was grown at 28° C for 3 days. A 20 ml YEB culture containing selective antibiotics was inoculated with fresh *Argobacterium* and grown overnight at 28° C in an orbital shaker. 200 ml YEB broth containing antibiotic selection was inoculated with all of the overnight culture and grown overnight at 28° C in an orbital shaker until $OD_{600} > 1.6$. Cultures were spun down at 5000 rpm for 10 min at room temperature and the pellet was resuspended in 5 % sucrose to $OD_{600} \sim 0.8$. Silwet L-77 (Lehle seeds, USA) at 500µl/l was added as surfactant. Plants to be transformed were inverted in the cell-suspension ensuring all flowerheads were submerged. Plants were agitated slightly to release air bubbles and left in the solution for approximately 5 sec. Plants were removed and dipping was repeated as before. Excess inoculum was removed by dabbing of influorescences onto kitchen roll. Plants were then placed into plactic bags, sealed with tape and placed overnight into the glasshouse away from direct light. Bags were removed and pots were moved to direct light and left to set seed.

2.2.5 Glufosinate selection of *Arabidopsis* transformants on soil

Seed collected from floral-dipped plants (see 2.2.4) were densely sown on soil and germinated as described before. Once cotyledons were fully opened but before true leaves appeared, young seedlings were sprayed with 0.1 % (v/v) Basta® (the commercial product of glufosinate). This treatment was repeated twice on a two day basis. Only transgenic *Arabidopsis* plants carrying the phosphinothricin acetyltransferase (*PAT*) gene that confers glufosinate-resistance survived while untransformed plants died.

2.2.6 Generation of *Arabidopsis* protoplasts

Arabidopsis leaf cells were digested with an enzyme solution to remove cell walls and release protoplasts.

Enzyme solution:		
Cellulase R10	1-1.5	%
Macerozyme R10	0.2-0.4	%
Mannitol	0.4	M
KCl	20	mM
MES	20	mM
pH 5.6; heat to 55° C for 10 min		
$CaCl_2$	10	mM
β-Mercaptoethanol	5	mM
BSA	0.1	%

W5:		
NaCl	154	mM
$CaCl_2$	125	mM
KCl	5	mM
MES	2	mM
pH 5.7		

Approximately 100 leaves of 2- to 3-week-old short-day grown plants were put into a 50 ml Erlenmeyer flask, 15 ml enzyme solution was added, leaves were vacuum-infiltrated twice for 3 min and incubated at 50 rpm on a rotary shaker for 2.5 h. The solution was filtered through an 80 µm nylon mesh into a 50 ml Falcon tube. Protoplasts were centrifuged for 5 min at 800 rpm (Heraeus Multifuge $3_{S\text{-}R}$), washed in 10 ml W5 and centrifuged as above. Protoplasts were resuspended in 5 ml W5.

2.2.7 Inoculation and maintenance of *Peronospora parasitica*

P. parasitica isolates were maintained as mass conidiosporangia cultures on leaves of their genetically susceptible *Arabidopsis* ecotypes over a 7 day cycle (see 2.1.2.1). Leaf tissue from infected seedlings was harvested into a 50 ml Falcon tube 7 d after inoculation. Conidiospores were collected by vigorously vortexing harvested leaf material in sterile dH_2O for 15 sec and after the leaf material was removed by filtering through miracloth (Calbiochem) the spore suspension was adjusted to a concentration of 4×10^4 spores/ml dH_2O using a Neubauer counting cell chamber. Plants to be inoculated had been grown under short day conditions as described above. *P. parasitica* conidiospores were applied onto 2-week-old seedlings by spraying until imminent run-off using an aerosol-spray-gun. Inoculated seedlings were kept under a propagator lid to create a high humidity atmosphere and incubated in a growth chamber at 18° C and a 10 h light period. For long term storage *P. parasitica* isolate stocks were kept as mass conidiosporangia cultures on plant leaves at -80° C.

2.2.8 Quantification of *P. parasitica* sporulation

To determine sporulation levels, seedlings were harvested 5 - 7 d after inoculation in a 50 ml Falcon tube and vortexed vigorously in 5 – 10 ml water for 15 sec. Whilst the conidiospores were still in suspension 10 µl were removed twice and spores were counted under a light microscope using a Neubauer counting cell chamber. For each tested *Arabidopsis* genotype, two pots containing approximately 30 seedlings were infected per experiment and harvested spores from all seedlings of each pot were counted twice with sporulation levels expressed as the number of conidiospores per gram fresh weight.

2.2.9 Histochemical analysis of *P. parasitica* development and necrotic plant tissue

Lactophenol trypan blue staining was used to visualise *P. parasitica* mycelium and necrotic plant tissue (Koch and Slusarenko, 1990). Leaf material was placed in a 15 ml Sarstedt tube (Nümbrecht, Germany) and immersed in lactophenol trypan blue. The tube was placed into a boiling water bath for 2 min followed by destaining in 5 ml chloral hydrate solution (2.5 g/ml water) for 2 h and a second time overnight on an orbital shaker. After leaf material was left for several hours in 70 % glycerol, samples were mounted onto glass microscope slides in 70 % glycerol and examined using a light microscope (Axiovert 135 TV, Zeiss, Germany) connected to a Nikon DXM1200 Digital Camera.

2.2.10 Maintenance of *P. syringae* pv. *tomato* (*Pst*) cultures

Pseudomonas syringae pv. *tomato* strains described in 2.1.2.2 were streaked onto selective NYG agar plates containing rifampicin (100 µg/ml) and kanamycin (50 µg/ml) from -80° C DMSO stocks. Streaked plates were incubated at 28° C for 48 h before storing at 4° C and refreshed weekly.

2.2.11 *P. syringae* pv. *tomato* (*Pst*) growth assay

Pst cultures of the denoted strains (see 2.1.2.2) were started from a small amount of bacteria grown on NYG agar plates containing rifampicin (100 µg/ml) and kanamycin (50 µg/ml) in 20 ml NYG broth containing rifampicin (100 µg/ml) and kanamycin (50 µg/ml). The 20 ml cultures were incubated overnight at 28° C and 200 rpm in a rotary shaker. 2.5 ml of the overnight cultures were used to inoculate 50 ml of NYG broth in 300 ml Erlenmeyer flasks supplemented with antibiotics. The flasks were incubated at 28° C and 200 rpm in a rotary shaker for 3 h. An ideal OD_{600} reading at this time point should be 0.2. Cultures were transferred to sterile 50 ml Falcon tubes and pelleted at 4500 rpm for 10 min at 20° C (Heraeus Multifuge $3_{S\text{-}R}$). Bacteria were washed by resuspending the pellet in 40 ml of 10 mM sterile $MgCl_2$ and subsequent centrifugation at 4500 rpm for 10 min at 20° C. The supernatant was promptly removed and each pellet resuspended in 50 ml of sterile 5 mM $MgCl_2$. For vacuum-infiltration the concentration of bacteria was adjusted to 5×10^5

cfu/ml in 600 ml of 5 mM $MgCl_2$ containing 0.002 % Silwet L-77 (Lehle seeds, USA). Single pots of 3 x 3 five-week-old plants, grown under short day conditions (see 2.2.1) were routinely used for bacterial growth assays. Two hours before vacuum-infiltration, plants were watered and kept under a dH_2O-humidified lid. Pots with plants were vacuum-infiltrated with bacteria by inverting the pots and carefully submerging all leaf material in 600 ml of diluted bacterial suspension contained within a plastic exsiccator. A vacuum was applied and maintained within the exsiccator for 3 min before being gradually released. Periodic swirling and tapping of the exsiccator helped to dislodge any air bubbles that accumulated at the surface of the leaves. Any non-infiltrated leaves remaining at this stage were removed by hand. The excess of bacterial solution was removed by inverting the pots and gently dipping of plants in water.

Day zero (d_0) samples were taken one hour after infiltration by using a cork borer (∅ 0.55 cm) to excise and transfer 4 leaf discs from 4 independent plants to a 1.5 ml centrifuge tube, resulting in a total excised area of 1 cm^2. This was repeated with a second batch of 4 leaf discs from 4 independent plants. The discs were then macerated with a plastic pestle in 100 µl of sterile 10 mM $MgCl_2$. Subsequently, 900 µl of sterile 10 mM $MgCl_2$ were added (10^{-1} dilution) and 100 ml of each sample were plated onto NYG agar (Rif^{100}, Kan^{50}). Day three (d_3) samples were taken in an identical manner to that of d_0 except that 4 leaf discs from 4 independent plants per infiltrated genotype were taken in triplicates. For each sample a dilution series ranging between 10^{-1} and 10^{-7} was made and 15 µl aliquots from each dilution were spotted sequentially onto a single NYG agar plate (Rif^{100}, Kan^{50}). All bacteria plates were incubated at 28° C for 48 h before colony numbers were counted.

2.2.12 Biochemical methods

2.2.12.1 *Arabidopsis* total protein extraction for immunoblot analysis

Total protein extracts were prepared from 3- to 5-week-old plant materials. Liquid nitrogen frozen samples were homogenized 2 x 15 sec to a fine powder using a Mini-Bead-Beater-8^{TM} (Biospec Products) and 1.2 mm stainless steel beads (Roth) in 2 ml centrifuge tubes. After the first 15 sec of homogenisation samples were transferred back to liquid nitrogen and the procedure was repeated. 150 µl of 2x SDS-PAGE sample buffer was added to 50 mg sample on ice. Subsequently, samples were briefly vortexed, boiled for 5 min and centrifuged at

20000 *g* and 4° C for 20 min in a bench top centrifuge. Supernatants were transferred to clean centrifuge tubes and stored at -20° C if not directly loaded onto SDS-PAGE gels.

2.2.12.2 Nuclear fractionation for immunoblot analysis

Nuclear fractionations were performed according to the protocol described by Kinkema *et al.* (2000), which is based on that described by Xia *et al.* (1997), with minor modifications: 2 g fresh weight of unchallenged leaf tissues grown under short day conditions (see 2.2.1) were homogenised in 4 ml Honda buffer using a mortar and pestle and then filtered through 62 µm (pore size) nylon mesh. Triton X-100 (10 %) was added to a final concentration of 0.5 % and after the solution was slowly mixed by swirling, incubated on ice for 15 min. The solution was then centrifuged at 1500 *g* for 5 min. An aliquot of the supernatant (S) fraction was saved and the pellet washed by gently resuspending in 3 ml Honda buffer containing 0.1 % Triton X-100. The sample was centrifuged again at 1500 *g* for 5 min. The pellet was gently resuspended in 3 ml Honda buffer and 1 ml aliquots were transferred to microcentrifuge tubes. The preparations were centrifuged at 100 *g* for 5 min to pellet starch and cell debris. The supernatants were transferred to new microcentrifuge tubes and centrifuged at 2000 *g* for 5 min to pellet the nuclei. Nuclear pellets were resuspended in 100 µl 2 x SDS-PAGE sample buffer, boiled for 10 min, and pooled. The nuclear extracts (N) and supernatant (S) fractions were run on 7.5 % or 10 % SDS-PAGE gels (see 2.2.12.5). To monitor the amount of cytosolic contamination in the nuclear extracts the described α-Hsc70 antibody was used (see 2.1.10). The described α-Histone H3 antibody was used as a nuclear marker (see 2.1.10).

2.2.12.3 Isolation of microsomal membranes

To isolate microsomal membranes 0.5 g of 4-week-old leaves grown in short day conditions (see 2.2.1) were homogenised in 0.5 ml extraction buffer (100 mM Tris, pH 7.5, 1 mM EDTA, 12 % sucrose, 2 mM DTT and protease inhibitor cocktail for plant cell and tissue extracts (Sigma) on ice using mortar and pestle. The homogenate was transferred to a microcentrifuge tube and centrifuged at 20000 *g* and 4°C for 10 min in a bench top centrifuge to remove cell debris. 100 µl of the supernatant were kept as a crude extract fraction whilst 600 µl of the supernatant were transferred to an ultracentrifugation tube (Beckmann) and centrifuged for 1 h at 100000 rpm and 4° C (Optima™ MAX-E ultracentrifuge, Beckmann Coulter, USA). 600 µl supernatant were kept as a soluble fraction and the pellet was washed with extraction buffer. After washing, the pellet was resuspended in 600 µl of extraction buffer using an ultrasonic bath. One volume of 2x SDS-PAGE sample buffer was added to the different fractions and samples were boiled for 8 min to denature proteins. Samples were frozen and kept at -20° C.

2.2.12.4 Co-Immunoprecipitation

Co-immunoprecipitations were performed on the Ws Myc-PAD4 transgenic line LM41-2 expressing 5x c-Myc tagged PAD4 under control of its native promoter (Feys *et al.*, 2001) and Ws-0 wild-type control plants. For each sample 1 g fresh weight of leaf tissue was ground in liquid nitrogen with a mortar and pestle to a fine powder. Two ml of extraction buffer (20 mM Tris-HCl, pH 8.0, 0.33 M sucrose, 10 mM EDTA, 5 mM DTT and protease inhibitor cocktail for plant cell and tissue extracts (Sigma)) were added and further homogenised by grinding on ice. Samples were centrifuged at 5000 *g* and 4° C for 45 min. 150 µl of supernatant were kept as an input fraction. Five µl of α-c-Myc antibody (see 2.1.10) were added to 1.2 ml of supernatant in a microcentrifuge tube and the solution incubated on an orbital shaker at 4° C for 2 h. After 35 µl of protein G sepharose™ (Amersham Biosciences) have been pre-washed twice with 1 ml of extraction buffer, the solution was added to the washed G sepharose™ and incubated on an orbital shaker at 4° C for 3 h to precipitate immunocomplexes. Samples were centrifuged at 1000 *g* and 4° C for 5 min. The pellet was washed with 750 µl washing buffer (50 mM HEPES, pH 7.4, 100 mM NaCl, 10 mM EDTA) by careful resuspension. The resuspended pellet was transferred to a new microcentrifuge tubes and centrifuged at 1000 *g* and 4° C for 5 min. The washing step was repeated twice without transferring the resuspended pellet to a new microcentrifuge tube. After the last washing step the pellet was resuspended in 50 µl of 2x SDS-PAGE sample buffer by vortexing, boiled for 5 min and centrifuged at 13000 rpm for 1 min. Supernatants were transferred to new microcentrifuge tubes and 15 µl loaded to a SDS-PAGE gel. Immunoblot detections were as described under 2.2.12.6. Samples were stored at -20° C.

2.2.12.5 Denaturing SDS-polyacrylamide gel electrophoresis (SDS-PAGE)

Denaturing SDS-polyacrylamide gel electrophoresis (SDS-PAGE) was carried out using the Mini-PROREAN® 3 system (BioRad) and discontinuous polyacrylamide (PAA) gels. Gels were made fresh on the day of use according to the manufacturer instructions. Resolving gels were poured between to glass plates and overlaid with 500 µl of water-saturated n-butanol or 50 % isopropanol. After gels were polymerised for 30 – 45 min the alcohol overlay was removed and the gel surface was rinsed with dH_2O. Excess water was removed with filter paper. A stacking gel was poured onto the top of the resolving gel, a comb was inserted and the gel was allowed to polymerise for 30 - 45 min. In this study, 7.5 % or 10 % resolving gels were used, overlaid by 4 % stacking gels. Gels were 0.75 mm or 1.5 mm in thickness.

Table 2.4. Formulation for different percentage resolving gels

Component[a]	7.5 % resolving gel	10 % resolving gel
H_2O	4.82 ml	4.1 ml
Resolving gel buffer	2.5 ml	2.5 ml
10 % SDS	0.1 ml	0.1 ml
30 % Acrylamide/Bis solution, 29:1 (BioRad)	2.5 ml	3.3 ml
TEMED (BioRad)	5.0 µl	5.0 µl
10 % APS[b]	75 µl	75 µl

Table 2.5. Constituents of a protein stacking gel

Component[a]	4 % stacking gel
H_2O	6.1 ml
Stacking gel buffer	2.5 ml
10 % SDS	0.1 ml
30 % Acrylamide/Bis solution, 29:1 (BioRad)	1.3 ml
TEMED (BioRad)	10 µl
10 % APS[b]	100 µl

[a] Add in stated order

[b] Store at -20° C

If protein samples were not directly extracted in 2x SDS-PAGE sample buffer (see 2.1.11) proteins were denatured by adding 1 volume of 2x SDS-PAGE sample buffer to the protein sample followed by boiling for 5 min.

After removing the combs under running water, each PAA gel was placed into the electrophoresis tank and submerged in 1x running buffer. A pre-stained molecular weight marker (Precision plus protein standard dual colour, BioRad) and denatured protein samples were loaded onto the gel and run at 80 - 100 V (stacking gel) and 100 – 150 V (resolving gel) until the marker line suggested the samples had resolved sufficiently.

2.2.12.6 Immunoblot analysis

Proteins that had been resolved on acrylamide gels were transferred to Hybond™-ECL™ nitrocellulose membrane (Amersham Biosciences) after gels were released from the glass plates and stacking gels were removed with a scalpel. PAA gels and membranes were pre-equilibrated in 1 x transfer buffers for 10 min on a rotary shaker and the blotting apparatus (Mini Trans-Blot® Cell, BioRad) was assembled according to the manufacturer instructions. Transfer was carried out at 100 V for 70 min. The transfer cassette was dismantled and membranes were checked for equal loading by staining with Ponceau S for 5 min before rinsing in copious volumes of deionised water. Ponceau S stained membranes were scanned and thereafter washed for 5 min in TBS-T before membranes were blocked for 1 h at room temperature in TBS-T containing 5 % blotting grade milk powder (Roth). The blocking solution was removed and membranes were washed briefly with TBS-T. Incubation with primary antibodies was carried out overnight by slowly shaking on a rotary shaker at 4° C in the following conditions: α-EDS1 1:500 in TBS-T + 2 % milk powder, α-c-Myc 1:5000 in TBS-T + 2 % milk powder, α-SAG101 1:500 in TBS-T + 5 % milk powder, α-Histone H3 1:5000 in TBS-T + 5 % milk powder and α-Hsc70 1:10000 in TBS-T + 1 % BSA. For antibody details see 2.1.10. Next morning the primary antibody solution was removed and membranes were washed 3 x 15 min with TBS-T at room temperature on a rotary shaker. Primary antibody-antigen conjugates were detected using a horseradish peroxidase (HRP)-conjugated goat anti-rabbit or goat anti-mouse secondary antibody (for antibody details see 2.1.10) diluted 1:5000 in TBS-T containing the same concentration of milk powder or BSA used for the precedent primary antibody. Membranes were incubated in the secondary antibody solution for 1 h at room temperature by slowly rotating. The antibody solution was removed and membranes were washed as described above. This was followed by chemiluminescence detection using the SuperSignal® West Pico Chemimuminescent kit or a 9:1 - 3:1 mixture of the SuperSignal® West Pico Chemimuminescent- and SuperSignal® West

Femto Maximum Sensitivity-kits (Pierce) according to the manufacturer instructions. Luminescence was detected by exposing the membrane to photographic film (BioMax light film, Kodak).

2.2.12.7 Histochemical staining for β-glucuronidase (GUS) activity

Plant material to be GUS-stained was covered with GUS-staining solution in appropriate reaction tubes. Tubes were placed in an exsiccator and a vacuum was applied for 3 - 5 min. Vacuum was released and this procedure was repeated twice. Tubes were closed and incubated over night at 37° C. After incubation of the leaves, the GUS staining solution was discarded. Plant material was rinsed with deionised water and tissues were cleared by putting into 70 % ethanol. The ethanol was exchanged several times until tissues were completely cleared and clear GUS-staining was visible. Tissues were stored in 70 % ethanol until examined by microscopy.

2.2.13 Molecular biological methods

2.2.13.1 Isolation of genomic DNA from *Arabidopsis* (Quick prep for PCR)

This procedure yields a small quantity of poorly purified DNA. However, the DNA is of sufficient quality for PCR amplification. If preps are to be used over a long period of time, they should be frozen in aliquots. The aliquot in use should be stored at 4° C. The cap of a 1.5 ml microcentrifuge tube was closed onto a leaf to clip out a section of tissue and 400 µl of DNA extraction buffer were added. A micropestle was used to grind the tissue in the tube until the tissue was well mashed. The solution was centrifuged at maximum speed for 5 min in a bench top microcentrifuge and 300 µl supernatant were transferred to a clean tube. 1 volume of isopropanol was added to precipitate DNA and centrifuged at maximum speed for 5 min in a bench top microcentrifuge. The supernatant was discarded carefully. The pellet was washed with 70 % ethanol and dried. Finally the pellet was dissolved in 100 µl 10 mM Tris-HCl pH 8.0 and 0.5 - 2 µl of the solution were used for PCR.

2.2.13.2 Isolation of total RNA from *Arabidopsis*

Total RNA was prepared from 3- to 6-week-old plant materials. Liquid nitrogen frozen samples (approximately 50 mg) were homogenized 2 x 15 sec to a fine powder using a Mini-Bead-Beater-8^{TM} (Biospec Products) and 1.2 mm stainless steel beads (Roth) in 2 ml centrifuge tubes. After the first 15 sec of homogenisation samples were transferred back to liquid nitrogen and the procedure was repeated. 1 ml of TRI$^{®}$ Reagent (Sigma) was added and samples were homogenised by vortexing for 1 min. For dissociation of nucleoprotein complexes the homogenised sample was incubated for 5 min at room temperature. 0.2 ml of chloroform was added and samples were shaken vigorously for 15 sec. After an incubation for 3 min at room temperature samples were centrifuged for 15 min at 12000 *g* and 4° C. 0.5 ml of the upper aqueous, RNA containing phase were transferred to a new microcentrifuge tube and RNA was precipitated by adding 0.5 volumes of isopropanol and incubation for 10 min at room temperature. Subsequently, samples were centrifuged for 10 min at 12000 *g* and 4° C. The supernatant was removed and the pellet was washed by vortexing in 1 ml of 75 % ethanol. Samples were again centrifuged for 5 min at 7500 *g* and 4° C, pellets were air dried for 10 min and dissolved in 50 µl DEPC-H_2O. All RNA extracts were adjusted to the same concentration with DEPC-H_2O. Samples were stored at -80° C.

2.2.13.3 Polymerase chain reaction (PCR)

Standard PCR reactions were performed using home made *Taq* DNA polymerase while for cloning of PCR products *Pfu* or *Pfx* polymerases were used (see 2.1.6.2) according to the manufacturer instructions. All PCRs were carried out using a PTC-225 Peltier thermal cycler (MJ Research). A typical PCR reaction mix and thermal profile is shown below.

Reaction mix (20 µl total volume):

Component[a]	**Volume**
Template DNA (genomic or plasmid)	0.1 - 20 ng
10 x PCR reaction buffer	2 µl
dNTP mix (2.5 mM each: dATP, dCTP, dGTP, dTTP)	2 µl
Forward primer (10 µM)	1 µl
Reverse primer (10 µM)	1 µl
Taq DNA polymerase (4U/µl)	0.5 µl
Nuclease free water	to 20 µl total volume

Thermal profile

Stage	**Temperature (°C)**	**Time period**	**No. of cycle**
Initial denaturation	94	3 min	1 x
Denaturation	94	30 sec	25 - 40
Annealing	50 - 60	30 sec	
Extension	72	1 min per kb	
Final extension	72	3 min	1 x

2.2.13.4 Site directed mutagenesis

Site directed mutagenesis was basically performed as described in the instruction manual of the QuickChange® site-directed mutagenesis kit of Stratagene®.

PCR reaction mix (25 µl total volume):

Component	**Volume**
Template plasmid (20 ng/µl)	1 µl
10 x *PfuTurbo*® reaction buffer	2.5 µl
dNTP mix (2.5 mM each: dATP, dCTP, dGTP, dTTP)	2.5 µl
Primer 1 (10 µM)	1.4 µl
Primer 2 (10 µM)	1.4 µl
PfuTurbo® DNA polymerase (2.5 U/µl)	0.5 µl
Nuclease free water	to 25 µl total volume

Thermal profile:

Stage	**Temperature (°C)**	**Time period**	**No. of cycle**
Initial denaturation	94	1 min	1 x
Denaturation	94	30 sec	12 - 18
Annealing	55	1 min	
Extension	72	2 min per kb	
Final extension	72	10 min	1 x

After the PCR, 0.5 µl *Dpn*I (20 U/µl) were added to the reaction mix to digest methylated, non-mutated, parental DNA and to select for mutation-containing synthesised DNA. The reaction was incubated for 1 h at 37° C before the endonuclease was heat-inactivated at 65° C for 20 min. 3 µl of the reaction mixture, containing the circular, nicked vector DNA with the desired mutations were then transformed into DH10B cells and plated on LB agar containing the appropriate antibiotic.

2.2.13.5 Reverse transcription-polymerase chain reaction (RT-PCR)

RT-PCR was carried out in two steps. SuperScript™ II RNase H$^-$ Reverse Transcriptase (Invitrogen) was used for first strand cDNA synthesis by combining 1 - 1.5 µg template total RNA, 1 µl oligo $dT_{18}V$ (0.5 µg/µl, V standing for an variable nucleotide), 5 µl dNTP mix (each dNTP 2.5 mM) in a volume of 13.5 µl (deficit made up with DEPC-H_2O). The sample was incubated at 65° C for 10 min to destroy secary structures before cooling on ice. Subsequently the reaction was filled up to a total volume of 20 µl by adding 4 µl of 5x reaction buffer (supplied with the enzyme), 2 µl of 0.1 M DTT and 0.5 µl reverse transcriptase. The reaction was incubated at 42° C for 60 min before the enzyme was heat inactivated at 70° C for 10 min. For subsequent normal PCR, 1 µl of the above RT-reaction was used as cDNA template. As template total RNA for the reverse transcription reaction was not DNase treated, a control reaction for each RNA preparation was performed in which the reverse transcription reaction was incubated without reverse transcriptase enzyme (enzyme replaced by equal volume of DEPC-H_2O) to check in the following PCR for contamination by genomic DNA.

2.2.13.6 Plasmid DNA isolation from bacteria

Standard alkaline cell lysis minipreps of plasmid DNA were carried out using the GFX™ micro plasmid prep kit from Amersham Biosciences according to the manufacturer´s instructions. Larger amounts of plasmid DNA for single cell transient gene expression assays were isolated using Qiagen Midi preparation kits.

2.2.13.7 Restriction endonuclease digestion of DNA

Restriction digests were carried out using the manufacturer´s recommended conditions. Typically, reactions were carried out in 0.5 ml tubes, using 1 µl of restriction enzyme per 10 µl reaction. All digests were carried out at the appropriate temperature for a minimum of 30 min.

2.2.13.8 DNA ligations

Typically, DNA ligations were carried out overnight at 16° C in a total volume of 10 µl containing 1 µl T4 DNA ligase (1 U/µl; Roche), ligation buffer (supplied by the manufacturer), 25 - 50 ng vector and 3- to 5-fold molar excess of insert DNA for sticky and blunt end ligations. In some cases ligations were performed overnight at 4° C, overnight at room temperature or for 1 - 3 h at room temperature.

2.2.13.9 Agarose gel electrophoresis of DNA

DNA fragments were separated by agarose gel electrophoresis in gels consisting of 1 – 2 % (w/v) SeaKem® LE agarose (Cambrex, USA) in TAE buffer. Agarose was dissolved in TAE buffer by heating in a microwave. Molten agarose was cooled to 50° C before 2.5 µl of ethidium bromide solution (10 mg/ml) was added. The agarose was pored and allowed to solidify before being placed in TAE in an electrophoresis tank. DNA samples were loaded onto an agarose gel after addition of 2 µl 6x DNA loading buffer to 10 µl PCR- or restriction-reaction. Separated DNA fragments were visualised by placing the gel on a 312 nm UV transilluminator and photographed.

2.2.13.10 Isolation of DNA fragments from agarose gel

DNA fragments separated by agarose gel electrophoresis were excised from the gel with a clean razor blade and extracted using the QIAEX®II gel extraction kit (Qiagen) according to the manufacturer’s protocol.

2.2.13.11 Generation of Gateway®-compatible vectors for protein-localisation and fluorescence resonance energy transfer (FRET) studies

To generate binary destination vectors for Gateway® cloning technology (Invitrogen), suitable for protein localisation and FRET protein-protein interaction studies, primer pair 5′-ATCCCCGGGATGGTGAGCAAGGGCGAGGAGC-3′ and 5′-AGTCTAGAGCTCTTACTTGTACAGCTCGTCCATGC-3′ (*Sma*I and *Xba*I sites underlined) was used to PCR amplify cyan fluorescent protein (*CFP*) and yellow fluorescent protein (*YFP*) from vector pMon999 (Shah *et al.*, 2001). PCR products for *CFP* and *YFP* were digested with *Sma*I and *Xba*I and ligated into the binary vector pXCS-HisHA (Witte *et al.*, 2004) digested by *Sma*I and *Xba*I, to result in pXCS-CFP and pXCS-YFP. A Gateway® recombination cassette (reading frame B, blunt *Eco*RV fragment, Invitrogen) was then ligated into the *Sma*I site of pXCS-CFP and pXCS-YFP. Clones with the right orientation of the Gateway® cassette were selected and named pXCSG-CFP and pXCSG-YFP. For fusions of CFP or YFP to the C-terminus of the protein of interest, LR reaction between an entry clone and the Gateway® destination vector was performed as described under 2.2.13.12. Vectors pXCSG-CFP and pXCSG-YFP allow the expression of fusion proteins under control of the highly active double 35S promoter of cauliflower mosaic virus (P_{35SS}). To allow the expression of fusion proteins under control of their native promoters, vectors pXCSG-CFP and pXCSG-YFP were digested with *Asc*I and *Xho*I to cut off P_{35SS}. *Pfu Turbo*® DNA polymerase (Stratagene®, Heidelberg, Germany) was used to fill-in the restriction enzyme-generated DNA overhangs. Subsequently, the linear, blunt-end vectors were re-ligated. Originated vectors were named pXCG-CFP and pXCG-YFP. All resulting expression construct, generated after LR reaction of an entry vector with the generated binary destination vectors, can also be used to stably transform *Arabidopsis* via *Agrobacterium*-mediated transformation (see 2.2.4). For vector maps see Figure 3.5.

2.2.13.12 Site specific recombination of DNA in Gateway®-compatible vectors

The pENTR™ Directional TOPO® Cloning kit was used for directionally cloning of blunt-end PCR products into pENTR™/D-TOPO® to generate an entry clone for entry into the Gateway® system according to the manufacturer's instructions. To transfer the fragment of interest into gene expression constructs, an LR reaction between the entry clone and a Gateway® destination vector (see also 2.2.13.11 for the generation of destination vectors) was performed.

Basic LR reaction approach:

LR reaction buffer (5x)	1	µl
Entry clone	70	ng
Destination vector	70	ng
LR clonase™ enzyme mix	1	µl
TE buffer	to 5	µl

Reactions were incubated for 1 h at room temperature before 0.5 µl proteinase K solution (supplied with the kit) were added. Reactions were incubated at 37° C for 10 min before completely transformed into *E. coli* strain DH10B (see 2.1.3.1).

2.2.13.13 DNA sequencing

DNA sequences were determined by the "Automatische DNA Isolierung und Sequenzierung" (ADIS) service unit at the MPIZ on Applied Biosystems (Weiterstadt, Germany) Abi Prism 377 and 3700 sequencers using Big Dye-terminator chemistry (Sanger *et al.*, 1977).

2.2.13.14 DNA sequence analysis

Sequence data were analysed mainly using SeqMan^{TM} II version 5.00 (DNASTAR, Madison, USA), EditSeq^{TM} version 5.00 (DNASTAR, Madison, USA) and Clone Manager 6 version 6.00 (Scientific and Educational software, USA).

2.2.13.15 Preparation of chemically competent *E. coli* cells

Media and solutions required for preparation of rubidium chloride *E. coli* chemically competent cells:

ΦB:			TFB1:			TFB2:		
Yeast extract	0.5	%	KAc	30	mM	MOPS	10	mM
Tryptone	2	%	$MnCl_2$	50	mM	$CaCl_2$	75	mM
$MgSO_4$	0.4	%	RbCl	100	mM	RbCl	10	mM
KCl	10	mM	$CaCl_2$	10	mM	Glycerol	15	%
pH	7.6		Glycerol	15	%	sterile-filter		
autoclave			pH	5.8				
			steril-filter					

5 ml of an *E. coli* strain DH10B over night culture grown in ΦB was added to 400 ml of ΦB and shaken at 37° C until the bacterial growth reached an OD_{600} 0.4 - 0.5. Cells were cooled on ice and all following steps were carried out on ice or in a 4° C cold room. The bacteria were pelleted at 5000 *g* for 15 min at 4° C. The pellet was gently resuspended in 120 ml ice-cold TFB1 solution and incubated on ice for 10 min. The cells were pelleted as before and carefully resuspended in 16 ml ice-cold TFB2 solution. 1.5 ml eppendorf reaction tubes containing 50 µl aliquots of cells were frozen in liquid nitrogen and stored at -80° C until use.

2.2.13.16 Transformation of chemically competent *E. coli* cells

A 50 µl aliquot of chemically competent cells was thawed on ice. 10 to 25 ng of ligated plasmid DNA (or ~ 5 µl of ligated mix from 10 µl ligation reaction) was mixed with the aliquot and incubated on ice for 30 min. The mixture was heat-shocked for 30 sec at 42° C and immediately put on ice for 1 min. 500 µl of SOC medium was added to the microcentrifuge tube and incubated at 37° C for 1 h on a rotary shaker. The transformation mixture was centrifuged for 5 min at 1500 *g*, resuspended in 50 µl LB broth and plated onto selective media plates.

2.2.13.17 Preparation of electro-competent *A. tumefaciens* cells

The desired *Agrobacterium* strain was streaked out onto YEB agar plate containing adequate antibiotics and grown at 28° C for two days. A single colony was picked and a 5 ml YEB culture, containing appropriate antibiotics, was grown overnight at 28° C. The whole overnight culture was added to 200 ml YEB (without antibiotics) and grown to an OD_{600} of 0.6. Subsequently, the culture was chilled on ice for 15 – 30 min. From this point onwards bacteria were maintained at 4° C. Bacteria were centrifuged at 6000 *g* for 15 min and 4° C and the pellet was resuspended in 200 ml of ice-cold sterile water. Bacteria were again centrifuged at 6000 *g* for 15 min and 4° C. Bacteria were resuspended in 100 ml of ice-cold sterile water and centrifuged as described above. The bacterial pellet was resuspended in 4 ml of ice-cold 10 % glycerol and centrifuged as described above. Bacteria were resuspended in 600 µl of ice-cold 10 % glycerol. 40 µl aliquots were frozen in liquid nitrogen and stored at -80° C.

2.2.13.18 Transformation of electro-competent *A. tumefaciens* cells

50 ng of plasmid DNA was mixed with 40 µl of electro-competent *A. tumefaciens* cells, and transferred to an electroporation cuvette on ice (2 mm electrode distance; Eurogentec, Seraing, Belgium). The BioRad Gene Pulse™ apparatus was set to 25 µF, 2.5 kV and 400 Ω. The cells were pulsed once at the above settings for a second, the cuvette was put back on ice and immediately 1 ml of YEB medium was added to the cuvette. Cells were quickly re-suspended by slowly pipetting and transferred to a 2 ml microcentrifuge tube. The tube was incubated for 3 h in an Eppendorf thermomixer at 28° C and 600 rpm. A 5 µl fraction of the transformation mixture was plated onto selection YEB agar plates.

2.2.14 Transient plant transformations

2.2.14.1 *Agrobacterium*-mediated transient transformation of *N. benthamiana* leaves

Prior to *A. tumefaciens* infiltration the following media needed to be prepared:

Induction medium (1 l):

K_2HPO_4	10.5	g
KH_2PO_4	4.5	g
$(NH_4)_2SO_4$	1.0	g
NaCitrate·$2H_2O$	0.5	g
$MgSO_4$ (1M)	1.0	ml
Glucose	1.0	g
Fructose	1.0	g
Glycerol	4.0	ml
MES	10.0	mM
pH	5.6	

autoclave
Prior to use add appropriate antibiotics
and 50 µg/ml Acetosyringone (3´,5´-Dimethoxy-4´-hydroxyacetophenone).

Infiltration medium:

MES	10	mM
$MgCl_2$	10	mM
pH	5.3 - 5.5	

Prior to use add 150 µg/ml Acetosyringone.

4 ml overnight cultures were grown in liquid YEB (including appropriate antibiotics) at 28° C. The culture was spun down, bacteria were resuspended in 5 ml induction medium and grown further for another 4 - 6 h. Cultures were spun down and the pellet was resuspended in infiltration medium to an OD_{600} of 0.4. The bacterial solution was then left at room temperature for 1 - 3 h. Young plants were watered a few hours before infiltrating healthy, fresh looking leaves with a needle-less 1 ml syringe on the underside. Samples of infiltrated leaf areas for protein extractions were taken 2 - 3 d after infiltration.

2.2.14.2 Single cell transient gene expression assay in *Arabidopsis* epidermal cells using particle bombardment

The biolistic particle delivery is a transient transformation method that uses helium pressure to introduce DNA coated on gold or tungsten particles (microcarriers) into living cells.

2.2.14.2.1 Preparation of *Arabidopsis* leaves for transfection

Detached 4-week-old *Arabidopsis* leaves, grown on soil under short day conditions (see 2.2.1), were placed on 1 % agar plates containing 85 µM benzimidazole. Leaves were placed in a light chamber at 22° C, 2 h prior bombardment.

2.2.14.2.2 Preparation of microcarriers

The following procedure prepares gold microcarriers for 10 bombardments. 30 mg of gold microcarriers (1.0 µm diameter; BioRad) were transferred into a 1.5 ml microcentrifuge tube. 1 ml of 70 % EtOH was added. The suspension was vigorously vortexed for 3 - 5 min on a platform vortexer. The suspension was left for 15 min to sediment the microcarriers. The microcarriers were pelleted by spinning for 5 sec in a bench-top centrifuge. The supernatant was removed and discarded. The pellet was rinsed for three times by adding 1 ml of sterile water, vigorously vortexing for 1 min, sedimentation of the particles for 1 min, pelleting the microparticles by spinning for 5 sec in a bench-top centrifuge and subsequent removal of the supernatant. After washing, 500 µl of sterile glycerol (50 % (v/v)) was added to adjust the microparticle suspension to a concentration of 60 mg/ml. The microcarriers can be stored at 4°C for up to 2 weeks.

2.2.14.2.3 Coating of microcarriers with DNA

Following procedure prepares DNA-coated microcarriers for one bombardment. The previously prepared microcarriers (see 2.2.14.2.2) were vortexed for 5 min on a platform vortexer to resuspend sedimented particles. 50 µl of the microcarrier suspension were removed while vortexing and transferred to a 1.5 ml microcentrifuge tube. For delivery of two constructs, equimolar plasmid amounts (maximum of 5 µg DNA in total) were mixed prior to the coating of particles. For single construct bombardments 5 µg DNA were used. While vigorously vortexed, the prepared DNA mixture, 50 µl $CaCl_2$ (2.5 M), and 20 µl spermidine (0.1 M) were added to the microcarrier suspension. The microcarriers were spun down for 2 sec in a bench-top centrifuge and the supernatant was discarded. 140 µl of 70 % ethanol were added and the suspension was vortexed at low speed for 2 sec before spinning the suspension for 2 sec. The supernatant was removed and discarded. 140 µl of 99.9 % ethanol were added and the suspension was again vortexed at low speed for 2 sec before spinning the suspension for 2 sec. The coated gold particles were resuspended in 50 µl of 99.9 % ethanol.

2.2.14.2.4 The particle bombardment

Seven macrocarriers (BioRad) were placed inside the macrocarrier holder of the Hepta Adapter™ (BioRad). 6 µl aliquots of DNA-coated microcarriers were removed from the suspension while vortexing and transferred to each of the seven macrocarriers. After complete evaporation of the ethanol, the Hepta Adapter™ was placed inside the BioRad particle delivery system (Biolistic PDS-1000/He™) and a vacuum of 27 mm Hg was applied. Rupture discs bursting at a pressure of 900 psi were used in the bombardment process. The bombarded leaves were kept in a light chamber at 22° C. FRET-analyses (see 2.2.16) and fluorescence microscopy were carried out 24 - 48 h after transfection.

2.2.15 Localisation studies using confocal laser scanning microscopy (CLSM)

Detailed analysis of intracellular fluorescence was performed by confocal laser scanning microscopy using a Zeiss LSM 510 META microscopy system (Zeiss, Germany) based on an Axiovert inverted microscope equipped with an Argon ion laser as an excitation source. CFP- and YFP-tagged proteins were excited by the 458 nm and the 514 nm laser lines. CFP fluorescence was selectively detected by an HFT 458 dichroic mirror and BP 470 – 500 band pass emission filter while YFP fluorescence was selectively detected by using an HFT 514 dichroic mirror and BP 535 – 590 band pass emission filter. A Plan-Apochromat 20x/0.75 lens was used for scanning of leaves. In order to avoid crosstalk between CFP and YFP, images were acquired in the multichannel tracking mode and analysed with Zeiss LSM510 software.

2.2.16 Fluorescence resonance energy transfer-acceptor photobleaching (FRET-APB)

For fluorescence resonance energy transfer-acceptor photobleaching (FRET-APB) analyses, the same microscopic system as described under 2.2.15 was utilised. Acceptor photobleaching experiments were performed essentially as described by Karpova *et al.* (2003). Cells were bleached in the acceptor YFP channel by scanning a region of interest (ROI) using 5 – 20 times 514 nm argon laser line at 100 % intensity. The bleach time ranged from 5 – 20 sec depending on size of the ROI. Before and after the acceptor bleaching, the CFP intensity images were collected to assess the changes in the donor fluorescence.

FRET efficiency (E_F) was calculated using the following formula $E_F = (I_6 - I_5) \times 100/I_6$, where I_6 is the CFP intensity after the photobleaching of YFP and I_5 is the intensity just before the photobleaching. This formula thus yields the increase in CFP fluorescence following a YFP bleach normalised by CFP fluorescence after the bleach (Karpova *et al.*, 2003). In order to monitor the changes in the levels of CFP fluorescence before the bleaching process, background FRET efficiency (B_F) was calculated using the following formula $B_F = (I_5 - I_4) \times 100/I_5$, where I_4 and I_5 refer to the CFP intensity at time points 4 and 5 preceding the bleaching. As background FRET was insignificantly low, background subtractions were not performed.

3 Results

The study is subdivided into three parts. The aim of the first section **(3.1)** was to analyse the tissue specific expression of EDS1, PAD4 and SAG101. Immunoblot analyses on EDS1 and Myc-PAD4 protein abundance in different *Arabidopsis* tissues are presented. In addition, microarray data have been utilised to compare *EDS1*, *PAD4* and *SAG101* transcriptional levels in these tissues. The microarray data shown for *EDS1* are compared with analyses of the transcriptional activity of the L*er* *EDS1* promoter (P_{EDS1}) by using stable transgenic P_{EDS1}*::GUS Arabidopsis* lines.

In the second section **(3.2)**, in order to explore signalling functions of EDS1, PAD4 and SAG101, I focus on the subcellular localisations of these three proteins and assess *in vivo* by fluorescence resonance energy transfer-acceptor photobleaching (FRET-APB) the nature of their associations within the cell. Biochemical approaches were utilised to verify the localisations observed with transiently expressed fluorescent protein (fp)-tagged versions of EDS1, PAD4 and SAG101.

In the third section **(3.3)** I have tested the involvement of SAG101 in plant innate immunity. Experiments using virulent and avirulent isolates of the oomycete pathogen *P. parasitica* and the bacterial pathogen *P. syringae* pv. *tomato* were performed to characterise the genetic and functional requirements of SAG101 and combined SAG101 and PAD4 activities in plant disease resistance signalling.

3.1 EDS1, PAD4 and SAG101 expression in different plant tissues

Plants are surrounded by large numbers of potential pathogens with distinct infection habits. Soil born bacteria, particular insects and phytopathogenic nematodes feed from root tissues or try to gain entrance into their host plants via the roots whereas fungal and oomycete spores are often propagated by the wind and infect aerial parts of the plant (e.g. downy mildews, powdery mildews and rust fungi). *EDS1* and *PAD4* are known to be expressed in healthy and pathogen challenged juvenile and mature leaves (Feys *et al.*, 2001) where they fulfil functions as defence regulators in resistance to oomycete, fungal and bacterial pathogens. *SAG101* transcription was reported to be strongly increased in senescent leaves (He and Gan, 2002). So far, nothing is known about the presence of EDS1, PAD4 and SAG101 proteins in various plant tissues apart from leaves. I therefore wanted to establish the abundance of these three proteins in the different plant tissues.

3.1.1 Immunoblot analysis of EDS1, PAD4 and SAG101 protein abundance

Immunoblot analyses with total protein extracts of healthy (pathogen-unchallenged) *Arabidopsis* tissues were performed. For protein detection, the stable transgenic *Arabidopsis* line LM41-2, expressing 5x c-Myc N-terminal tagged PAD4 under control of the native L*er* *PAD4* promoter in Ws *pad4-5* background (Feys *et al.*, 2001) was chosen and is denoted Myc-PAD4 throughout this work. This line complements the *pad4-5* mutant phenotype and was utilised due to the lack of a workable PAD4 antibody. Figure 3.1 shows the expression pattern of EDS1 (A) and Myc-PAD4 (B) in flowerbuds, cauline leaves, stems, young rosette leaves, senescent rosette leaves and roots.

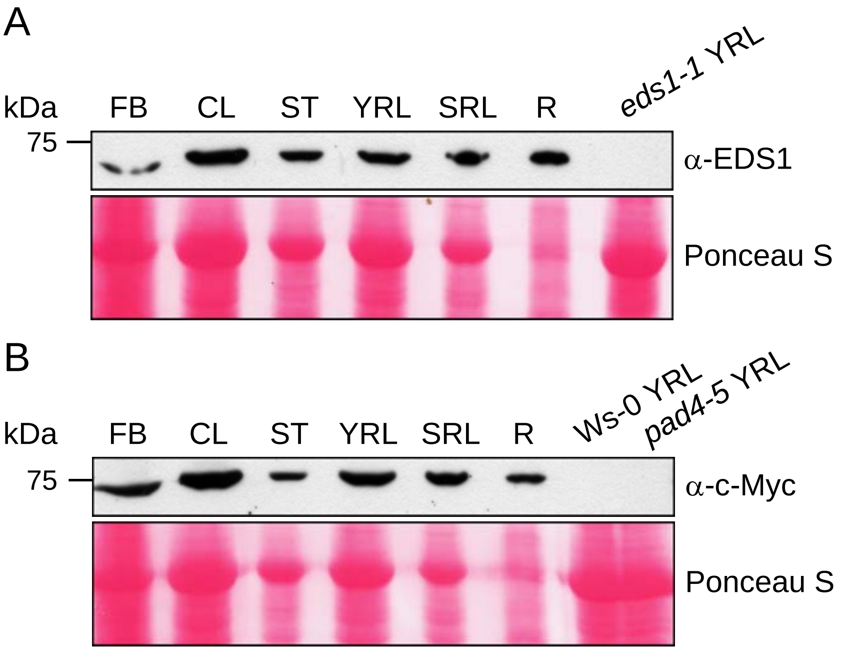

Fig. 3.1. Immunoblot detection of EDS1 and c-Myc tagged PAD4 in different tissues of *Arabidopsis* Myc-PAD4. Total protein extracts of different tissues from the stable transgenic plant line LM41-2, expressing 5x c-Myc tagged PAD4 under control of the native L*er* *PAD4* promoter were separated on a 10 % SDS polyacrylamide gel. Separated proteins were transferred to nitrocellulose membrane. **(A)** EDS1 proteins were detected by using a rabbit polyclonal α-EDS1 antibody, **(B)** Myc-PAD4 proteins by using a mouse monoclonal α-c-Myc antibody. Negative control for (A) was an *eds1-1* null mutant and Ws-0 and a *pad4-5* null mutant for (B). Loading of the gels was standardised by using the same amount of tissue fresh weight for protein extractions and monitored by Ponceau S staining of the membrane. Molecular weight markers in kDa is shown on the left. **FB:** flowerbuds; **CL:** cauline leaves; **ST:** stem; **YRL:** young rosette leaves; **SRL:** senescent rosette leaves; **R:** roots.

Due to the vast differences in Rubisco content in the different tissues, loading of the SDS-PAGE gels was not standardised by loading the same protein amount but by using the same amount of fresh weight of the different tissues for total protein extractions. The immunoblot analysis (Figure 3.1) showed that EDS1 and Myc-PAD4 are present in all the tested plant tissues of the Myc-PAD4 line. No EDS1 protein was detectable in young rosette leaves of *eds1-1* mutant plants (A) and no Myc-PAD4 protein was detectable in either Ws-0 wild-type plants or in *pad4-5* mutant plants. In three independent experiments, consistently highest EDS1 and PAD4 protein levels were obtained in cauline leaves, young rosette leaves and roots, whereas lowest protein amounts were detectable in flowerbuds and stems. However, J. Bautor found under her experimental conditions that EDS1, PAD4 and SAG101 protein levels were increased in senescent leaves when compared to juvenile or mature leaves. Immunoblots shown in this figure were chosen to clearly demonstrate the ubiquitous presence of EDS1 and PAD4 in the analysed tissues. Attempts to monitor SAG101 protein levels in the same total protein extracts of unchallenged tissues, using a rabbit polyclonal SAG101 antibody, failed under the experimental conditions, although it is known that SAG101 is present in mature leaves (Feys *et al.*, submitted). It was only feasible to detect SAG101 protein in subcellular fractions (see 3.2.1) or after pathogen infection where protein levels were elevated (see 3.3.1). However, *SAG101* transcripts were clearly detectable via RT-PCR analysis in all of the tested tissues (data not shown), demonstrating the existence of *SAG101* mRNA throughout these tissues and not only upon initiation of leave senescence as indicated by He and Gan (2002), although J. Bautor could show that SAG101 protein levels increase incrementally in juvenile, mature and senescent rosette leaves (unpublished data). The presence of *SAG101* transcripts in all of the analysed tissues and its increased expression in senescent leaves was strengthened by microarray data presented under 3.1.2.

3.1.2 Gene expression analysis of *EDS1*, *PAD4* and *SAG101*

In addition to the protein expression data for EDS1 and PAD4 (see 3.1.1), the publically available *Arabidopsis* microarray database GENEVESTIGATOR (Zimmermann *et al.*, 2004) was accessed to retrieve expression patterns of *EDS1*, *PAD4* and *SAG101* in distinct tissues. Expression data were compiled and are presented in Figure 3.2. Due to two closely linked *EDS1* copies, *EDS1A* (At3g48090) and *EDS1B* (At3g48080), present as tandem repeat on the lower arm of chromosome 3 in accession Columbia-0, expression levels for both copies of *EDS1* are presented.

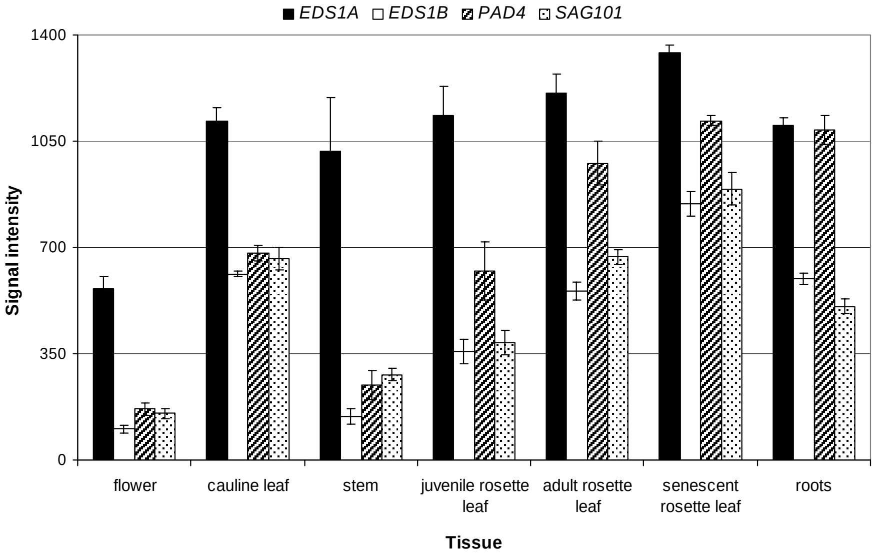

Fig. 3.2. Tissue specific gene expression levels of *EDS1A*, *EDS1B*, *PAD4* and *SAG101*. Gene expression levels for *EDS1A*, *EDS1B*, *PAD4* and *SAG101* were retrieved from the GENEVESTIGATOR database (www.genevestigator.ethz.ch) for the indicated tissues.

The microarray data support the finding that *SAG101* is expressed throughout all tissues tested. Furthermore, results obtained by immunoblot analysis for EDS1 and PAD4 described in 3.1.1 correlate with the gene expression data. Lowest expression of *EDS1* and *PAD4* was observed in pooled floral tissues and *PAD4* was also expressed at low levels in stems. A general trend was an increase in transcript abundance of both copies of *EDS1*, *PAD4* and *SAG101* from juvenile rosette leaves to adult rosette leaves and senescent rosette leaves which would be consistent with results of J. Bautor who found incrementally increased protein levels of EDS1, PAD4 and SAG101 in juvenile, mature and senescent rosette leaves. However, the here presented protein data point towards a slightly stronger abundance of EDS1 and PAD4 in young rosette leaves in comparison to senescent leaves.

Generally, *EDS1A* is expressed at higher levels than *PAD4* or *SAG101*, whereas *EDS1B* expression was lower. This might point to a possible drawback of the microarray data in comparing *EDS1A* and *EDS1B* expression levels. *EDS1A* shows higher homology than *EDS1B* to the *EDS1* sequences of for example L*er* and Ws-0. Since data coming from microarray experiments performed with other ecotypes than Col-0 were integrated into the data sets, hybridisations of these *EDS1* sequences with *EDS1A* will be favoured resulting in a stronger microarray signal of *EDS1A* compared to *EDS1B*. To take this into account, *EDS1A* gene expression data should mainly be considered when comparing *EDS1*, *PAD4* and

SAG101 levels. High expression of *EDS1A* and *PAD4* in roots correlated with high protein levels of these two proteins in four independent immunoblot experiments. The microarray data presented for *EDS1A* were next compared to the transcriptional activity of the *EDS1* promoter (P_{EDS1}) in different plant tissues by using P_{EDS1}*::GUS* stable transgenic *Arabidopsis* lines.

3.1.3 Transcriptional activity of the *EDS1* promoter in different plant tissues using P_{EDS1}*::GUS* stable transgenic plants

To monitor transcriptional activity of the native *EDS1* promoter (P_{EDS1}) in different tissues, stable transgenic *Arabidopsis* lines containing the L*er EDS1* promoter fused to the *E. coli uidA* gene were utilised. These lines were generated by G. Cook at the Sainsbury Laboratory in Norwich in Ws-0 and Col-0 accession. Four independent lines, two in accession Ws-0 and two in Col-0 were grown on soil under short day conditions (see 2.2.1) to analyse *EDS1* promoter activity through GUS expression in pathogen unchallenged tissues. Whole plants or different tissues were collected at different developmental stages of the plants, directly infiltrated with GUS staining solution and incubated overnight at 37° C. Plants were stained after 14 d and 28 d of growth. Flowers, cauline leaves, stems, young rosette leaves, senescent rosette leaves and roots were collected from 8-week-old plants. Figure 3.3 shows the line G573C in accession Ws-0 as a representative of the four different lines tested, which all displayed consistent GUS staining patterns. GUS activity could be seen throughout all tissues although stems displayed only weak and diffuse staining. This was the only contrast seen when comparing the GUS data with the gene expression microarray data presented in Figure 3.2 and might be due to the fact that the lignified stems are difficult to infiltrate with GUS staining solution and thus no substrate is accessible for the enzymatic reaction. This is supported by the fact that elevated GUS activity was detectable in stems segments where they had been cut for staining and unlikely to be a wound induction as stem segments were infiltrated with GUS staining solution directly after cutting. Moreover staining of P_{EDS1}*::GUS* leaves 24 h after wound-injury did not result in *GUS* induction which is typically seen for wound-responsive promoters or promoter elements (data not shown). Strong β-glucuronidase activity was detectable in roots, especially in root hairs and lateral root initials, young and senescent rosette leaves and cauline leaves. Leaves and roots of 2- and 4-week old seedlings also displayed β-glucuronidase activity. Stems of 2-week-old seedlings, stem segments and flowers showed GUS activity which was overall lower compared to the other tissues. Two-week-old seedlings also showed GUS staining in the transition zone between roots and stem. Staining in flowers was locally restricted to stigmata. Developing siliques exhibited GUS staining at their tips as well as at their base. The β-glucuronidase activity staining data of the P_{EDS1}::*GUS* line in general confirmed the immunoblot data for EDS1 presented under 3.1.1 as well as the *EDS1* gene expression data described in 3.1.2.

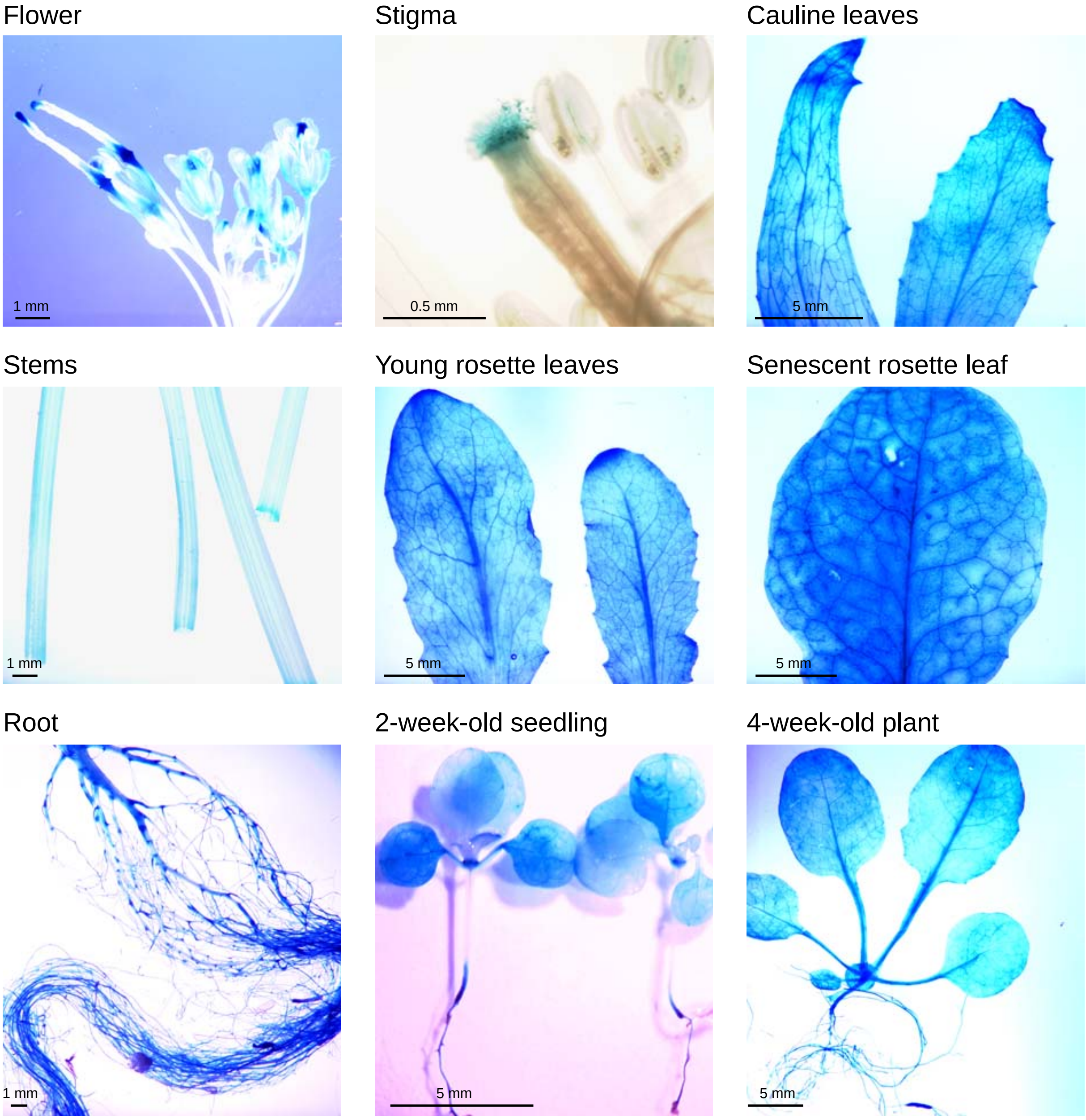
Flower
Stigma
Cauline leaves
Stems
Young rosette leaves
Senescent rosette leaf
Root
2-week-old seedling
4-week-old plant

Fig. 3.3 GUS stained tissues and seedlings of the Ws-0 stable transgenic line G573C expressing the *uidA* gene under control of the native L*er* *EDS1* promoter. Plants were grown on soil under short day conditions and not challenged with pathogens. Different tissues were collected from 8-week-old plants, vacuum-infiltrated with GUS staining solution and incubated over night at 37° C. Whole plants were stained at the indicated time points. Tissues were cleared with 70 % Ethanol to visualise β-glucuronidase activity. Pictures are representative of two independent experiments using 4 different transgenic lines, both in Ws-0 and Col-0 ecotype backgrounds. Sizes of scale bars are indicated in the pictures.

Previous analyses have shown that *EDS1* expression is induced upon pathogen challenge (Falk *et al.*, 1999; Feys *et al.*, 2001) and moreover, this study demonstrated that EDS1 protein levels increased upon inoculation with virulent *P. parasitica* (Figure 3.16). However, infection of 2-week-old P_{EDS1}*::GUS* lines with virulent and avirulent *P. parasitica* isolated did not result in obviously enhanced GUS activity in cells adjacent to HR lesions in the incompatible interactions or in cells surrounding growing pathogen mycelium in compatible interactions. This may be due to the already high P_{EDS1}-driven *GUS* expression in unchallenged leaves.

3.1.4 Summary of EDS1, PAD4 and SAG101 expression patterns

The immunoblot, microarray and P_{EDS1}*::GUS* data presented in 3.1.1 – 3.1.3 demonstrate the presence of EDS1 in all tissues tested. The immunoblot data for Myc-PAD4 also revealed that Myc-PAD4 is present in total protein extracts of the various tissues (see 3.1.1) but generally expression of *PAD4* seems to be lower in comparison to *EDS1* (see 3.1.2). Although no protein data of SAG101 were obtained, microarray data strongly suggest the presence of SAG101 in the different tissues. The failure to detect SAG101 in total extracts of the diverse tissues was most likely due to the sensitivity of the antibody detection. B. Feys was able to monitor SAG101 protein in soluble extracts of unchallenged, mature leaves (Feys *et al.*, submitted). Additionally, under the experimental conditions it was possible to detect SAG101 in a subcellular fraction derived from unchallenged leaves in which the SAG101 protein was enriched (see 3.2.1). The affinity of the SAG101 antibody against its antigen appears to be also rather weak. Furthermore, expression of SAG101 in unchallenged leaf tissues seems to be low. SAG101 became detectable in pathogen challenged total leave extracts, pointing towards a strong pathogen inducibility of *SAG101* expression (see below under 3.3.1). The failure to detect increased P_{EDS1}-driven *GUS* expression upon pathogen challenge is likely due to already high P_{EDS1}-driven GUS expression in unchallenged leaves.

3.2 Subcellular localisation of EDS1, PAD4 and SAG101 and analysis of their *in vivo* interactions via fluorescence resonance energy transfer (FRET)

Nothing was known about the subcellular localisations of EDS1, PAD4 and SAG101 and in which cellular compartment(s) these proteins fulfil their respective functions. EDS1 and PAD4 proteins are predicted to be soluble from their amino acid sequences. The proteins have no obvious signal peptide or transmembrane domains. However, EDS1 possesses two possible bipartite nuclear localisation signals (NLS) (Falk *et al.*, 1999) (double lysine (K) motive at amino acid positions 366 and 440). In addition, EDS1 contains a putative coiled-coil domain extending from amino acids 359 – 383 that is not found in either SAG101 or PAD4. Figure 3.4 shows a sequence alignment of the predicted L*er* EDS1, PAD4 and SAG101 proteins. Obvious nuclear localisation signals in PAD4 are not present. The N-terminal halves of EDS1 and PAD4 relate these proteins to lipases/esterases with the typical GXSXG motive, containing a catalytic serine (S). Together with an aspartic acid (D) and a histidine (H) these three amino acids constitute a catalytic triad in lipases. Although SAG101 shares sequence homologies with lipases the putative catalytic serine and aspartic acid typical for α/β-fold hydrolase catalytic triads are missing. The predicted SAG101 sequence contains a putative signal peptide cleavage site at amino acid position 28 and a monopartite nuclear localisation signal (4 lysine (K) motif, amino acids 48 – 51). Furthermore, EDS1 and PAD4 each possess a putative nuclear export sequence (NES), indicated as EDS1-NES and PAD4-NES in Figure 3.4, respectively. Amino acids relevant for the nuclear export signal are marked above the corresponding sequence. These amino acids fall into a leucine rich region, which is framed by vertical black bars. Nuclear export signals were found using the NetNES 1.1 prediction server, available under www.cbs.dtu.dk (la Cour *et al.*, 2004). No obvious nuclear export signal was found in the protein sequence of SAG101.

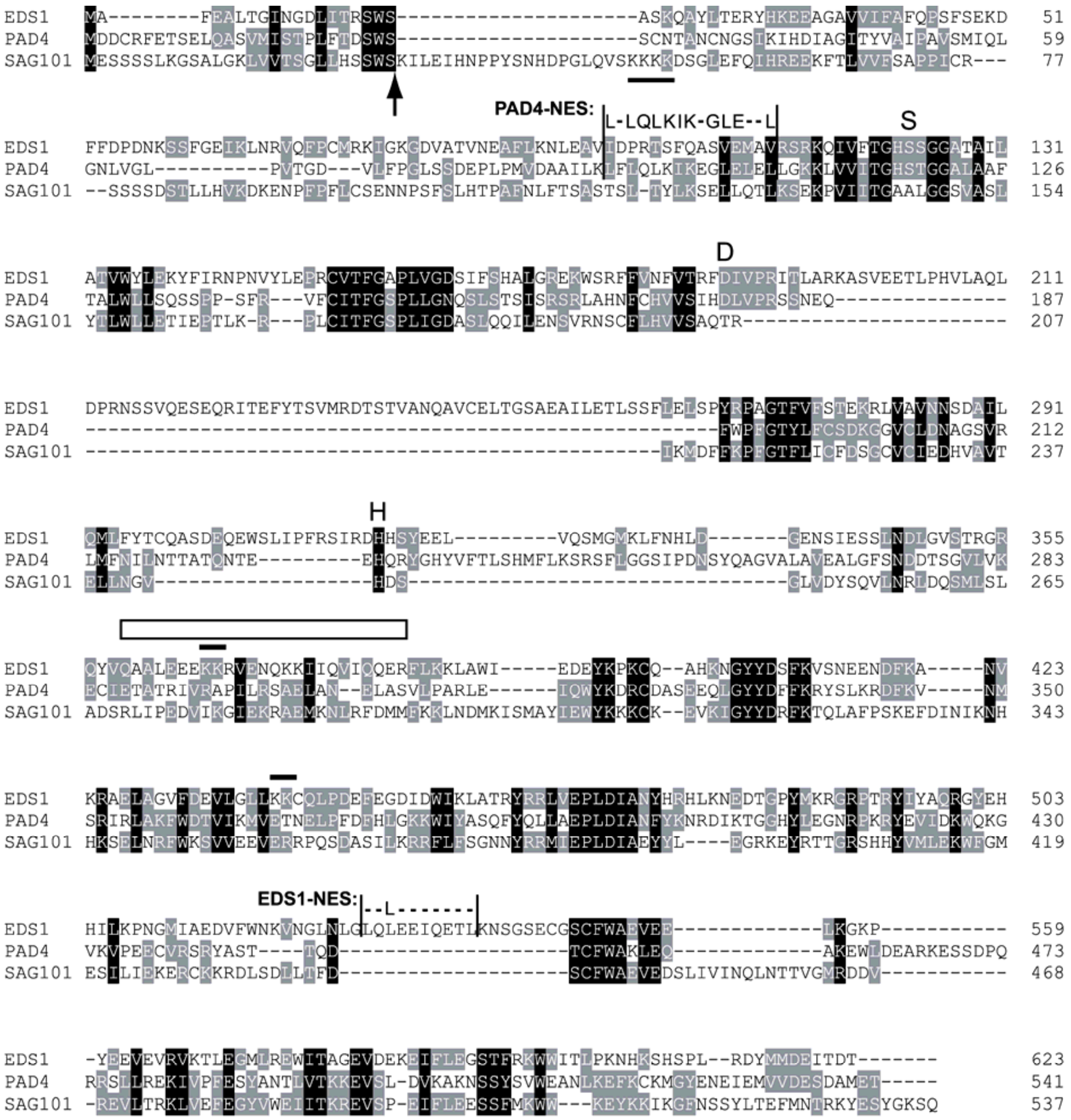

Fig. 3.4. Sequence alignment of L*er* EDS1, PAD4 and SAG101 proteins. Structural motifs within the sequences are indicated as followed: The putative catalytic triad in EDS1 and PAD4 consisting of a serine (S), an aspartic acid (D) and a histidine (H) are highlighted above the sequences by the corresponding amino acid letter. The putative bipartite nuclear localisation signal in EDS1 is highlighted with black bars above the EDS1 sequence, the possible nuclear localisation signal in SAG101 is indicated by a black bar below the SAG101 sequence. An arrow below the SAG101 sequence displays the putative signal peptide cleavage site. The putative coiled-coil domain found in EDS1 is indicated by an open rectangle above the sequence. Nuclear export signals (NES) found in the sequences of EDS1 and PAD4 are accentuated as EDS1-NES and PAD4-NES, respectively, with the relevant amino acids displayed above the corresponding sequence. Relevant amino acids of the nuclear export signal lie in leucine rich region, which is marked by vertical black bars. The alignment was generated using GeneDoc software (Nicholas, K. B. and Nicholas H. B. jr. (1997): GeneDoc, a tool for editing and annotating multiple sequence alignments. Distributed by the author: www.psc.edu/biomed/genedoc).

In order to gain insights into the subcellular localisation of EDS1, PAD4 and SAG101 and to explore measuring of protein-protein interactions in living plant cells by fluorescence resonance energy transfer (FRET) analysis, Gateway® compatible destination vectors were generated (see 2.2.13.11), that allow expression of a protein of interest as a fusion protein with a C-terminal cyan fluorescent protein (CFP) or yellow fluorescent protein (YFP) tag, both under control of the respective native promoter or the double 35S promoter of cauliflower mosaic virus (P_{35SS}). These binary vectors can also be used to stably transform plants via *Agrobacterium*-mediated transformation and are suitable for protein localisation and FRET protein-protein interaction studies. Vector maps of the generated destination vectors are shown in Figure 3.5.

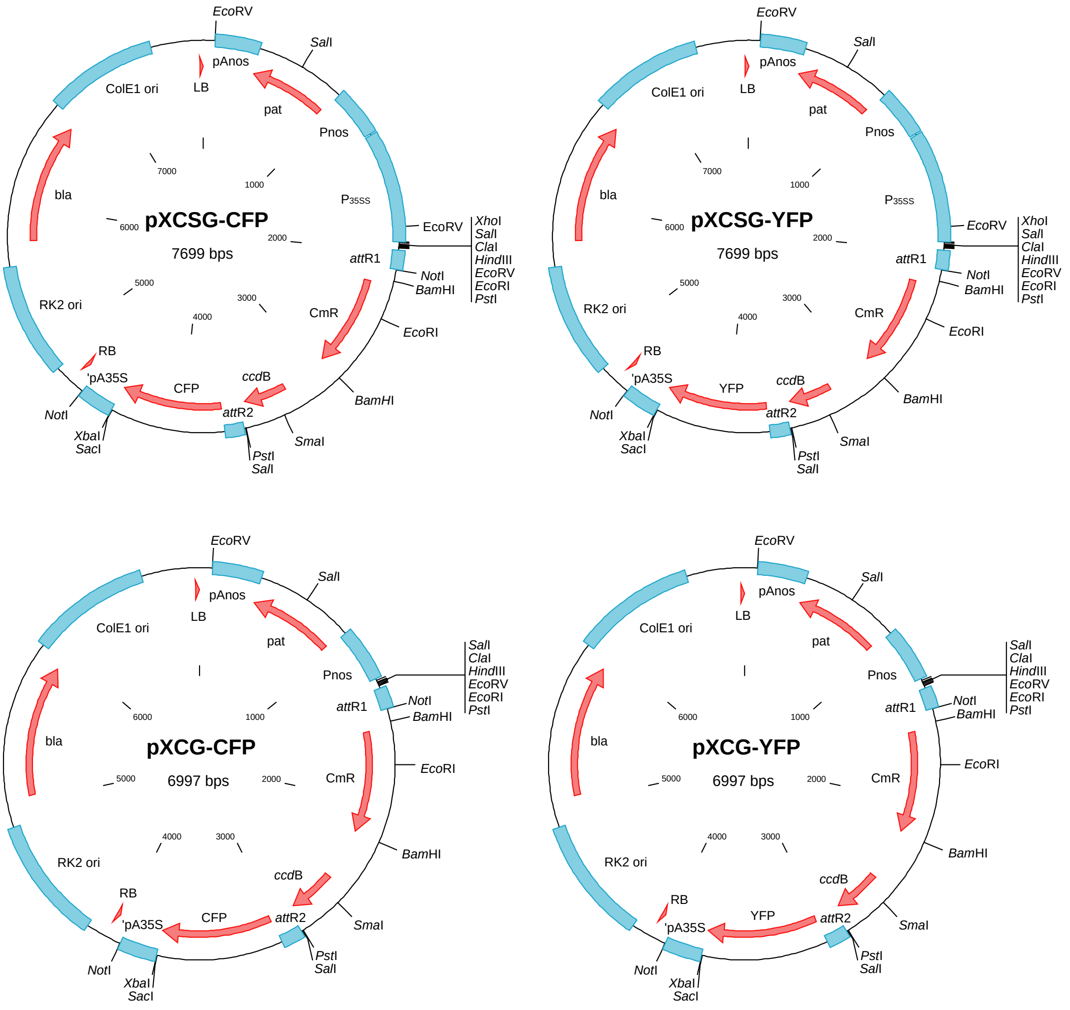
EcoRV
SalI
pAnos
LB
ColE1 ori
pat
Pnos
7000
1000
bla
P35SS
EcoRV
XhoI
SalI
ClaI
HindIII
EcoRV
EcoRI
PstI
6000
pXCSG-CFP
7699 bps
2000
attR1
NotI
BamHI
5000
RK2 ori
3000
4000
CmR
EcoRI
RB
'pA35S
CFP
ccdB
BamHI
attR2
NotI
SmaI
XbaI
SacI
PstI
SalI
EcoRV
SalI
pAnos
LB
ColE1 ori
pat
Pnos
7000
1000
bla
P35SS
EcoRV
XhoI
SalI
ClaI
HindIII
EcoRV
EcoRI
PstI
6000
pXCSG-YFP
7699 bps
2000
attR1
NotI
BamHI
5000
RK2 ori
3000
4000
CmR
EcoRI
RB
'pA35S
YFP
ccdB
BamHI
attR2
NotI
SmaI
XbaI
SacI
PstI
SalI
EcoRV
SalI
pAnos
LB
ColE1 ori
pat
Pnos
SalI
ClaI
HindIII
EcoRV
EcoRI
PstI
6000
1000
NotI
BamHI
attR1
bla
pXCG-CFP
5000
6997 bps
2000
CmR
EcoRI
4000
3000
RK2 ori
BamHI
ccdB
RB
'pA35S
CFP
attR2
SmaI
NotI
XbaI
SacI
PstI
SalI
EcoRV
SalI
pAnos
LB
ColE1 ori
pat
Pnos
SalI
ClaI
HindIII
EcoRV
EcoRI
PstI
6000
1000
NotI
BamHI
attR1
bla
pXCG-YFP
5000
6997 bps
2000
CmR
EcoRI
4000
3000
RK2 ori
BamHI
ccdB
RB
'pA35S
YFP
attR2
SmaI
NotI
XbaI
SacI
PstI
SalI

Fig. 3.5. Plasmid maps of the generated Gateway®-compatible, binary destination vectors for protein localisation and FRET protein-protein interaction studies. Essential features and restriction sites are depicted in the maps. **pXCSG** vectors allow expression of C-terminal fluorescent protein tagged fusion-proteins under control of the double 35S promoter of cauliflower mosaic virus (**P_{35SS}**), whereas **pXCG** vectors allow expression under control of the respective native promoters. **(CFP)** cyan fluorescent protein; **(YFP)** yellow fluorescent protein; **(*att*R1)** attachment site R1; **(*att*R2)** attachment site R2; **(*ccd*B)** negative selection marker; **(LB)** left border; **(RB)** right border; **(pat)** phosphinothricin acetyltransferase gene conferring glufosinate-resistance; **(bla)** β-lactamase gene conferring ampicillin resistance; **(CmR)** chloramphenicol resistance.

3.2.1 Subcellular localisation of EDS1, PAD4 and SAG101

For subcellular localisation studies the fluorescent proteins CFP and YFP were fused to the C-terminus of EDS1, PAD4 and SAG101. For this purpose the vectors shown in Figure 3.5 were utilised. Genomic L*er EDS1* sequence or L*er* cDNAs for *PAD4* and *SAG101* were cloned into the Gateway® entry vector pENTR/D-TOPO (Invitrogen). LR reactions (see 2.2.13.12) with the generated destination vectors resulted in the desired constructs that were used in single cell transfection assays via particle bombardment (see 2.2.14.2). Gold particles, coated with the desired vector constructs were ballistically bombarded into epidermal cells of detached *Arabidopsis eds1-1/pad4-5* leaves. Fusion proteins were expressed under control of the double 35S promoter (P_{35SS}). Expression of the full length fusion proteins was verified by transient expression of the constructs in *N. benthamiana* leaves via *Agrobacterium*-mediated transient transformation and subsequent immunoblot analysis using a mouse-monoclonal GFP antibody, recognising both CFP and YFP. No free CFP or YFP was detectable in the immunoblots (data not shown). For co-expression of two different proteins, equimolar vector amounts were coated onto gold particles. Detailed analysis of intracellular fluorescence was performed by confocal laser scanning microscopy (CLSM) using a Zeiss LSM 510 META microscopy system based on an Axiovert inverted microscope equipped with an Argon ion laser as an excitation source (for details see 2.2.15). Figure 3.6 (A) shows an epidermal cell co-expressing EDS1-YFP and PAD4-CFP. EDS1 and PAD4 co-localised both in the cytosol and inside the nucleus. The same localisation of EDS1 and PAD4 was obtained when the two proteins were separately expressed in single epidermal cells, both under control of P_{35SS} or their native promoters (data not shown). Subcellular localisation of EDS1 was not affected by using a different vector backbone (pGreenII) expressing EDS1 with an N-terminal GFP tag under control of its native promoter and under control of P_{35SS} (data not shown). Fluorescent protein (fp)-tagged EDS1 was still able to enter the nucleus after bombardment of *pad4/sag101* double mutant plants, indicating that EDS1 does not depend on SAG101 or PAD4 to enter the nucleus. In contrast to the localisation of EDS1 and PAD4, it was found that SAG101 is exclusively localised inside the nucleus as shown by co-transfection of EDS1 and SAG101 in Figure 3.6 (B). The same localisation for SAG101 was obtained when expressed alone (data nor shown). Consistently if EDS1 was co-expressed with SAG101, a significantly stronger signal for EDS1 fluorescence was observed in the nucleus and only a weak signal was still present in the cytosol than when bombarded alone (data not shown) or in combination with PAD4 (see comparison between 3.6 A and B). The signal for EDS1-YFP

(Figure 3.6 B) in the cytosol was only detectable after increasing the YFP channel signal intensity of the laser scanning microscope. Localisations of EDS1, PAD4 and SAG101 are consistent with features found in the sequences of these three proteins (Figure 3.4). Both EDS1 and SAG101 possess nuclear localisation signals, whereas a nuclear export signal found in EDS1 and PAD4 is absent in SAG101.

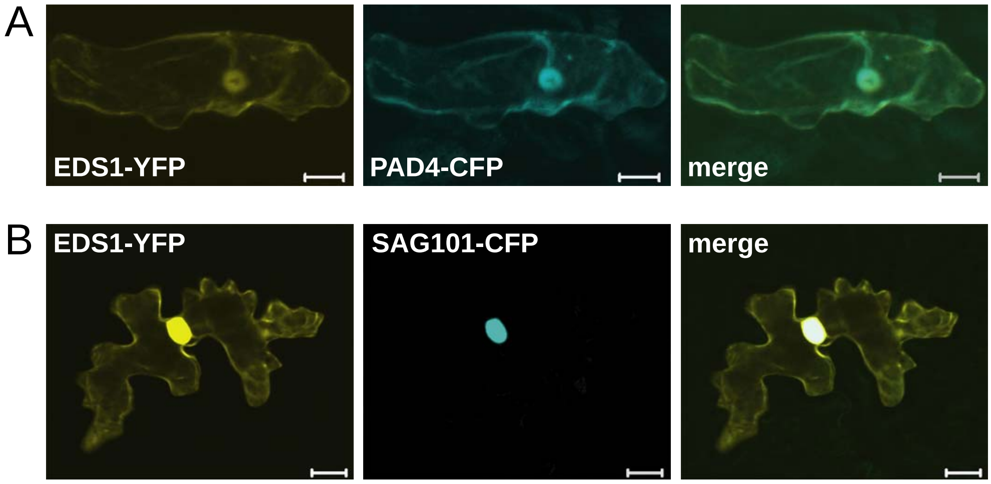

Fig. 3.6. Subcellular localisation of EDS1, PAD4 and SAG101 in transfected *Arabidopsis* epidermal cells. *Arabidopsis* epidermal cells were co-transfected in a single cell bombardment assay with **(A)** fluorescently tagged EDS1 and PAD4 or **(B)** EDS1 and SAG101 and analysed by confocal laser scanning microscopy. Fusion proteins were expressed under control of the double 35S promoter. Images were taken 24 h after transfection and show 3D reconstructions from individual image stacks. Scale bar: 20 µm

To exclude the possibility that transiently overexpressed proteins were mislocalised and to confirm that the observed localisations were not due to bombardment artefacts, nuclear extracts from Col-0 or the Myc-PAD4 transgenic line were generated and the presence of native EDS1 and SAG101 or Myc-PAD4 in those extracts was measured by immunoblot detection. Nuclear extracts were generated as described under 2.2.12.2 from 4-week-old unchallenged plants. Nuclear fractions (N) and supernatant fractions (S) from which nuclei were removed, were loaded onto SDS-PAGE gels and blotted onto nitrocellulose membranes. As shown in Figure 3.7 A and B, EDS1 and Myc-PAD4 were found in nuclei as well as in supernatant fractions depleted of nuclei, whereas SAG101 was only present in nuclei (Figure 3.7 C). No signals were obtained for EDS1, PAD4 and SAG101 in the corresponding mutant controls *eds1-1* (A), *pad4-5* (B) and *sag101-1* (C). Immunodetection of the marker proteins Histone H3 as a nuclear protein, and Hsc70 as a cytosolic protein served as internal controls to validate the results obtained for EDS1, PAD4 and SAG101 subcellular localisation. No contamination with nuclear extracts was detectable in the supernatant fraction and minimal contamination of cytosolic proteins was present in the nuclear fraction. In addition, Ponceau S staining of the membranes revealed no obvious Rubisco contamination in nuclear extracts.

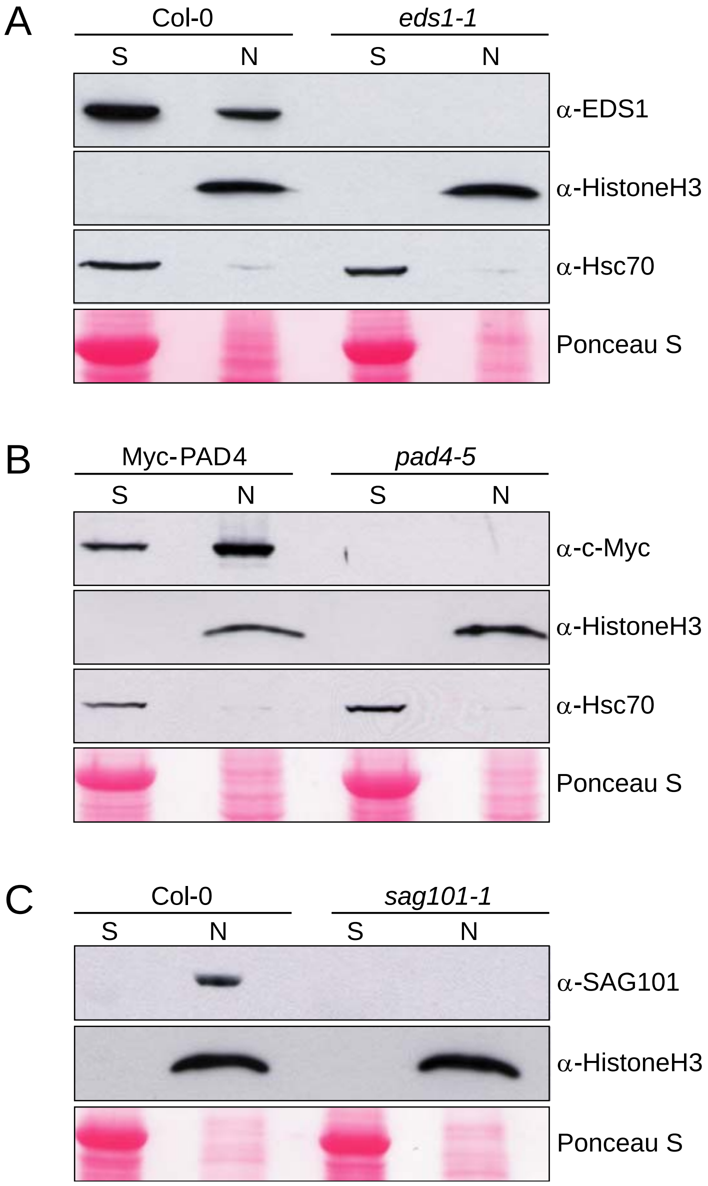
A
Col-0
eds1-1
S N S N
α-EDS1
α-HistoneH3
α-Hsc70
Ponceau S
B
Myc-PAD4
pad4-5
S N S N
α-c-Myc
α-HistoneH3
α-Hsc70
Ponceau S
C
Col-0
sag101-1
S N S N
α-SAG101
α-HistoneH3
Ponceau S

Fig. 3.7. Immunoblot analysis of EDS1, Myc-PAD4 and SAG101 in subcellular fractions of unchallenged leaf tissues. **N**: nuclear protein extracts and **S**: total protein supernatant fractions depleted of nuclei were generated from 4-week-old unchallenged leaves of the indicated *Arabidopsis* lines. Proteins were separated on 10 % SDS polyacrylamide gels and blotted onto nitrocellulose membranes. Membranes were probed with **(A)** α-EDS1, **(B)** α-c-Myc or **(C)** α-SAG101 antibodies. After detection, membranes were stripped and re-probed with an antibody against cytosolic Hsc70, which served as a cytosolic marker and an antibody against HistoneH3, which was used as a nuclear marker. Protein amounts in the different fractions were monitored by Ponceau S staining of the membrane. For details see materials and methods under 2.2.12.2.

I concluded from these results that the intracellular localisations deduced from transient bombardment of fp-tagged EDS1, PAD4 and SAG101 likely reflect their physiological localisations in the cell.

The functionality of the fp-tagged EDS1 fusion protein constructs was further assessed by generation of stable transgenic plants. Thus, *eds1-1* mutant plants were stably transformed with the genomic L*er EDS1* sequence fused to *CFP* and *YFP* in the vector backbones described in Figure 3.5. Fusion proteins were expressed under control of P_{35SS} or under control of the native 1.4 kb region of the L*er EDS1* promoter (P_{EDS1}) (Feys *et al.*, 2001). Homozygous, single insertion lines were selected of which four are shown in Figure 3.8. The stably expressed, fp-tagged EDS1 lines also displayed cytoplasmic and nuclear localisation. Panel (A) displays whole leaves viewed under a fluorescence microscope. Strong fluorescence signals were obtained from lines expressing fusion proteins under control of P_{35SS} whereas fluorescence for the endogenous promoter driven lines was weak although signals for EDS1 in the cytosol and nucleus were detected. No CFP or YFP fluorescence signal was obtained for non-transgenic Ws-0 wild-type control plants (data not shown). In order to increase the signal intensity for the *EDS1* promoter driven lines, protoplasts were generated as protoplasts no longer have fluorescence quenching effects of the cell wall. However, detectable fluorescence in the protoplasts derived from leaves of lines expressing the fusion proteins by the *EDS1* promoter was still weak in contrast to protoplasts derived from P_{35SS} driven lines (Figure 3.8 B). Chloroplast appeared as dark, negative stains in the protoplasts indicating that EDS1 fluorescence was truly cytosolic. One further aspect in the generation of protoplasts lies in the possibility to simultaneously trigger responses in a large number of cells by simply adding chemical compounds to the medium. Experiments are in progress to resolve a possible passaging of EDS1 and/or PAD4 between cytosol and nucleus by addition of the nuclear export inhibitor Leptomycin B to the protoplast medium, since nuclear export signals were found in both EDS1 and PAD4 (Figure 3.4 and 4.2.1).

To rule out that the signal obtained for EDS1 localisation inside the nuclei was due to diffusion of free CFP or YFP (potentially cleaved from the fusion protein), the stable transgenic lines were further examined by immunoblot analysis, using a mouse monoclonal anti-GFP antibody. No free CFP or YFP was present in these lines (data not shown). Importantly, the generated lines complemented the *eds1-1* mutant phenotype in response to infection with the avirulent *P. parasitica* isolate Noco2, by exhibiting a clear hypersensitive response (data not shown).

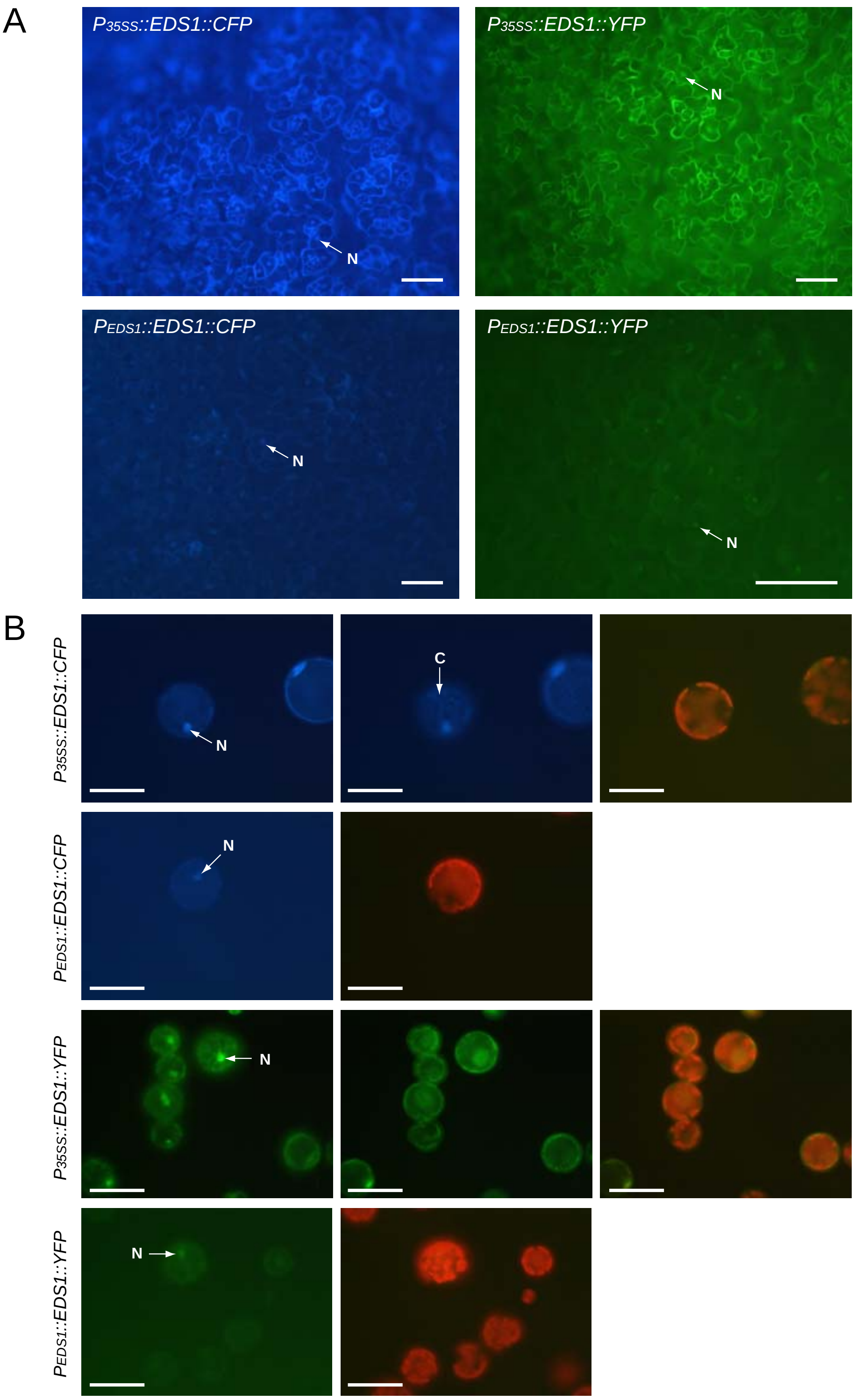
A
P35SS::EDS1::CFP
N
P35SS::EDS1::YFP
N
PEDS1::EDS1::CFP
N
PEDS1::EDS1::YFP
N
B
P35SS::EDS1::CFP
N
C
PEDS1::EDS1::CFP
N
P35SS::EDS1::YFP
N
PEDS1::EDS1::YFP
N

Fig. 3.8. Leaves and protoplasts of stable transgenic plants expressing fluorescent protein-tagged EDS1 under control of the double 35S or native L*er* EDS1 promoter. Stable transgenic *Arabidopsis* lines were generated by *Agrobacterium*-mediated transformation of *eds1-1* mutant plants. The genomic sequence of L*er* *EDS1* was fused in frame via its C-terminus to the fluorescent proteins CFP or YFP. For construct detail see Materials and Methods 2.2.13.11. **(A)** Whole leaves and **(B)** protoplasts derived from the same leaves were analysed using a Zeiss Axiovert 135 TV fluorescence microscope connected to a Nikon DXM1200 Digital Camera. N: nuclei; C: chloroplasts; Protoplasts were generated from 2-week-old leaf material. Constructs used for transformation are indicated (A) in the pictures or (B) on the left. No CFP or YFP fluorescence was visible in Ws-0 wild-type control plants (data not shown). Scale bar: 50 µm

In parallel, stable transgenic lines with fluorescent protein C-terminal tagged PAD4 were generated by N. Medina-Escobar. Overexpression as well as native promoter (*P_{PAD4}*) expression lines were shown to complement the *pad4-5* mutant phenotype into which the constructs were transformed upon Noco2 infection (data not shown). Generation of stable transgenic fp-tagged SAG101 lines is in progress. The aim of generating stable transgenic lines expressing fp-tagged EDS1, PAD4 and SAG101 is to gain insights to possible subcellular localisation dynamics upon triggering of the resistance response via pathogens or another stimulus like redox stress. Also, the different lines can be crossed to monitor possible changes in protein-protein interactions between these proteins via FRET analysis in pathogen challenged tissues.

Further subcellular fractionation experiments were performed to test for the existence of other possible EDS1 and PAD4 intracellular pools, for example inside or attached to membranes. Microsomal membrane (M) fractions were generated from 4-week-old unchallenged leaves of the Myc-PAD4 transgenic line LM41-2 and control lines as shown in Figure 3.9. Proteins were separated on 10 % SDS-PAGE gels and analysed by immunoblotting. Development of the blots revealed that both EDS1 (Figure 3.9 A) and Myc-PAD4 (Figure 3.9 B) proteins were detectable in crude (C) as well as in soluble (S) fractions. EDS1 protein was undetectable in microsomal membrane (M) fractions, whereas a feint band for Myc-PAD4 was detectable in the membrane fraction of Myc-PAD4 (Figure 3.9 B). The presence of the feint Myc-PAD4 band in the microsomal membrane fraction was likely to be a contamination by soluble proteins. The cellular fractionation method used for generation of the fractions (see 2.2.12.3) only used one pellet-washing step which might have been insufficient to remove all soluble protein from the microsomal membrane fraction. This finding was supported by the fact that a feint band also was obtained in the microsomal membrane fractions for the soluble marker protein Hsc70 (Figure 3.9).

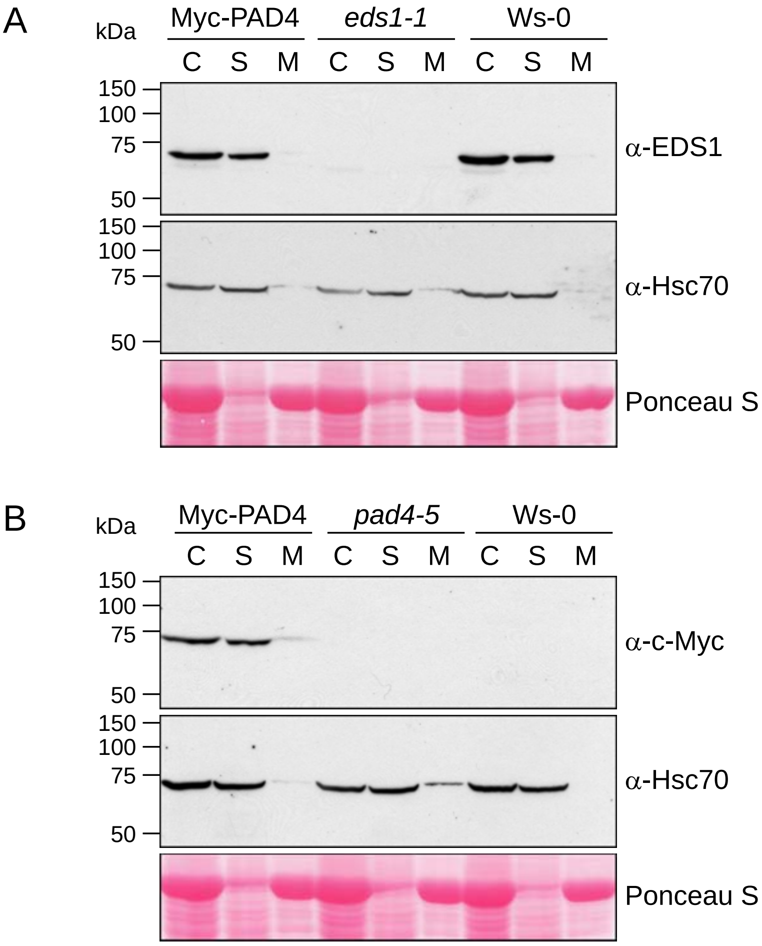

Fig 3.9. Immunoblot analysis of EDS1 and Myc-PAD4 in subcellular fractions of unchallenged leaf tissues. Crude (C), soluble (S) and microsomal membrane (M) fractions were generated from 4-week-old unchallenged leaf tissues of the indicated *Arabidopsis* lines. Proteins were separated on 10 % SDS polyacrylamide gels and blotted onto nitrocellulose membranes. Membranes were probed with **(A)** α-EDS1 or **(B)** α-c-Myc antibodies. An antibody against cytosolic Hsc70 was used as a marker to monitor contamination of soluble proteins in the microsomal membrane fractions. Molecular weight markers in kDa are shown on the left.

In summary, experiments to monitor subcellular localisation of EDS1, PAD4 and SAG101 using cell biology and biochemical approaches revealed that EDS1 and PAD4 are localised in the cytosol as well as inside the nucleus, whereas SAG101 is exclusively localised inside the nucleus. In addition, EDS1 and PAD4 were shown to be soluble proteins that are either not or only very low abundant in microsomal membrane fractions. The fact that EDS1 but not PAD4 fluorescence was consistently stronger inside the nucleus and weaker in the cytosol after co-bombardment with SAG101 than after bombardment of EDS1 with PAD4 or alone suggested that EDS1 may be preferentially held inside the nucleus by SAG101 through direct interaction. To further test this hypothesis Fluorescence resonance energy transfer (FRET) experiments were carried out to possibly monitor direct EDS1-SAG101 association in living plant cells.

3.2.2 EDS1 dimerises in the cytosol and interacts with SAG101 inside the nucleus

In a biochemical approach B. Feys found that SAG101 associates with EDS1 *in planta*. B. Feys affinity-purified HA (hemagglutinin)- and TAP (tandem affinity purification)-tagged EDS1 from soluble protein extracts of unchallenged leaf material of 5-week-old HA-EDS1 or TAP-EDS1 transgenic *Arabidopsis* lines, expressing the respective transgene under control of the native *EDS1* promoter. One EDS1 associated protein was identified by MALDI- and Q-TOF mass spectrometry and shown to be SAG101 (Feys *et al.*, submitted). Nevertheless, the nature of this association was not known. Co-expression studies of EDS1 and SAG101 in transiently transfected *Arabidopsis* epidermal cells, presented under 3.2.1, further suggested that SAG101 might directly interact with EDS1 inside the nucleus. In order to address whether the SAG101-EDS1 interaction is direct, fluorescence resonance energy transfer (FRET) experiments were accomplished.

FRET is a phenomenon whereby a fluorescent molecule, the donor (cyan fluorescent protein, CFP), transfers energy by a nonradiative mechanism to a neighbouring chromophore, the acceptor (yellow fluorescent protein, YFP) and occurs when proteins fused to donor and acceptor fluorescent dyes physically interact. The absorption spectrum of the acceptor chromophore must hereby overlap with the fluorescence emission spectrum of the donor. FRET is highly dependent on the proximity between the donor and acceptor and in general only occurs when the molecules are separated by less than 100 Å (Gadella *et al.*, 1999). FRET is manifested by a decrease in the fluorescence intensity of the donor fluorophore and increases the fluorescence of the acceptor fluorophore due to the transfer of energy from the donor towards the acceptor. FRET can be measured by quantifying an increase in donor fluorescence (CFP) after photobleaching the acceptor (YFP) (Karpova *et al.*, 2003). This method of acceptor photobleaching (APB) utilises the effect that energy transfer is reduced or eliminated when the acceptor is bleached, thereby resulting in an increase in donor fluorescence. Figure 3.10 illustrates the FRET principle for protein-protein interactions.

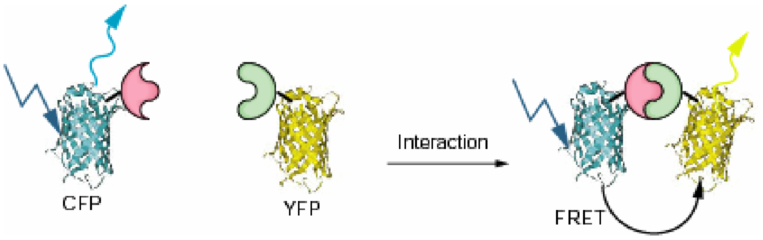

Fig. 3.10. The FRET principle for protein-protein interactions. Upon protein-protein interaction FRET is manifested by a decrease in the fluorescence intensity of the donor fluorophore (CFP) and will increase the fluorescence of the acceptor (YFP). Upon photobleaching the acceptor YFP, FRET is further manifested by an increase in donor (CFP) fluorescence. CFP, cyan fluorescent protein; YFP, yellow fluorescent protein; dark blue arrow indicates excitation; cyan and yellow arrows indicate fluorescence; non-CFP or YFP fusion proteins are represented in pink and green; The figure was taken from Gadella *et al.* (1999).

FRET-APB experiments to directly study the physical interaction between EDS1 and SAG101 were performed with the same constructs described under 3.2.1 for localisation studies (see also Figures 3.5 and 3.6). The fluorescent proteins CFP and YFP were fused to the C-terminus of L*er* EDS1 and SAG101. The CFP and YFP fusion proteins were used as donor-acceptor pairs in FRET-APB analysis. Fusion proteins for FRET studies were expressed under control of P_{35S} and transfected via particle bombardment into single epidermal cells of detached *Arabidopsis eds1-1/pad4-5* leaves (see 2.2.14.2). FRET-APB experiments were generally carried out 24 h after particle bombardment using a LSM 510 META microscopy system (Zeiss) equipped with an Argon ion laser. Cells were bleached in the acceptor YFP channel by scanning a region of interest (ROI) using 5 – 20 times 514 nm argon laser line at 100 % intensity. Before and after the acceptor bleaching, CFP intensity was measured for changes in donor fluorescence. In the case of EDS1 and SAG101 nuclei were bleached as the compartment where interaction could take place. Figure 3.11 A, shows a representative example for the FRET-APB analysis between EDS1-YFP and SAG101-CFP. On bleaching of the EDS1-YFP acceptor fluorophore there was a sharp and sudden increase in the fluorescence intensity of the donor fluorophore SAG101-CFP. This demonstrates a clear interaction between EDS1 and SAG101 inside the nucleus. Figure 3.11 B shows that no such increase in donor-fluorescence was obtained when FRET-APB was performed between free CFP and YFP inside the nucleus. Additionally, no FRET signals were derived when co-expressing EDS1-CFP with free YFP or EDS1-CFP with the nuclear localised transcription factor WRKY14-YFP (Figure 3.12). The same results for the EDS1-SAG101 interaction were obtained when fp-tags were swapped between EDS1 and SAG101

(Figure 3.12). Bleaching of SAG101-YFP in this case resulted in an increase of EDS1-CFP fluorescence.

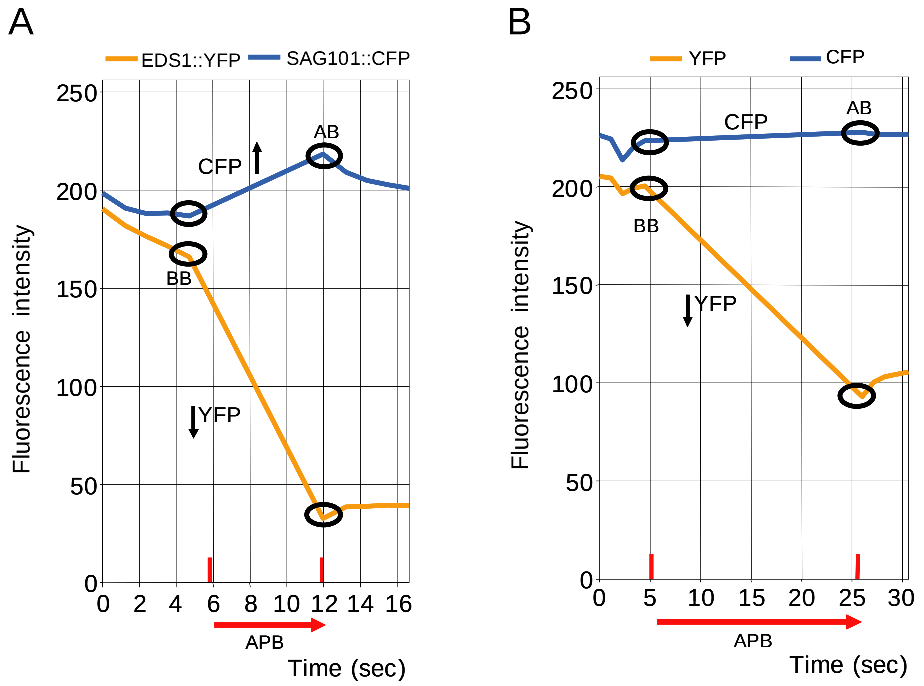

Fig. 3.11. FRET-APB analysis in nuclei of cells expressing EDS1-YFP and SAG101-CFP or free CFP and YFP. *Arabidopsis* epidermal cells were co-transfected via particle bombardment with **(A)** EDS1-YFP and SAG101-CFP or **(B)** free YFP and CFP. Proteins were expressed under control of the double 35S promoter and APB was carried out 24 h after transfection. Donor and acceptor fluorescence intensity was quantified at several time points before and after APB. A representative example for donor and acceptor fluorescence intensities of bleached nuclei is shown for each co-transfection. **(A)** Quantification of donor and acceptor fluorescence intensity before and after APB shows a substantial increase in donor (CFP) fluorescence, demonstrating physical interaction between EDS1 and SAG101 inside the nucleus. **(B)** No such an increase in donor fluorescence upon APB can be seen in control nuclei, co-expressing non-interacting free YFP and CFP. **APB:** acceptor photobleaching; **Black circles** show the start (**BB:** before bleach) and end (**AB:** after bleach) of the bleach cycle. Increase or decrease in fluorescence is indicated by black arrows. **Vertical red bars** and **red arrows** below the diagrams indicate the time window in which the acceptor YFP was bleached. For further details see Materials and Methods.

In order to get a complete impression of the physical interaction between EDS1 and SAG101, mean FRET efficiencies of 30 sample sites from independent cells were calculated as described in Materials and Methods under 2.2.16. For calculations of nuclear mean FRET efficiencies for the control donor-acceptor pairs EDS1-CFP/YFP, EDS1-CFP/WRKY14-YFP and CFP/YFP at least 15 independent sample sites were used. Mean FRET efficiencies of 7.76 ± 3.5 % were obtained for energy transfer between SAG101-YFP as an acceptor and EDS1-CFP as a donor (average ± standard deviation), as illustrated in Figure 3.12. Only low-level random FRET signals were recorded in the control FRET-APB experiments of the nuclear localised donor-acceptor pairs EDS1-CFP/YFP (-1.16 ± 4.07 %), EDS1-CFP/WRKY14-YFP (0.68 ± 3.86 %) and CFP/YFP (-0.91 ± 3.72 %). Representative pictures of pseudo-coloured nuclei for each indicated donor-acceptor pair below the bar chart in Figure 3.12, showing donor-fluorescence before and after bleach, further revealed, that only in the case of EDS1-CFP and SAG101-YFP an increase in donor fluorescence (red colour) could be seen.

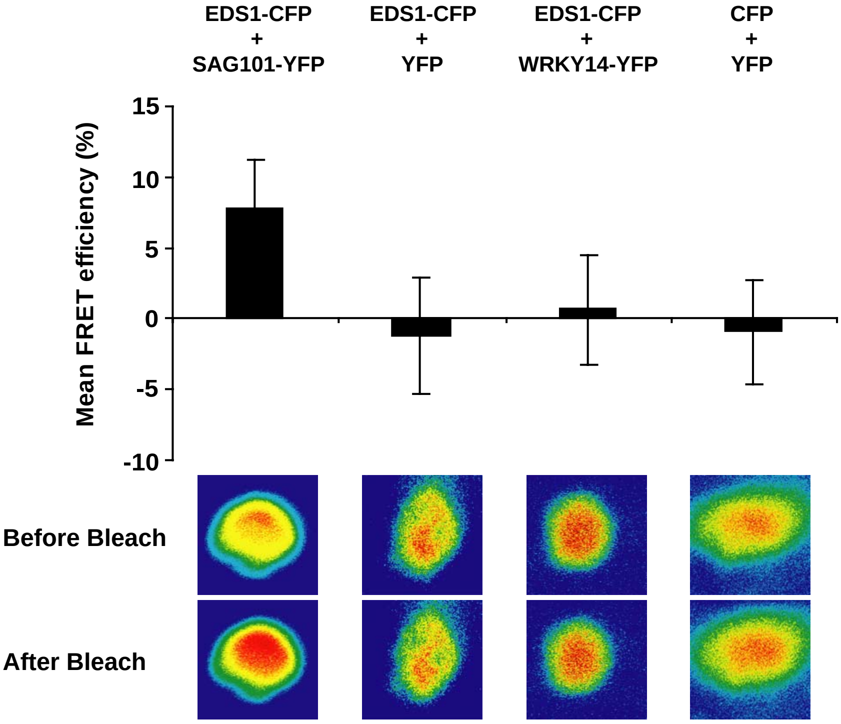

Fig. 3.12. FRET-APB analysis of the nuclear interaction between fluorescently tagged EDS1 and SAG101. *Arabidopsis* detached *eds1-1/pad4-5* leaves were co-transfected via particle bombardment with the indicated fusion-protein constructs. FRET-APB was carried out 24 h after transfection. Mean FRET-efficiencies ± standard deviations from at least 15 sample sites are shown. Representative pictures of pseudo-coloured nuclei show donor-fluorescence before and after bleach for each indicated co-transfection below the bars. An increase of donor-fluorescence (red colour) can only be seen if protein-protein interaction occurs. For further details see Materials and Methods.

Taken together, these data demonstrate direct interaction between EDS1 and SAG101 inside the nuclei of living *Arabidopsis* cells. Although SAG101 was identified by B. Feys as an EDS1 associated protein in soluble plant extracts, subcellular localisation and FRET-APB experiments carried out in this work were able to uncover the nucleus as the relevant subcellular compartment where EDS1-SAG101 interaction takes place. Moreover, the FRET-APB experiments presented here uncovered that the EDS1-SAG101 interaction is direct. The unbiased biochemical approach carried out by B. Feys and the targeted cell-biological experiments presented here together provide compelling evidence of direct *in planta* interaction between EDS1 and SAG101.

Yeast two-hybrid assays preceding this work revealed that EDS1 can dimerise in yeast (Feys *et al.*, 2001) but direct EDS1-EDS1 interaction was not demonstrated *in planta*. One of the aims of this study was to uncover possible EDS1 homomeric associations *in vivo* utilising FRET-APB. As EDS1 was shown to be localised in the cytosol and inside the nucleus (see 3.2.1), this method provides the possibility to resolve spatially potential EDS1-EDS1 complexes in living tissues. For this purpose, the same constructs used for EDS1 localisation studies and for the generation of stable transgenic plants were used (see 3.2.1). L*er* genomic sequence of *EDS1* was C-terminally fused to *CFP* and *YFP*. Constructs expressing the fusion proteins EDS1-CFP and EDS1-YFP under control of P_{35S}, were transfected via particle bombardment into detached *Arabidopsis eds1-1/pad4-5* leaves and used as donor-acceptor pair in FRET-APB studies. FRET-APB was carried out as described for the EDS1-SAG101 interaction and in Materials and Methods (see 2.2.16). Due to the localisation of EDS1 in the cytosol and nucleus and the possibility that dimers could be present in both compartments, regions of interest (ROI) in both the cytosol and the nucleus were examined by FRET-APB. Mean FRET efficiencies of at least 15 sample sites from independent cells were calculated as described in Materials and Methods (see 2.2.16). As shown in Figure 3.13, clear FRET signals were obtained for EDS1-EDS1 interaction in the cytosol (7.7 ± 4.23 %) whereas no FRET signals above random background FRET were obtained for EDS1-EDS1 in nuclei (0.39 ± 2.55 %). Only random FRET signals were also recorded for the control FRET-APB donor-acceptor pairs EDS1-CFP/YFP (-2.09 ± 3.24 %) and CFP/YFP (-1.58 ± 1.1 %) in the cytosol. For nuclear FRET-APB controls, see Figure 3.12.

Using CLSM and FRET-APB it was possible not only to demonstrate EDS1 homo-dimerisation *in planta* but also to resolve spatially that dimerisation occurs in the cytosol but is absent in the nucleus, suggesting a difference in the nature of EDS1 interactions between these two compartments.

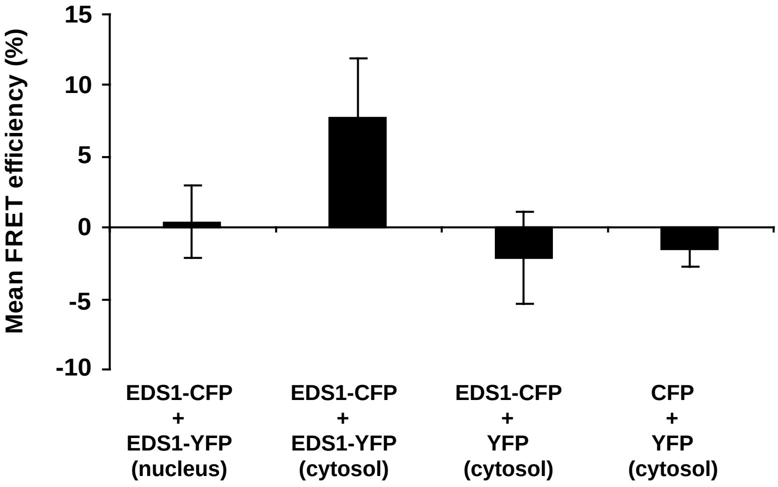

Fig. 3.13. FRET-APB analysis of the homodimerisation of fluorescently tagged EDS1. *Arabidopsis* detached *eds1-1/pad4-5* leaves were co-transfected via particle bombardment with the indicated fusion-protein constructs. FRET-AB was carried out 24 h after transfection. Mean FRET-efficiencies ± standard deviations from at least 15 sample sites are shown. For further details see Materials and Methods.

I tested whether the known interaction between EDS1 and PAD4 in healthy and pathogen challenged soluble plant extracts (Feys *et al.*, 2001) was reproducible by FRET-APB. Under the conditions tested mean FRET efficiencies did not significantly differ from background FRET signals, neither for the cytosol (2.27 ± 4 %) nor for the nucleus (0.46 ± 2.88 %) (Figure 3.14.). No detectable interaction between EDS1 and PAD4 could be due to the fact that only a small pool of EDS1 interacts with PAD4 (Feys *et al.*, submitted) or that the EDS1-PAD4 interaction is extremely weak or transient. Alternatively, the molecular orientations of the fp-tags might preclude transfer of fluorescence-energy between this special donor-acceptor pair. No specific FRET signals were also obtained between SAG101 and PAD4 in the nucleus or for PAD4-PAD4 in the cytosol or nucleus (data not shown).

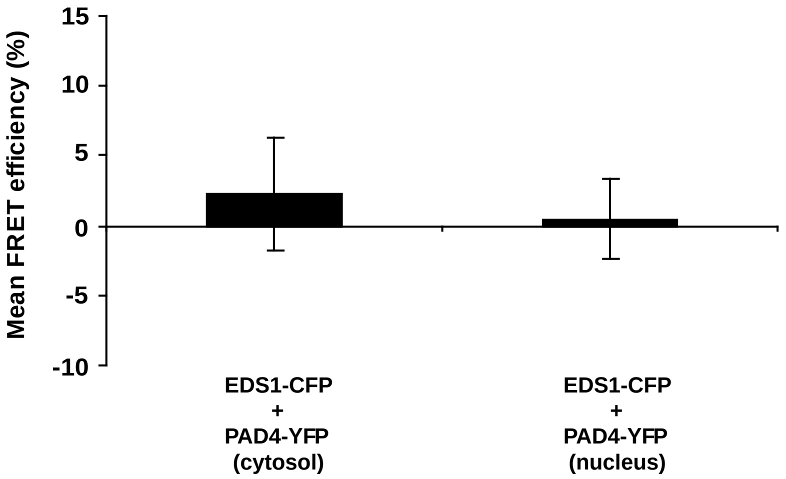

Fig. 3.14. FRET-APB analysis of fluorescently tagged EDS1 and PAD4. *Arabidopsis* detached *eds1-1/pad4-5* leaves were co-transfected via particle bombardment with EDS1-CFP and PAD4-YFP. FRET-AB was carried out 24 h after transfection. Mean FRET-efficiencies ± standard deviations from at least 15 sample sites are shown. Mean FRET efficiencies do not significantly differ from random FRET signals as displayed in Figure 3.12. and 3.13. For further details see Materials and Methods.

3.2.3 Summary of EDS1, PAD4 and SAG101 localisation and protein-protein interaction studies

Single cell bombardment of *Arabidopsis* leaves and *in planta* protein-protein interaction studies by FRET-APB were utilised to monitor the subcellular localisations and interactions of EDS1, SAG101 and PAD4. EDS1 and PAD4 co-localised in the cytosol and in the nucleus whereas SAG101 exclusively localised to the nucleus. Stronger EDS1-YFP fluorescence was found in the nucleus when EDS1-YFP was co-bombarded with SAG101-CFP than when bombarded alone, in combination with PAD4 or several nuclear localised WRKY transcription factors implying that SAG101 may hold EDS1 inside the nucleus. This fact, together with findings of B. Feys that SAG101 is part of an EDS1 complex in soluble leaf extracts prompted to examine a physical interaction between EDS1 and SAG101 by FRET analysis and led to the identification of SAG101 as a direct EDS1-interacting partner inside nuclei of healthy (pathogen-unchallenged) *Arabidopsis* cells. Moreover, FRET experiments discovered that EDS1 dimerises in the cytosol of unchallenged cells. This direct EDS1-EDS1 interaction was not detected in the nucleus. The data demonstrated that EDS1 forms molecular and spatial distinct associations in the cell.

3.3 Investigating the role of SAG101 in *Arabidopsis* innate immunity

SAG101 displays some pockets of sequence homology to the defence regulatory proteins EDS1 and PAD4 (see Introduction and Figure 3.4). Additionally, it was possible to show direct interaction between SAG101 and EDS1 inside nuclei of pathogen unchallenged leaf tissues (see 3.2.2). It was not known whether SAG101 functions in plant disease resistance signalling. The discovery of SAG101 being a direct EDS1 partner prompted me to investigate the role of SAG101 in plant innate immunity.

3.3.1 *SAG101* expression is induced upon infection with compatible and incompatible *P. parasitica* isolates

A first hint, apart from the interaction of SAG101 with EDS1 (described in this work), that SAG101 might be involved in disease resistance signalling, resulted from infection phenotypes of a published SAG101 enhancer trap line Sel139 (for senescence enhancer trap line 139) (He and Gan, 2002). In this line, a T-DNA containing a *GUS* reporter gene behind a minimal 35S promoter sequence had inserted 266 bp downstream from the poly(A) site of *SAG101* in accession Columbia-*glaborous1* (Figure 3.15 A). Analyses of enhancer trap lines in generally utilise the fact that a minimal promoter fused to a reporter gene alone has no transcriptional activity but when the construct inserts in the proximity of a chromosomal gene the cis regulatory elements of the chromosomal gene promoter direct expression of the reporter gene. Two-week-old Sel139 seedlings were infected with compatible and incompatible *P. parasitica* isolates and stained for GUS activity 7 days after infection. Figure 3.15 B shows that the expression of the GUS reporter gene is induced upon infection with the Col-*gl* incompatible *P. parasitica* isolates Cala2, Emoy2 and Emwa1 around HR lesions. *RPP* genes recognising the different isolates are indicated in the pictures. Interestingly, the expression of the GUS reporter gene was also induced upon infection with the compatible *P. parasitica* isolates Emco5 and Noco2 around growing oomycete mycelium, indicating an involvement of SAG101 not only in *R* gene-mediated but also in basal resistance responses. No GUS activity was detectable after spaying Sel139 plants with H_2O.

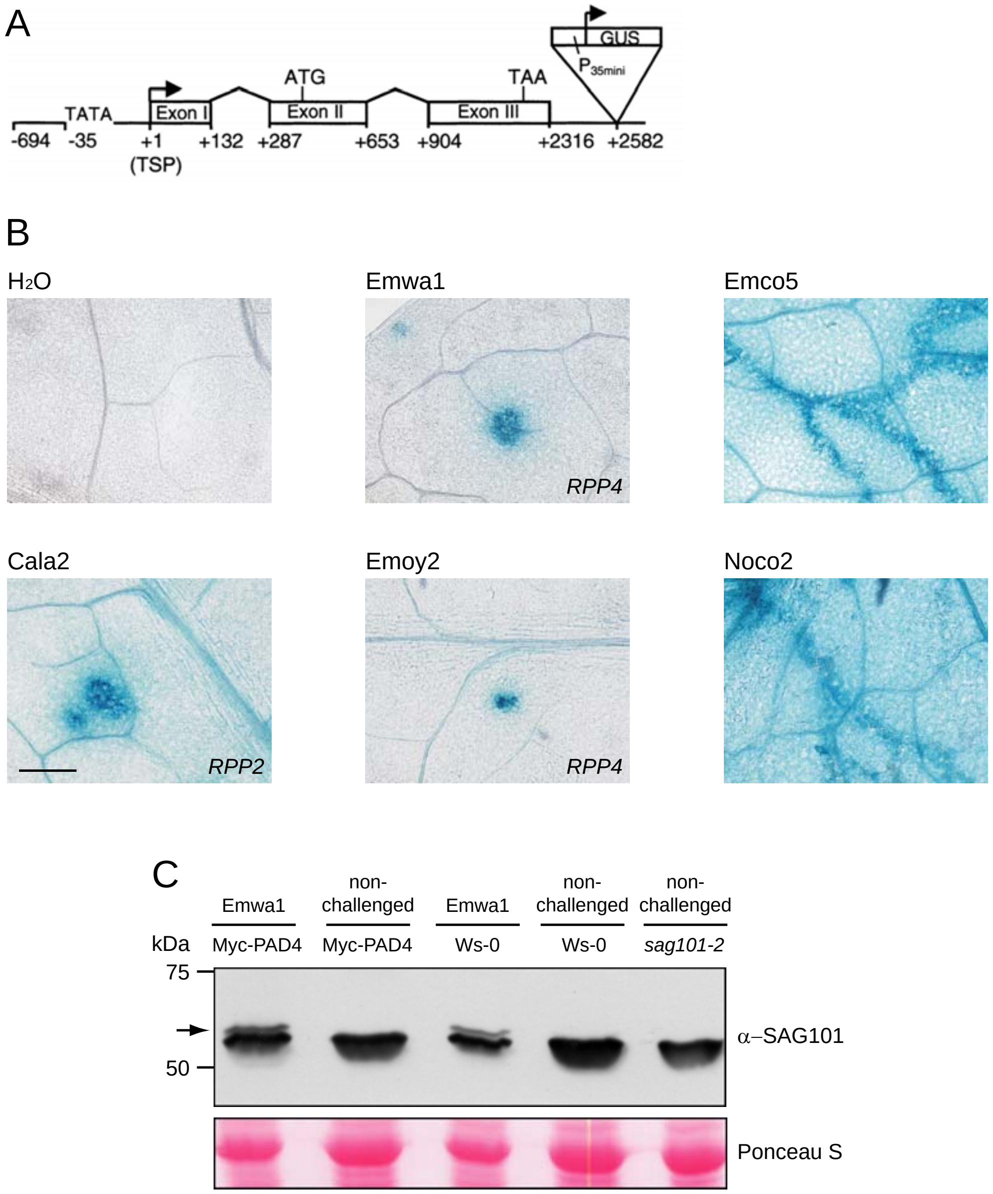
A
GUS
P_{35mini}
ATG
TAA
TATA
Exon I
Exon II
Exon III
-694
-35
+1
(TSP)
+132
+287
+653
+904
+2316
+2582
B
H2O
Emwa1
Emco5
RPP4
Cala2
Emoy2
Noco2
RPP2
RPP4
C
Emwa1
non-challenged
Emwa1
non-challenged
non-challenged
kDa
Myc-PAD4
Myc-PAD4
Ws-0
Ws-0
sag101-2
75
50
α–SAG101
Ponceau S

Fig. 3.15. Analysis of *SAG101* expression and protein abundance upon infection with compatible and incompatible *P. parasitica* isolates. Expression of *SAG101* was monitored by infecting seedlings of the Col-*gl SAG101* enhancer trap line Sel139 (He and Gan, 2002) with compatible and incompatible *P. parasitica* isolates followed by GUS activity staining and by immunoblot detection of SAG101 after infection with compatible *P. parasitica*. **(A)** Col-*gl SAG101* gene structure with insertion of the T-DNA in Sel139 (Figure taken from He and Gan, 2002). ATG, translational start codon; P_{35mini}, 35S minimal promoter of CaMV (-60 region); TAA translational stop codon; TATA, TATA box; TSP, transcriptional start point. **(B)** 2-week-old seedlings of the *SAG101* enhancer trap line Sel139 described in (A) were inoculated with the indicated compatible and incompatible *P. parasitica* isolates and stained for GUS reporter gene activity 7 dpi. *R* genes recognising the respective incompatible *P. parasitica* isolate are highlighted in the pictures. Strong GUS activity was detectable around HR lesions in the incompatible interactions (Cala2, Emoy2 and Emwa1) and around growing mycelium in the compatible interactions (Emco5 and Noco2). Scale bar: 200 µm. **(C)** Elevated levels of SAG101 protein were detectable in total protein extracts derived from Ws-0 and Myc-PAD4 plants 7 d after infection with the Ws-0 compatible *P. parasitica* isolate Emwa1. The same result was obtained after infection of Col-0 plants with the compatible *P. parasitica* isolate Noco2. SAG101 protein is indicated with an arrow. A non-specific cross-reacting band is present in all lines. Molecular weight markers in kDa are shown on the left.

As already mentioned, it was not feasible under the experimental conditions to detect SAG101 by immunoblot analysis of total protein extracts derived from unchallenged leaf tissues. However, it was possible to observe SAG101 protein in total protein extracts derived from Ws-0 or the Myc-PAD4 transgenic line LM41-2 after infection with the Ws-0 compatible *P. parasitica* isolate Emwa1 (Figure 3.15 C). The same result was obtained from protein extracts derived from Col-0 plants infected with the Columbia compatible *P. parasitica* isolate Noco2 (data not shown). These data demonstrate that the enhanced expression of the GUS reporter gene in the *SAG101* enhancer trap line upon compatible and incompatible *P. parasitica* infections likely reflects enhanced transcription of the *SAG101* gene by its promoter, since elevated SAG101 protein levels were detectable upon compatible *P. parasitica* infections by immunoblot analysis.

In order to assess if an increase of immunodetectable SAG101 protein after infection with compatible *P. parasitica* is also accompanied with an increase in EDS1 and PAD4 protein amounts, the same total protein extracts derived from Ws-0 and Myc-PAD4 leave tissues 7 days after infection with the Ws-0 compatible *P. parasitica* isolate Emwa1 were probed with α-c-Myc and α-EDS1 antibodies. Protein levels in these tissues were also compared with their abundance in unchallenged tissues. Figure 3.16 demonstrates that EDS1 and PAD4 proteins, like SAG101, are more abundant in tissues infected with compatible *P. parasitica* 7 days after infection. No Myc-PAD4 signal was obtained for non-transgenic Ws-0 lines (Figure 3.16 A) and no signal was detectable for EDS1 in control *eds1-1* extracts (Figure 3.16 B). This is the first demonstration of a clear increase in EDS1 and PAD4 protein abundance in a compatible interaction with *P. parasitica* (for comparison see Feys *et al.*, 2001). Upregulation of EDS1 and PAD4 upon virulent pathogen challenge probably reflects their roles as essential components of basal plant defences. The increase in *SAG101* expression upon infection with compatible and incompatible *P. parasitica* (Figure 3.15 B) as well as the detectable increase in SAG101 protein abundance in a compatible interaction (Figure 3.15 C) prompted me to examine the role of SAG101 in plant disease signalling in more detail.

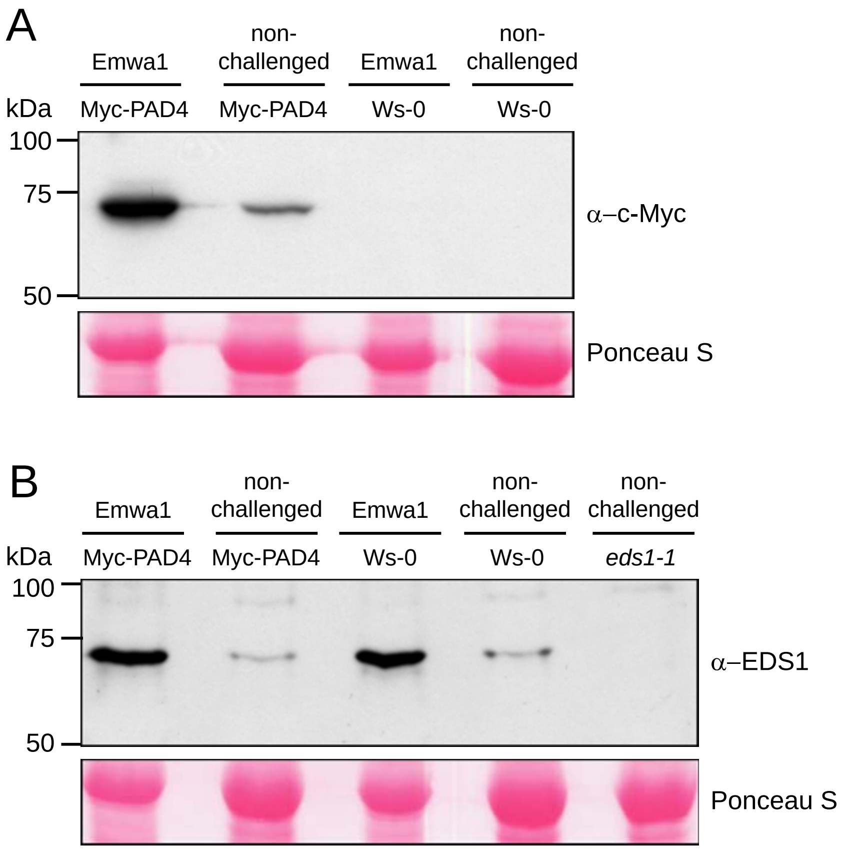
A
Emwa1
non-challenged
Emwa1
non-challenged
kDa
Myc-PAD4
Myc-PAD4
Ws-0
Ws-0
100
75
50
α–c-Myc
Ponceau S
B
Emwa1
non-challenged
Emwa1
non-challenged
non-challenged
kDa
Myc-PAD4
Myc-PAD4
Ws-0
Ws-0
eds1-1
100
75
50
α–EDS1
Ponceau S

Fig. 3.16. Immunoblot analysis of EDS1 and Myc-PAD4 protein abundance upon infection with compatible *P. parasitica* Emwa1. Total protein extracts for immunoblot detection were generated from Ws-0 and Myc-PAD4 plants, 7 d after inoculation with the compatible *P. parasitica* isolate Emwa1. **(A)** Myc-PAD4 and **(B)** EDS1 protein abundance was compared to non-inoculated control samples. No signal for Myc-PAD4 was obtained in non-transgenic Ws-0 plants (A) as no signal for EDS1 was obtained in *eds1-1* mutant plants (B). Although Ponceau S staining of the membrane shows a reduced overall protein content in Emwa1 infected tissues, increased signal intensities for Myc-PAD4 and EDS1 were obtained. Molecular weight markers in kDa are shown on the left.

3.3.2 SAG101 signals in plant innate immunity

In order to assess whether SAG101 is necessary for plant defence, two independent *sag101* knock-out lines in accession Col-0 that were homozygous for d*Spm* transposon inserted within exonic sequences of the *SAG101* gene were isolated by B. Feys at the Sainsbury Laboratory in Norwich, and are referred to as *sag101-1* and *sag101-2* (Tissier *et al.*, 1999). Both alleles were shown by immunoblot analysis to be null at the level of SAG101 protein accumulation (Feys *et al.*, submitted).

3.3.2.1 Loss of *RPP2* resistance in *pad4-1/sag101* double mutants

For phenotypic characterisation of the *sag101* mutants upon pathogen infection, 2-week-old plants were spray inoculated with conidiospores (4 x 10^4 ml^{-1}) of the avirulent *P. parasitica* isolate Cala2 which is recognised by *RPP2* in Col-0, and stained 7 days after inoculation with lactophenol trypan blue (LTB) for visualisation of necrotic plant cells and pathogen mycelium (see 2.2.9). Both, *sag101-1* and *sag101-2* exhibited *RPP2*-triggered programmed cell death (HR) at pathogen infection sites as in the wild-type parental line, Col-0 (Figure 3.17).

This response was in contrast to Col-0 *pad4-1* that has weakened *RPP2* resistance, manifested as trailing plant cell necrosis after staining leaves with LTB (Figure 3.17) that is associated with occasional sporulation of the oomycete pathogen. To address whether *SAG101* could be redundant with *PAD4* and if the *pad4-1* and *sag101* mutations might display an additive or synergistic effect upon *P. parasitica* infection, *pad4-1/sag101* double mutant plants were generated by L. Moisan and B. Feys (Feys *et al.*, submitted). Leaves of *pad4-1/sag101-1* as well as *pad4-1/sag101-2* double mutants exhibited loss of *RPP2*-mediated resistance upon *P. parasitica* Cala2 infection that was as extreme as susceptibility of *eds1-1* null mutants in accession Ws-0 (Figure 3.17), manifested as LTB stained free mycelium growth of the pathogen. Ws-0 wild-type plants prevented pathogen growth through expression of an *RPP1A* triggered HR. Macroscopically, *pad4-1/sag101* double mutant plants displayed heavy sporulation that was comparable to *eds1-1* and *eds1-2* mutant plants in accessions Ws-0 and L*er*, respectively (Figure 3.18 and data not shown). A null *eds1* mutant in Col-0 was not available for phenotypic comparison within the same genotype (see below).

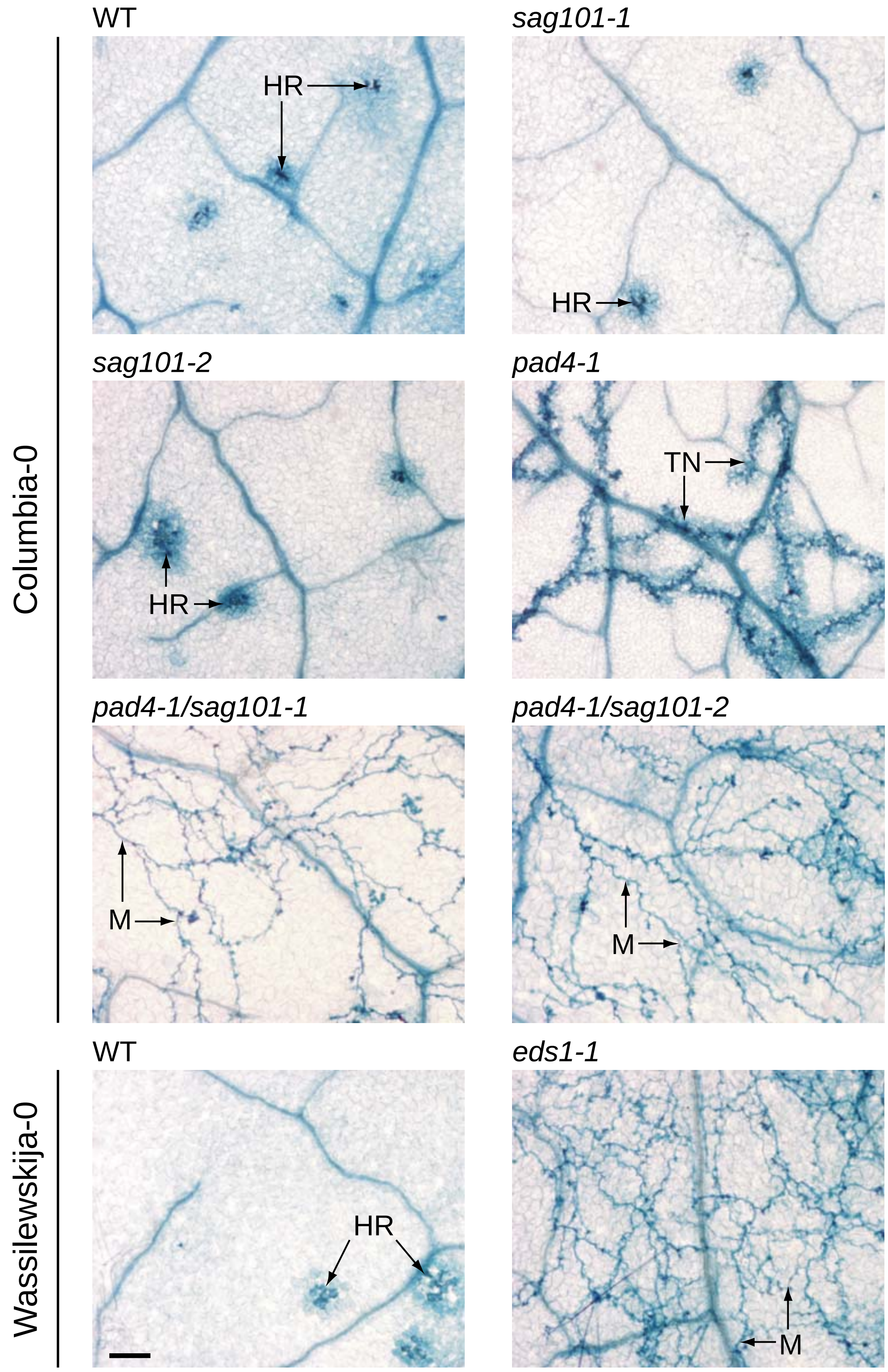
WT
sag101-1
HR
HR
HR
sag101-2
pad4-1
HR
HR
TN
pad4-1/sag101-1
pad4-1/sag101-2
M
M
WT
eds1-1
HR
M
Columbia-0
Wassilewskija-0

Fig. 3.17. Infection phenotypes of leaves inoculated with *P. parasitica* Cala2. 2-week-old seedlings were spray-inoculated with 4 x 10^4 conidiospores ml^{-1} of *P. parasitica* isolate Cala2, which is recognised by *RPP2* in Col-0 and *RPP1A* in Ws-0. Leaves were stained with lactophenol trypan blue 7 d after inoculation to visualise pathogen mycelium and necrotic plant cells. Genotypes are indicated above the pictures, ecotype backgrounds are indicated on the left. Free mycelium growth can be seen in *pad4/sag101* double and *eds1-1* mutants. HR: hypersensitive response; TN: trailing necrosis; M: mycelium. Scale bar: 150 µm.

To examine further whether the *pad4-1/sag101* double mutants exhibit loss of *RPP2*-mediated resistance that is as extreme as susceptibility of *eds1* mutant plants, sporulation levels of *P. parasitica* Cala2 infected leave tissues were quantified 6 days after inoculation (for details see 2.2.8) and are displayed in Figure 3.18.

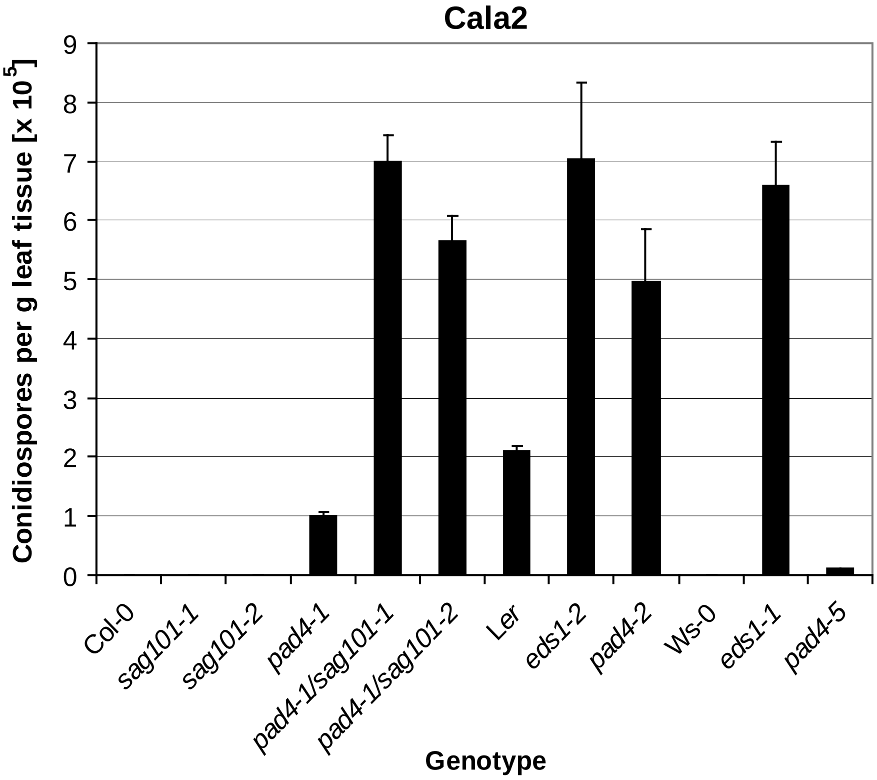

Fig. 3.18. Resistance phenotypes of *Arabidopsis* lines infected with *P. parasitica* Cala2. Sporulation levels of *P. parasitica* isolate Cala2 on the indicated *Arabidopsis* wild-type and mutant lines was quantified 6 d after spray-inoculation of 2-week-old seedlings with 4 x 10^4 conidiospores ml^{-1}. Cala2 is recognised by *RPP2* in Col-0 and by *RPP1A* in Ws-0 but is virulent on L*er*. *Pad4-1* and *sag101* single and double mutations are in Col-0. Backgrounds are L*er* for *eds1-2* and *pad4-2* and Ws-0 for *eds1-1* and *pad4-5*. For each tested *Arabidopsis* genotype, two pots containing approximately 30 seedlings were infected and harvested spores from all seedlings of each pot were counted twice. Sporulation levels resulting from the four counts are expressed as the average number of conidiospores per gram fresh weight ± standard deviation. Experiments were repeated twice with congenerous results. Similar results were obtained when *sag101* and *pad4-1* single and double mutants were tested for *RPP4* recognition of *P. parasitica* isolate Emwa1.

Quantification of sporulation on the tested genotypes correlated with the phenotypes observed after staining Cala2 infected leaf material with LTB. Both *sag101* single mutants that displayed HR upon Cala2 infection (Figure 3.17) did not support pathogen sporulation on leaves and thus resembled the Col-0 wild-type parental line. *Pad4-1* mutant plants that exhibited delayed or weakened *RPP2* resistance, resulting in the described trailing necrosis phenotype, permitted low but significant pathogen sporulation. In contrast to *pad4-1* and *sag101* single mutants, *pad4-1/sag101-1* and *pad4-1/sag101-2* double mutant plants that allowed unimpeded pathogen growth as revealed by LTB staining (Figure 3.17), were completely disabled in *RPP2*-mediated resistance and allowed pathogen sporulation that was as extreme as on *eds1* null mutants in accessions L*er* (*eds1-2*) or Ws-0 (*eds1-1*). A similar result for *pad4/sag101* double mutant plants was obtained after infection with *P. parasitica* Emwa1 which is recognised by *RPP4* (data not shown).

High sporulation levels on *pad4-2* mutant leaves in the Cala2 susceptible accession L*er* confirmed known defects of *pad4* mutants in basal resistance responses resulting in enhanced disease susceptibility of *pad4* in compatible interactions (Glazebrook *et al.*, 1996). In conclusion, these results demonstrate that the combined activities of PAD4 and SAG101 in resistance to avirulent *P. parasitica* strains are at least equivalent to *eds1*.

3.3.2.2 Loss of basal resistance in *pad4-1/sag101* double mutants

EDS1 and PAD4 are essential regulators of basal resistance responses to obligate biotrophic pathogens, controlling defence signal amplification and accumulation of SA (Zhou *et al.*, 1998; Jirage *et al.*, 1999; Feys *et al.*, 2001). Mutations in basal defence components characteristically cause hypersusceptibility to virulent pathogen strains (Glazebrook *et al.*, 1996; Parker *et al.*, 1996). In order to address whether SAG101 might also be involved within the basal resistance layer in restricting the growth of virulent pathogens, *sag101-1* and *sag101-2* single mutants as well as *pad4-1/sag101-1* and *pad4-1/sag101-2* double mutant plants were infected with *P. parasitica* isolate Noco2 which is virulent on parental Col-0 wild-type plants. Sporulation levels on infected leaf tissues was quantified 6 days after inoculation as displayed in Figure 3.19. *Sag101-1* and *sag101-2* single mutant plants did not support sporulation of compatible *P. parasitica* Noco2 above levels ascertained for Col-0 wild-type plants. This was again in contrast to *pad4-1* mutant plants (compare with Figure 3.17). As mutations in *PAD4* are known to cause an enhanced disease susceptibility phenotype upon infection with compatible, biotrophic pathogens (Glazebrook *et al.*, 1996), this phenotype confirmed that *pad4-1* plants are hypersusceptible to Noco2 infection. Surprisingly, basal resistance to virulent *P. parasitica* Noco2 was significantly more disabled in *pad4-1/sag101-1* and *pad4-1/sag101-2* than in *pad4-1* alone and as severe as in *eds1* mutant plants in L*er* (*eds1-2*) and Ws-0 (*eds1-1*) accessions (Figure 3.19). Since *pad4* in other

Arabidopsis accessions (L*er* and Ws-0) disables basal resistance as fully as *eds1* (Figure 3.18 and data not shown), this result was unexpected and suggest that the *pad4-1/sag101* combination creates a "super-susceptible" background to virulent *P. parasitica* Noco2 in accession Col-0.

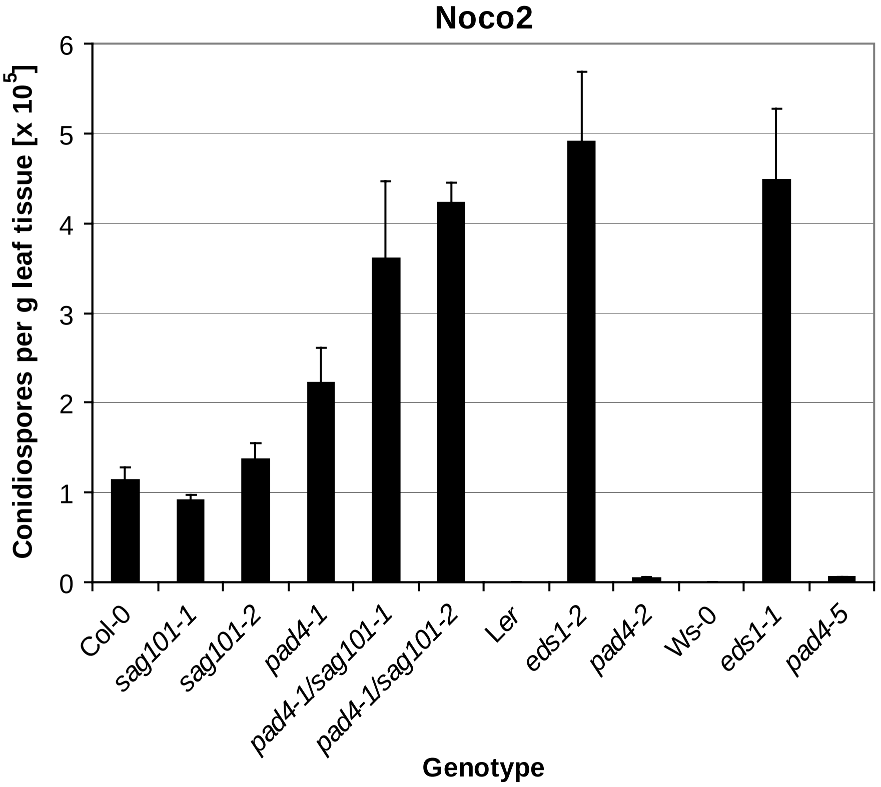

Fig. 3.19. Resistance phenotypes of *Arabidopsis* lines infected with *P. parasitica* Noco2. Sporulation levels of *P. parasitica* isolate Noco2 on the indicated *Arabidopsis* wild-type and mutant lines was quantified 6 d after spray-inoculation of 2-week-old seedlings with 4 x 10^4 conidiospores ml^{-1}. Noco2 is virulent on Col-0 but recognised by *RPP5* in L*er* and *RPP1* in Ws-0. *Pad4-1* and *sag101* single and double mutations are in Col-0. Backgrounds are L*er* for *eds1-2* and *pad4-2* and Ws-0 for *eds1-1* and *pad4-5*. For each tested *Arabidopsis* genotype, two pots containing approximately 30 seedlings were infected and harvested spores from all seedlings of each pot were counted twice. Sporulation levels resulting from the four counts are expressed as the average number of conidiospores per gram fresh weight ± standard deviation. Experiments were repeated twice with similar results.

Taken together, the results demonstrate that the sum of SAG101 and PAD4 activities are at least equivalent to EDS1 in restriction of the growth of virulent *P. parasitica* Noco2. In comparison to the single *pad4-1* mutant, *pad4-1/sag101* double mutants are "super-susceptible" to virulent *P. parasitica* Noco2 in accession Col-0.

3.3.2.3 EDS1 protein is stabilised by its interacting partners PAD4 and SAG101

This study and experiments carried out by B. Feys showed that PAD4 and SAG101 are direct interacting partners of EDS1 *in planta* (Feys *et al.*, 2001; Feys *et al.*, submitted) and thus could have stabilising effects on EDS1 which may be the primary defence signalling molecule. I addressed whether the severe loss of *R* gene-mediated and basal-resistance phenotype observed in *pad4/sag101* double mutants (Figures 3.18 and 3.19) could be accounted for by a depletion of EDS1 protein levels through destabilisation upon removal of its interacting partners. Total protein extracts of *sag101-1*, *sag101-2* and *pad4-1* single as well as *pad4-1/sag101-1* and *pad4-1/sag101-2* double mutants were examined for EDS1 protein abundance by immunoblot analysis and compared to the level in parental Col-0 wild-type leaves (set as 100 %). Figure 3.20 demonstrates that EDS1 protein levels are depleted incrementally in *sag101*, *pad4* and *pad4/sag101* leaf tissues.

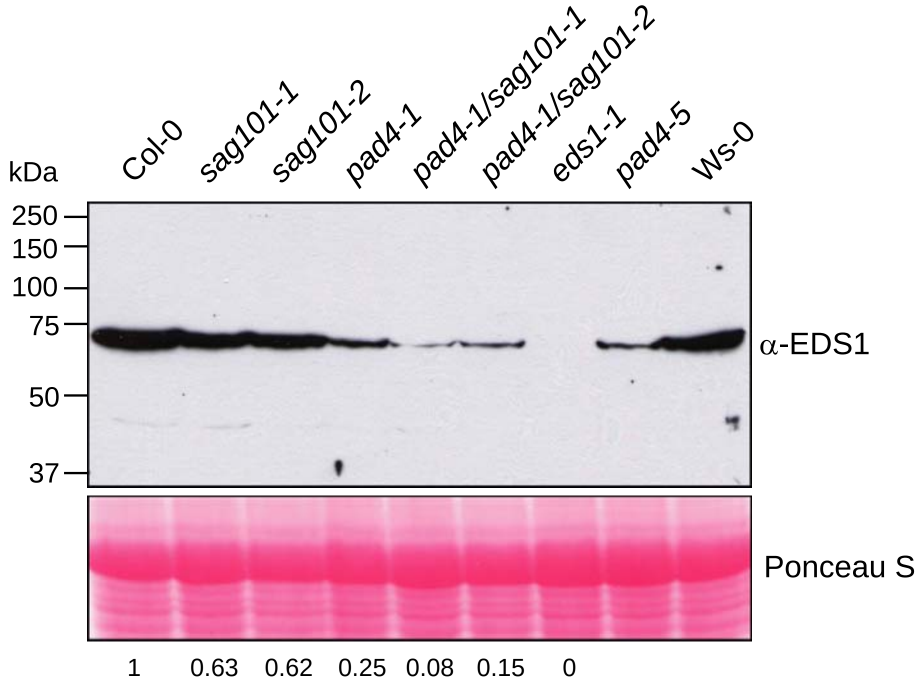

Fig. 3.20. Immunoblot analysis of EDS1 protein abundance in *Arabidopsis* mutant lines. Total protein extracts for immunoblot analysis were derived from 3-week-old plants of the indicated wild-type and mutant lines and separated on a 10 % SDS polyacrylamide gel. Separated proteins were transferred to nitrocellulose membrane and EDS1 protein was detected by using a rabbit polyclonal EDS1 antibody. *Sag101*, *pad4-1* and *pad4/sag101* mutants are in Col-0, *eds1-1* and *pad4-5* are in Ws-0 ecotype. Numbers below the immunoblot indicate band intensities relative to the EDS1-signal obtained for wild-type Col-0, measured by ImageQuant 5.2 software. Equal loading is shown by Ponceau S staining of the membrane. Molecular weight markers in kDa are shown on the left.

Whereas EDS1 was reduced to ~60 % of Col-0 wild-type levels in *sag101* single mutants (63 % and 62 % in *sag101-1* and *sag101-2*, respectively) and 25 % in *pad4-1* single mutant plants, only residual EDS1 protein levels (~10 %) was detectable in *pad4-1/sag101* double mutants (8 % and 15 % in *pad4-1/sag101-1* and *pad4-1/sag101-2*, respectively). Due to the lack of an available *eds1* mutant in Col-0 (see also 3.3.2.4), protein extracts of the null *eds1-1* mutant in Ws-0 ecotype served as a negative control in this immunoblot analysis. Overall EDS1 protein levels in accession Ws-0 was slightly lower then in accession Col-0 and might account for the somewhat lower EDS1-signal obtained for the Ws *pad4-5* mutant compared to Col *pad4-1* (Figure 3.20).

These data show that SAG101 and PAD4 contribute additively to EDS1 protein abundance. Since mutations in *pad4* were shown to have only minimal influence on pathogen induced *EDS1* mRNA levels (Feys *et al.*, 2001), it is likely that SAG101 and PAD4 act post-transcriptionally and most likely at the level of EDS1 protein stabilisation. Moreover, B. Feys demonstrated that EDS1 is strictly required for accumulation of both SAG101 and PAD4 as SAG101 protein was undetectable on immunoblots in an *eds1-1* mutant background and Myc-PAD4 protein was almost undetectable in the absence of EDS1 in the identical *eds1-1* mutant background (Feys *et al.*, submitted). RT-PCR analysis of the same material revealed that transcription of *SAG101* and *PAD4* mRNAs was similar in *eds1* mutant and wild-type plants indicating that EDS1 acts post-transcriptionally at the level of PAD4 and SAG101 protein accumulation. The data presented in this study and in Feys *et al.* (submitted) show that EDS1, PAD4 and SAG101 have mutually stabilising effects on their interacting partners.

3.3.2.4 SAG101 and PAD4 have defence regulatory functions beyond stabilising EDS1

From the pathogen assays (Figures 3.17 – 3.19) and immunoblot data on EDS1 protein abundance (Figure 3.20) I hypothesised that diminished EDS1 protein levels below certain thresholds could account for the weakened resistance in *pad4-1* and complete loss of resistance in *pad4-1/sag101* double mutant plants, reflecting their stabilisation of EDS1. To test this hypothesis, a Col-0 line was included in the analysis in which endogenous *EDS1* was stably silenced using a double stranded RNAi (dsRNAi) construct, and is denoted Col-*eds1*RNAi (Feys *et al.*, submitted). Due to two closely linked and highly sequence related Col-0 *EDS1* genes (82 % nucleotide identity), *EDS1A* (At3g48090) and *EDS1B* (At3g48080) lying in tandem repeat on the lower arm of chromosome 3, an *EDS1* null T-DNA knock-out in Col-0 was not available and silencing of these two genes via an dsRNAi approach was the method of choice. Both *EDS1* genes individually were shown to be functional and able to complement the *eds1* phenotype when stably transformed into L*er eds1-2* mutant plants and expressed under control of the L*er EDS1* promoter (J. Bautor, A. Cabral and J. Parker, unpublished data). The Col-*eds1*RNAi line was generated by A. de Cruz-Cabral and C. Neu at the MPIZ in Cologne and was utilised to compare directly its disease resistance phenotype and EDS1 protein abundance with those phenotypes of Col-0 *pad4-1/sag101*. In addition to Col-*eds1*RNAi, individual T-DNA insertion lines for *EDS1A* (SALK_057149) and *EDS1B* (SALK_019545) were included in my analysis. First, the Col-*eds1*RNAi and both *EDS1* insertion lines were characterised by semi-quantitative RT-PCR (see 2.2.13.5) for EDS1 transcript abundance as shown in Figure 3.21. Total RNA for reverse transcription and subsequent PCR analysis was isolated from unchallenged leaf tissues (see 2.2.13.2).

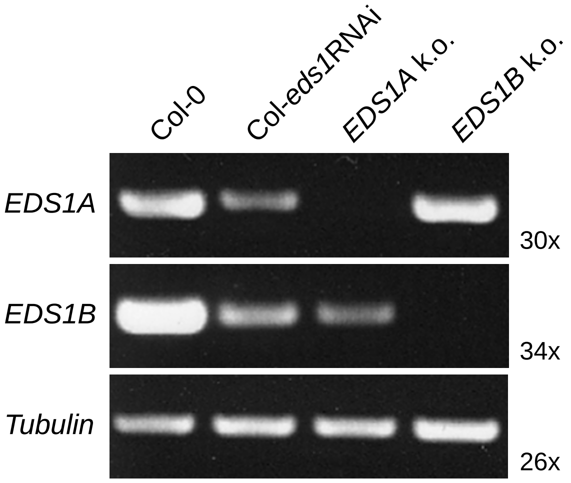

Fig. 3.21. RT-PCR analysis on the abundance of *EDS1* transcripts in Col *eds1* mutant lines. Total RNA for reverse transcription was extracted from 3-week-old unchallenged leaf tissues. Equal application of template RNA for reverse transcription is shown by a control PCR reaction detecting Tubulin first strand cDNA. Transcripts detected are indicated on the left, plant lines are indicated above the agarose gel pictures. Numbers of cycles used in PCR reactions are indicated on the right.

EDS1 transcript levels of the two *EDS1* genes were effectively silenced in Col-*eds1*RNAi and only detectable after raising cycle numbers in the RT-PCR program to 30x (*EDS1A*) and 34x (*EDS1B*) (Figure 3.21). No *EDS1A* transcripts were detectable in the *EDS1A* T-DNA insertion line and *EDS1B* transcripts were also absent in the *EDS1B* T-DNA insertion line. *EDS1A* transcript levels were unaffected in the *EDS1B* insertion line that was downstream of the *EDS1A* gene. Interestingly, the insertion line in *EDS1A* that was upstream of *EDS1B*, was also depleted in *EDS1B* transcripts to levels similar to those in Col-*eds1*RNAi.

To test the hypothesis that weakened resistance phenotype in *pad4-1* and loss of resistance phenotype in *pad4-1/sag101* mutant plants is due to diminished EDS1 protein levels, total protein extracts from 4-week-old unchallenged leave tissues of these lines were analysed by immunoblotting. As can be seen on the anti-EDS1 immunoblot in Figure 3.22, *pad4-1/sag101* double mutant plants displayed strong depletion of EDS1 when compared with parental Col-0 (consistent with the results shown in Figure 3.20). Nevertheless, EDS1 protein in Col-*eds1*RNAi accumulated to significantly lower levels than in *pad4-1/sag101*.

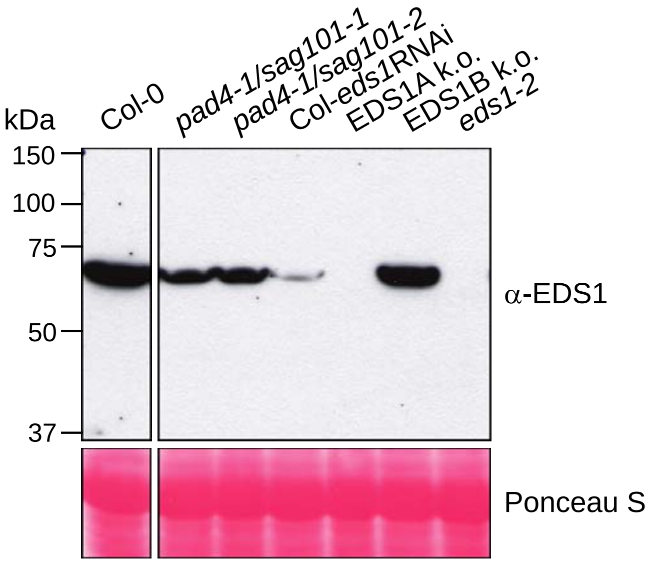

Fig. 3.22. Immunoblot analysis of *Arabidopsis* mutants depleted in EDS1. Total protein extracts were generated from 4-week-old unchallenged leaves of the indicated *Arabidopsis* lines. Proteins were separated on a 10 % SDS polyacrylamide gel. Separated proteins were transferred to nitrocellulose membrane and EDS1 protein was detected by using a rabbit polyclonal EDS1 antibody. All mutant lines are in accession Col-0 except *eds1-2* which is in accession L*er*. Equal loading is shown by Ponceau S staining of the membrane. Molecular weight markers in kDa are shown on the left.

No signal for EDS1 was obtained in *eds1-2* mutant controls. EDS1 protein was also undetectable in the *EDS1A* insertion line. This can be rationalised by the fact that absence of EDS1A protein in this line is accompanied with a strong depletion of *EDS1B* mRNA levels to levels observed in Col-*eds1*RNAi, as shown in the RT-PCR analysis in Figure 3.21. Moreover, it was established that EDS1B protein is less efficiently recognised by the polyclonal α-EDS1 antibody than EDS1A (J. Bautor and J. Parker, personal communication) and could account for the failure to detect EDS1 in the *EDS1A* insertion line. The

EDS1-signal detected in the *EDS1B* insertion line was comparable to Col-0 wild-type and correlated with the RT-PCR data (Figure 3.21). Even though *EDS1B* is not expressed in this line, *EDS1A* transcripts accumulate to the same level seen in Col-0 wild-type.

EDS1 protein accumulated to significantly lower levels in Col-*eds1*RNAi than in both *pad4-1/sag101-1* and *pad4-1/sag101-2* (Figure 3.22). In spite of this, Col-*eds1*RNAi leaves exhibited stronger *RPP2*-mediated resistance upon infection with the Col-0 incompatible *P. parasitica* isolate Cala2 as demonstrated in Figure 3.23.

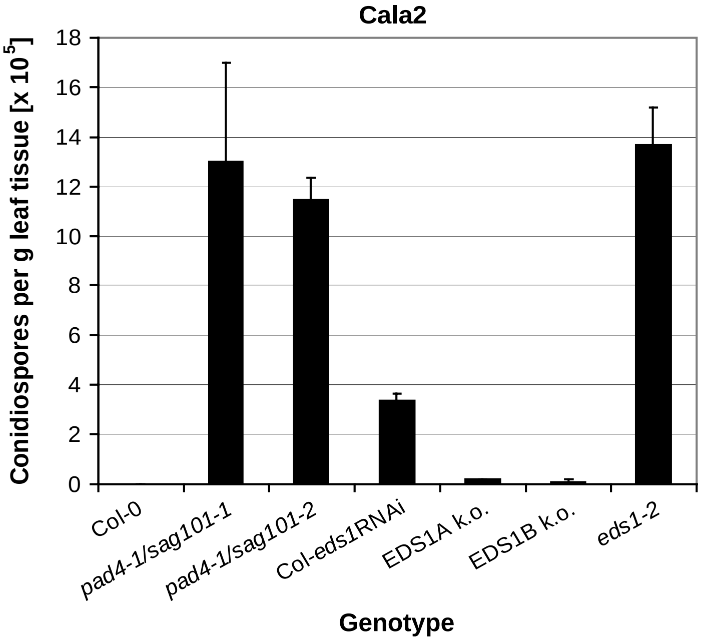

Fig. 3.23. *RPP2* resistance of *Arabidopsis* lines depleted in EDS1. Sporulation levels of *P. parasitica* isolate Cala2 on the indicated *Arabidopsis* lines was quantified 6 d after spray-inoculation of 2-week-old seedlings with 4 x 10^4 conidiospores ml^{-1}. Cala2 is recognised by *RPP2* in Col-0. All mutants are in accession Col-0 except *eds1-2* which is in L*er*. For each tested *Arabidopsis* genotype, two pots containing approximately 30 seedlings were infected and harvested spores from all seedlings of each pot were counted twice. Sporulation levels resulting from the four counts are expressed as the average number of conidiospores per gram fresh weight ± standard deviation. Experiments were repeated twice with congenerous results. Similar results were obtained when these mutants were tested for *RPP4* recognition of *P. parasitica* isolate Emwa1.

Pad4-1/sag101 mutants displayed loss of *RPP2*-mediated resistance that was as severe as in *eds1-2* mutant plants (see also Figure 3.18). Both the single *EDS1* knock-out lines in *EDS1A* and *EDS1B* did not support significant sporulation of *P. parasitica* Cala2 and were resistant as Col-0 wild-type. This is consistent with the finding that both copies of *EDS1* can complement the *eds1* mutant. The finding that Col-*eds1*RNAi plants support higher sporulation than *EDS1A* knock-out plants that have lower overall accumulation of EDS1 protein might be explained if *EDS1B* expression is still inducible upon pathogen infection whereas silencing in Col-*eds1*RNAi suppresses *EDS1* expression and up-regulation more effectively.

I reasoned from these data that PAD4 and SAG101 are likely to have intrinsic signalling capabilities beyond just stabilising EDS1 in TIR-NB-LRR type R protein-triggered resistance and that the complete loss of this resistance in *pad4/sag101* double mutant plants is not simply caused by the reduction of EDS1 protein. I concluded further that extremely low EDS1-levels are sufficient to fulfil its signalling function in *R* gene-mediated resistance.

The Col-*eds1*RNAi line was then compared to *pad4/sag101* double mutants in its response to virulent *P. parasitica* isolate Noco2. Sporulation levels of *P. parasitica* Noco2 were quantified 7 days after inoculation of leaves (for details see 2.2.8). As shown in Figure 3.24, *pad4-1/sag101* double mutants displayed complete loss of basal resistance as seen before that was as severe as in the control *eds1-2* mutant in accession L*er* (see also Figure 3.19).

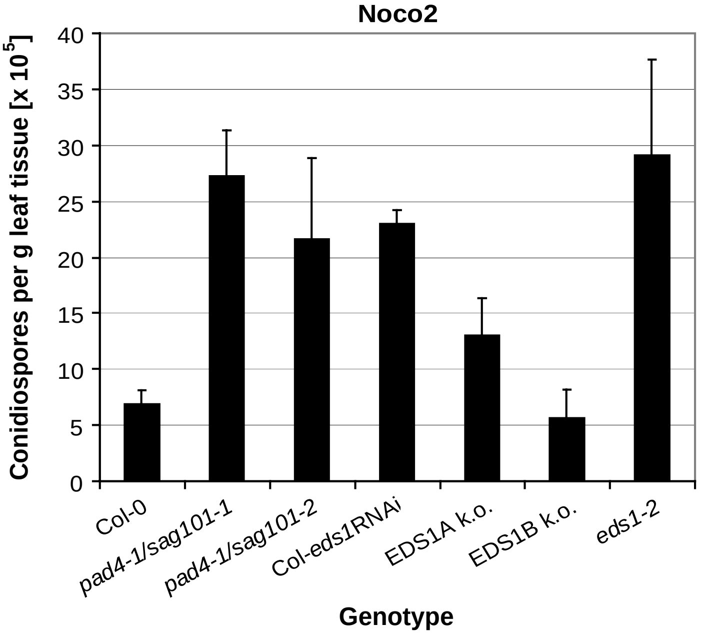

Fig. 3.24. Basal resistance of *Arabidopsis* lines depleted in EDS1. Sporulation levels of *P. parasitica* isolate Noco2 on the indicated *Arabidopsis* lines was quantified 7 d after spray-inoculation of 2-week-old seedlings with 4 x 10^4 conidiospores ml^{-1}. Noco2 is virulent on Col-0. All mutants are in accession Col-0 except *eds1-2* which is in L*er*. For each tested *Arabidopsis* genotype, two pots containing approximately 30 seedlings were infected and harvested spores from all seedlings of each pot were counted twice. Sporulation levels resulting from the four counts are expressed as the average number of conidiospores per gram fresh weight ± standard deviation. Experiments were repeated twice with similar results.

The Col-*eds1*RNAi line displayed a similar degree of susceptibility as *pad4/sag101* double mutants to virulent *P. parasitica* Noco2, which was in contrast to the differential infection phenotype seen between these lines in *R* gene-mediated resistance after inoculation with the incompatible *P. parasitica* isolate Cala2 (Figure 3.23). *EDS1B* knock-out plants did not support sporulation of the pathogen above levels seen on Col-0 wild-type, whereas *EDS1A* knock-out plants exhibited sporulation levels that were intermediate between Col-*eds1*RNAi and *EDS1B* insertion lines. In several experiments sporulation-levels on the *EDS1A* insertion line were either lower or within the range of the Col-*eds1*RNAi line.

These results suggest that maintenance of a certain EDS1 threshold is important for full expression of basal resistance. This threshold seems to be higher for basal resistance than for *R* gene-mediated resistance (see also Figure 3.23).

3.3.2.5 The combined activities of PAD4 and SAG101 are required for TIR-NB-LRR type *R* gene-mediated and basal resistance against bacterial pathogens

To analyse if loss of *R* gene-mediated and basal disease resistance phenotypes of *pad4/sag101* double mutant plants is restricted to infections with the oomycete pathogen *P. parasitica* or is a more general phenomenon, the genetic requirement for combined PAD4 and SAG101 in resistance to virulent and avirulent strains of the bacterial pathogen *Pseudomonas syringae* pv. *tomato* (*Pst*) strain DC3000 was tested. Infection of plants with *Pst* DC3000 expressing either of the avirulence genes *avrRps4* and *avrRpm1*, whose gene products are recognised by the TIR-type NB-LRR R protein RPS4 and the CC-NB-LRR R protein RPM1, respectively, could further reveal if loss of R protein-mediated resistance in *pad4/sag101* falls into the EDS1 signalling pathway.

Five-week-old *Arabidopsis* plants of the different mutant and wild-type lines were vacuum-infiltrated with 5 x 10^5 cfu ml^{-1} as described in Materials and Methods (see 2.2.11). Samples were taken to determine the number of viable bacteria as described in Materials and Methods (see 2.2.11). Figure 3.25 displays the infection phenotypes of the different mutant lines after infiltration of virulent *Pst* DC3000. This strain contains an empty vector control and does not express any *Avr* gene (see 2.1.2.2). Growth trends of virulent *Pst* DC3000 confirmed the data obtained for infections with virulent *P. parasitica* Noco2. *Sag101* single mutants did not show loss of resistance to virulent DC3000 compared to parental Col-0. Basal resistance in *pad4-1/sag101* double mutant plants was suppressed as strongly as in *eds1* mutant plants in L*er* (*eds1-2*) and Ws-0 (*eds1-1*) accessions. However, in contrast to infections with virulent *P. parasitica* Noco2, *pad4-1* permitted growth of DC3000 to the same level as in *pad4/sag101* double mutants. Therefore, *pad4/sag101* plants do not seem to be "super-susceptible" in response to virulent *Pst* DC3000 as seen after Noco2 infection (Figure 3.19). This is complied with the fact that mutations in *pad4* generally compromise basal resistance to levels observed in *eds1* (see *eds1-2* and *pad4-2* (L*er* background) and *eds1-1* and *pad4-5* (Ws-0 background) in Figure 3.25 which allow bacterial growth to the same extent). The Col-*eds1*RNAi line enhanced growth of virulent *Pst* DC3000 to levels seen in *pad4/sag101* that was also found for the infection phenotype of virulent *P. parasitica* Noco2 (Figure 3.24).

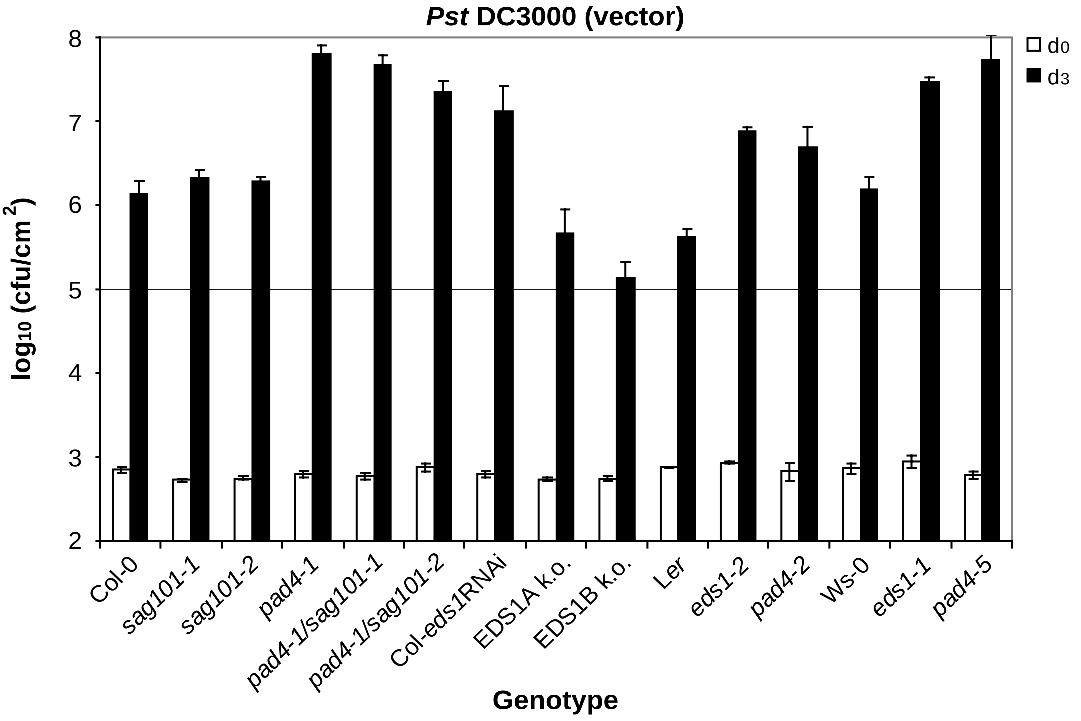

Fig. 3.25. *In planta* growth of virulent *P. syringae* pv. *tomato* strain DC3000. 5-week-old plants were vacuum-infiltrated with a bacterial suspension of virulent *Pst* DC3000 at 5 x 10^5 cfu ml^{-1} and bacterial titers measured at day zero (d_0) and day three (d_3). Mutant lines are in accession Col-0 except *eds1-2* and *pad4-2* (accession L*er*) and *eds1-1* and *pad4-5* (accession Ws-0). Bacterial growth is expressed as mean values of viable bacteria per cm^2 leaf tissue ± standard deviation, resulting from two replicate samplings for d_0 and three replicate samplings for d_3 values. For details see text and Materials and Methods (2.2.11). This experiment was repeated with similar results.

T-DNA insertions in *EDS1A* or *EDS1B* did not enhance growth of virulent *Pst* DC3000 above levels in Col-0 wild-type. For *EDS1A* knock-out plants which lack functional EDS1A protein and in addition are strongly depleted in *EDS1B* transcript abundance (Figure 3.21) this could be reasoned by a strong pathogen-inducibility of *EDS1B* expression by virulent DC3000. EDS1 protein was shown before to accumulate to hightened levels after infection of Ws-0 and Myc-PAD4 plants with the virulent *P. parasitica* isolate Emwa1 (Figure 3.16).

Bacterial growth of *P. syringae* pv. *tomato* strain DC3000 expressing *avrRps4* was then examined on the various *Arabidopsis* lines. Leaves were vacuum-infiltrated and bacterial titers were determined as described in Materials and Methods. Growth of *Pst* DC3000 expressing *avrRps4* is displayed in Figure 3.26. TIR-NB-LRR type *R* gene-mediated resistance in *pad4-1/sag101* double mutant plants was completely abolished as seen for *eds1* mutant plants in L*er* (*eds1-2*) and Ws-0 (*eds1-1*) accessions. Bacterial growth in *pad4-1* was intermediate between *sag101* and *pad4/sag101*. *Sag101* single mutants did not support bacterial growth above Col-0 wild-type levels.

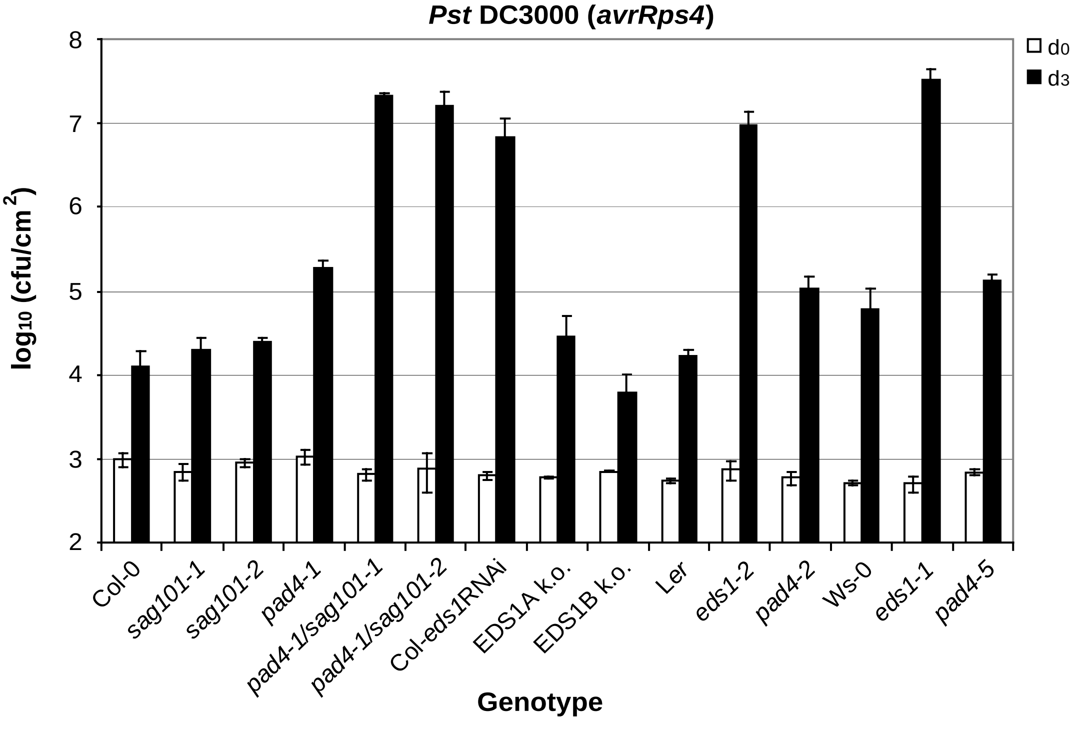

Fig. 3.26. *In planta* growth of *P. syringae* pv. *tomato* strain DC3000 expressing *avrRps4*. 5-week-old plants were vacuum-infiltrated with a bacterial suspension of *Pst* DC3000 expressing *avrRps4* at 5 x 10^5 cfu ml^{-1} and bacterial titers measured at day zero (d_0) and day three (d_3). Mutant lines are in accession Col-0 except *eds1-2* and *pad4-2* (accession L*er*) and *eds1-1* and *pad4-5* (accession Ws-0). Bacterial growth is expressed as mean values of viable bacteria per cm^2 leaf tissue ± standard deviation, resulting from two replicate samplings for d_0 and three replicate samplings for d_3 values. For details see text and Materials and Methods (2.2.11). This experiment was repeated with similar results.

The Col-*eds1*RNAi line enhanced growth of *Pst* DC3000 expressing *avrRps4* almost to levels seen in *pad4/sag101*. Bacterial growth in Col-*eds1*RNAi in an independent experiment was intermediate between *pad4-1* and *pad4-1/sag101* levels which would correspond to the results seen for Col-*eds1*RNAi when infected with *P. parasitica* isolate Cala2, recognised by *RPP2*. However, the difference between Col-*eds1*RNAi and *pad4-1/sag101* upon *P. parasitica* Cala2 infection was more pronounced as seen for infection with DC3000 expressing *avrRps4* (Figures 3.23 and 3.26).

The T-DNA insertion lines in *EDS1A* or *EDS1B* did not enhance bacterial growth above Col-0 wild-type levels. The fact that Col-*eds1*RNAi plants supported higher bacterial growth as *EDS1A* knock-out plants, which lack EDS1A and display depletion of *EDS1B* transcripts in the range of Col-*eds1*RNAi could again be explained therefore that *EDS1B* expression is still pathogen inducible whereas silencing in Col-*eds1*RNAi is effective to suppress *EDS1* expression and induction.

These results confirm the complete loss of *R* gene-mediated resistance in *pad4/sag101* double mutants conditioned by *RPP2* (Figure 3.18) and *RPP4* (data not shown) after infection with the incompatible *P. parasitica* isolates Cala2 and Emwa1, respectively and show that the combined activities of PAD4 and SAG101 are required to restrict the growth of incompatible bacterial and oomycete pathogens in TIR-NB-LRR type *R* gene-conditioned resistance.

Finally it was examined whether the combined activities of PAD4 and SAG101 are also genetically required for disease resistance signalling conditioned by the CC-NB-LRR type *R* gene *RPM1*. For this purpose the bacterial growth of *Pst* DC3000 expressing *avrRpm1* was examined within the *Arabidopsis* lines tested before. Plants were vacuum-infiltrated and bacterial titers were determined as described in Materials and Methods (see 2.2.11). As shown in Figure 3.27, neither of the tested *Arabidopsis* mutants displayed a significant enhancement in disease susceptibility towards infection with *Pst* DC3000 expressing *avrRpm1* compared to the corresponding wild-type controls.

This result demonstrates that the combined activities of PAD4 and SAG101 are either not required or can be overridden in resistance conferred by the CC-NB-LRR type *R* gene *RPM1*.

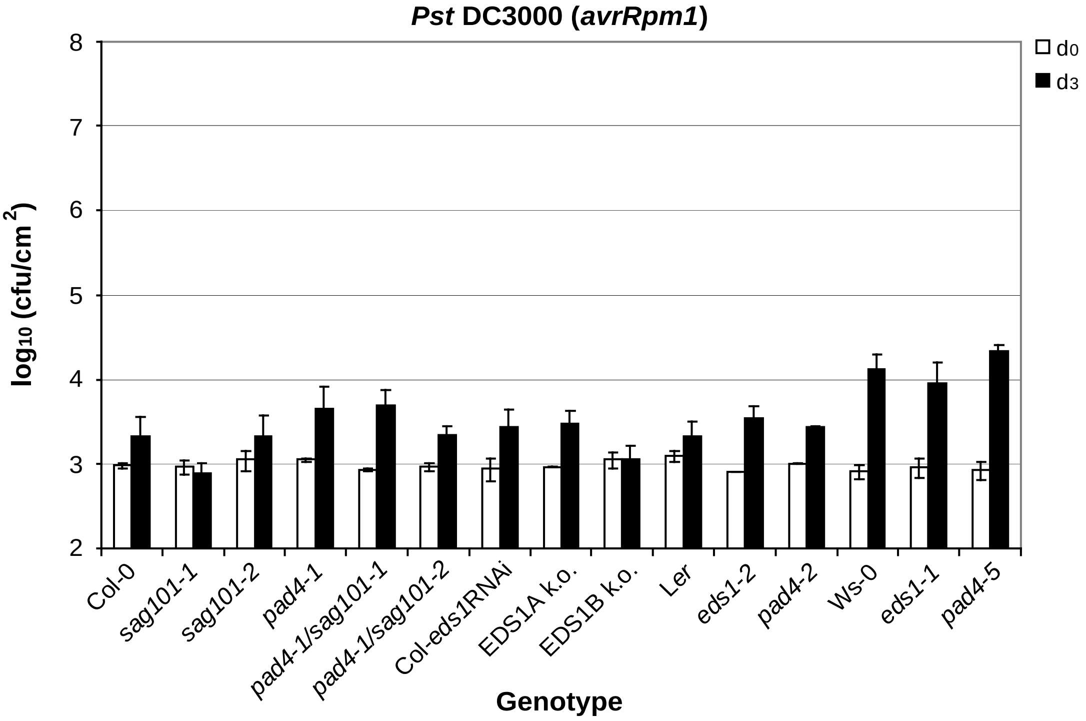

Fig. 3.27. *In planta* growth of *P. syringae* pv. *tomato* strain DC3000 expressing *avrRpm1*. 5-week-old plants were vacuum-infiltrated with a bacterial suspension of *Pst* DC3000 expressing *avrRpm1* at 5 x 10^5 cfu ml^{-1} and bacterial titers measured at day zero (d_0) and day three (d_3). Mutant lines are in accession Col-0 except *eds1-2* and *pad4-2* (accession L*er*) and *eds1-1* and *pad4-5* (accession Ws-0). Bacterial growth is expressed as mean values of viable bacteria per cm^2 leaf tissue ± standard deviation, resulting from two replicate samplings for d_0 and three replicate samplings for d_3 values. For details see text and Materials and Methods (2.2.11).

3.3.3 Summary of the role of SAG101 in plant innate immunity

The results described in chapter 3.3 show that SAG101 a direct EDS1-interactor inside the nucleus signals in plant innate immunity. *Sag101* single mutant plants did not display a detectable disease resistance phenotype in *R* gene-mediated or in basal plant resistance. In order to test whether SAG101 could be redundant with PAD4, *pad4/sag101* double mutants were generated. Those double mutant plants exhibited complete loss of TIR-NB-LRR type *R* gene-mediated resistance against avirulent oomycete and bacterial pathogens as well as loss of basal resistance against virulent isolates of these pathogens. Impairment of *pad4/sag101* double mutants in both of these responses was at least as severe as in *eds1* mutant plants and shows that the combined activities of PAD4 and SAG101 are essential for full resistance and programmed cell death triggered by TIR-NB-LRR type R proteins and expression of basal defences against virulent pathogens. The activities of PAD4 and SAG101 were either not needed or could be overridden in resistance conferred by the CC-NB-LRR type *R* gene, *RPM1*. SAG101 therefore contributes a significant activity to the EDS1-regulated resistance pathway.

Both EDS1 interacting partners, SAG101 and PAD4, were shown to stabilise EDS1 protein and to be required for full EDS1 accumulation. However, loss of disease resistance in *pad4/sag101* plants that are strongly depleted in EDS1 protein, is not simply due to the reduction of EDS1 level, since a Col-*eds1*RNAi line that is even further depleted in EDS1, displayed significantly stronger resistance against incompatible *P. parasitica* isolates. PAD4 and SAG101 are therefore likely to have intrinsic signalling capabilities beyond just stabilising EDS1, at least in TIR-NB-LRR type *R* gene triggered resistance. The fact, that Col-*eds1*RNAi plants displayed a similar degree of susceptibility as *pad4/sag101* to virulent bacterial and oomycete pathogens furthermore suggests that maintenance of a certain threshold of EDS1 is important for full expression of basal resistance and that EDS1 levels required for expression of R protein-triggered responses are below those that are required for effective signal relay in basal resistance.

4 Discussion

Arabidopsis EDS1 and its interacting partner, PAD4, constitute a regulatory hub that is essential for basal resistance against virulent pathogens and is engaged by TIR-type NB-LRR proteins in signalling isolate-specific pathogen recognition. By virtue of their inherent domain structures, EDS1 and PAD4 together with SAG101, a third lipase-like protein, constitute a unique protein-triade in higher plants. The domains of sequence homology of SAG101 to EDS1 and PAD4 and the finding that SAG101 is part of an EDS1 complex in soluble protein extracts of healthy (pathogen-unchallenged) leaf tissues suggested an involvement of SAG101 within the EDS1 and PAD4 defence regulatory pathway. However, experimental proof for this assumption was missing. Also, the subcellular compartments in which EDS1, PAD4 and SAG101 fulfil their respective signalling functions were not known. A key aim of this study was to uncover the subcellular localisations of EDS1, PAD4 and SAG101 and the molecular and spatial nature of EDS1 associations within the cell. Another aim was to determine a possible role of SAG101 in plant innate immunity and whether this is related to EDS1 and PAD4 signalling. In order to gain insights to possible further signalling properties of EDS1, PAD4 and SAG101 another aspect of this study was to analyse the tissue specific expression of these three lipase-like proteins. The results achieved will be summarised, evaluated and discussed.

4.1 *EDS1*, *PAD4* and *SAG101* are expressed in all major plant organs

EDS1 and PAD4 proteins are present in healthy and pathogen challenged juvenile and mature leaves (Feys *et al.*, 2001) where they fulfil functions as defence regulators in resistance to oomycete, fungal and bacterial pathogens (Glazebrook *et al.*, 1996; Parker *et al.*, 1996; Feys *et al.*, 2001; Xiao *et al.*, 2001; Xiao *et al.*, 2005). *SAG101* transcription was shown to increase in senescent leaves of *Arabidopsis* accession Col-*glabrous1* (He and Gan, 2002). Nothing so far was known about *EDS1*, *PAD4* and *SAG101* expression in different plant tissues. Knowledge of their tissue specific expression patterns could point to further signalling properties in response to multiple pathogen classes with distinct infection habits. EDS1 and PAD4 were shown to interact in healthy and pathogen challenged leaf tissues (Feys *et al.*, 2001). This study and Feys *et al.* (submitted) furthermore revealed that EDS1 is able to homodimerise and interact with SAG101 *in planta*. Feys *et al*. (submitted) also demonstrated that PAD4 and SAG101 protein accumulation in leaf tissues strictly required the presence of their interacting partner EDS1 (see also 4.2.2). If this is a phenomenon throughout the plant then a prediction would be that PAD4 and SAG101 proteins are only present in tissues where EDS1 is expressed.

In order to monitor the tissue specific expression of EDS1, PAD4 and SAG101 the Myc-PAD4 transgenic line LM41-2 expressing 5x c-Myc-tagged PAD4 under its native promoter (Feys *et al*., 2001) was chosen for immunoblot analyses of total protein extracts derived from unchallenged tissues, such as flowerbuds, cauline leaves, stems, young rosette leaves, senescent rosette leaves and roots. The Myc-PAD4 line expresses EDS1, SAG101 and also the *Myc-PAD4* transgene at wild-type physiological levels (Feys *et al*., submitted) and was chosen due to the lack of a workable PAD4 antibody. As demonstrated in Figure 3.1, EDS1 and PAD4 proteins were detectable in all of the analysed tissues and confirmed the assumption that PAD4 is present in tissues where EDS1 is expressed. This correlates with the finding that PAD4 functions in combination with EDS1 (Feys *et al*., 2001; Rustérucci *et al*., 2001; Feys *et al*., submitted). Three independent experiments revealed consistently highest abundance of EDS1 and PAD4 in cauline leaves, young rosette leaves and roots, whereas these two proteins were expressed at lower levels in flowerbuds and stems. The abundance of EDS1 and PAD4 in leaf tissues is consistent with their known functions as essential signalling components in resistance against certain leaf diseases (Parker *et al*., 1996; Feys *et al*., 2001; Xiao *et al*., 2001; Xiao *et al*., 2005). As EDS1 and PAD4 were also highly abundant in roots (Figures 3.1- 3.3 and data not shown) these proteins may also be involved in disease resistance signalling processes against certain root pathogens. Work in the past was focussed on EDS1 and PAD4 functions in aerial tissues, so experimental proof for this speculation is lacking.

The constitutive expression of EDS1 and PAD4 throughout all plant tissues is consistent with a role as signalling components in plant innate immunity in which signal perception and transduction require pre-existing proteins. Moreover, the presence of EDS1 in all of these tissues could be rationalised by its early signalling activity that is necessary for the oxidative burst and expression of the hypersensitive response (HR) in TIR-NB-LRR triggered defence (Feys *et al*., 2001; Rustérucci *et al*., 2001). A fast signal relay through the EDS1 signalling pathway upon pathogen perception would logically require preformed EDS1 protein. The coexistence of PAD4 in these tissues might account for the second function known for EDS1 that recruits PAD4 for defence potentiation through the accumulation of SA

(Feys *et al.*, 2001). However, it still needs to be proven whether EDS1 and PAD4 interact in tissues other than leaves as demonstrated by Feys *et al.* (2001).

The existence of EDS1 and PAD4 throughout the different tissues might also be correlated with their function in establishment of systemic acquired resistance (SAR). The failure of *eds1* and *pad4* in both signal emission from local tissues and distal signal perception (L. Jorda, A. Maldonado and J. Parker, unpublished data) implies that in wild-type plants both proteins are present in local and distal tissues and coincides with their known role as defence potentiators (Feys *et al.*, 2001; Rustérucci *et al.*, 2001). As the establishment of SAR is associated with elevated levels of SA both at the site of infection and in systemic tissues (Mou *et al.*, 2003), a possible role of EDS1 and PAD4 might lie in the activation or amplification of responses via an SA-dependent positive feedback loop in both local and systemic tissues (Feys *et al.*, 2001). Recently, SABP2 (SA-binding protein 2), a methyl salicylate (MeSA) esterase with high SA-binding binding affinity purified from tobacco, was found by virus-induced gene silencing (VIGS) to be necessary for full expression of basal and systemic resistance to tobacco mosaic virus (TMV) (Kumar and Klessig, 2003). Interestingly, SABP2, like EDS1 and PAD4, belongs to the α/β-fold hydrolase super family and shares the GXSXG motif containing the active site serine as part of a catalytic triade with EDS1 and PAD4 (Figure 3.4) (Kumar and Klessig, 2003; Forouhar *et al.*, 2005). Forouhar *et al.* (2005) proposed that both short- and long-distance transmission of SA synthesised at the site of infection involves converting it first into the more hydrophobic MeSA that can cross membranes more easily. They further suggest a role for SABP2 in the hydrolysis of biologically inactive MeSA into active SA in the target cell as part of the signal transduction pathways that activates SAR and, perhaps, local defence responses as well (Forouhar *et al.*, 2005). Another protein, *Arabidopsis* DIR1, a putative apoplastic lipid transfer protein, contributes to long-distance signalling in systemic resistance and is proposed to function in cooperation with a mobile signal, preferentially a lipid or lipid derived molecule, either as a translocator for release of the signal into the vascular tissue or as a chaperone to transmit the signal through the plant (Maldonado *et al.*, 2002). Although it remains to be established whether SABP2 and/or DIR1 are systemic components of an EDS1 and PAD4 driven amplification system, the involvement of these four proteins in SAR-signalling points towards the possibility of lipids or lipid-derived molecules being mobile signals in SAR (Durrant and Dong, 2004). So far it is not known whether also SAG101 is involved in SAR.

Attempts to monitor SAG101 protein levels in the same tissue protein extracts of Myc-PAD4 plants by immunoblot analysis failed under the experimental conditions. This was most likely due to the sensitivity of the rabbit polyclonal SAG101 antibody that gave high background signals in total protein extracts and whose affinity towards its antigen appeared to be weak. However, B. Feys (Sainsbury Laboratory, Norwich, UK) was able to demonstrate the presence of SAG101 protein in soluble extracts of 4-week-old unchallenged Myc-PAD4 leaf tissues (Feys *et al.*, submitted). Under the experimental conditions used in my study it was only feasible to detect SAG101 in total protein extracts after pathogen induction (Figure 3.15) or after an enrichment of the protein in nuclear fractions (Figure 3.7), arguing for a low abundance of SAG101 in unchallenged tissues and its strong pathogen inducibility. RT-PCR analysis revealed the presence of *SAG101* transcripts in the different tissues demonstrating the existence of *SAG101* mRNA (data not shown). However, J. Bautor (MPIZ, Cologne) detected incrementally increased SAG101 protein levels in juvenile, mature and senescent rosette leaves suggesting increased transcription of *SAG101* in senescent tissues as was demonstrated by He and Gan (2002). The finding that *SAG101* transcripts were detectable in all tissues was strengthened by *Arabidopsis* gene expression microarray data (Zimmermann *et al.*, 2004) (see 3.1.2) that were accessed to retrieve the expression levels of *SAG101* as well as of *EDS1* and *PAD4* in the different tissues. Although *SAG101* transcription increases incrementally in juvenile rosette leaves, adult rosette leaves and senescent rosette leaves, consistent with protein data of J. Bautor (see above), transcripts were abundant in all tissues (Figure 3.2). Lowest *SAG101* transcript abundance in flowers and stems (Figure 3.2) correlated with lowest EDS1 and PAD4 protein abundance in these tissues compared to the other tissues examined (see 3.1.1). Overall, *SAG101* transcript levels were lower compared to *EDS1* and *PAD4* in the different tissues and might also have contributed to the failure to detect SAG101 protein in the diverse unchallenged tissues.

The EDS1 immunoblot and microarray data were compared with the transcriptional activity of the native EDS1 promoter (P_{EDS1}) by using P_{EDS1}*::GUS* stable transgenic *Arabidopsis* lines (see 3.1.3). Four independent soil grown lines in accession Ws-0 and Col-0 were analysed for *EDS1* promoter activity in pathogen unchallenged tissues via GUS activity staining. The four lines displayed consistent GUS staining patterns. GUS staining observed in these lines was in general, consistent with the immunoblot and microarray data. Thus P_{EDS1}*::GUS* is expressed in all plant tissues, although stems displayed only weak and diffuse GUS staining (Figure 3.3.). This was the only difference when comparing GUS and microarray data (Figures 3.2 and 3.3) since the microarray data indicated a stronger expression of *EDS1* in stems (see *EDS1A* in Figure 3.2). Low GUS activity in stems could be due to the fact that lignified stems were more difficult to infiltrate with GUS staining solution than other tissues and thus substrate accessibility for the enzymatic reaction was limited. This was further supported by the fact that increased GUS activity was detectable in the area of stem segments that had been cut for staining (Figure 3.3 and data not shown). This most likely displayed a better substrate accessibility rather than wound induction as the stems were infiltrated with GUS staining solution directly after cutting. Also, staining of *P_{EDS1}::GUS* leaves 24 h after wound-injury did not result in *GUS* induction typically seen for wound-responsive promoters or promoter elements (data not shown; S. Rietz, MPIZ, personal communication). The low EDS1 protein abundance in total flower extracts was supported by the GUS staining data which revealed that the *P_{EDS1}::GUS* expression in flowers was locally restricted to the tips of stigmata as well as the tips and bases of siliques (Figure 3.3). The GUS staining patterns further supported the finding of high *EDS1* expression in roots, in particular in root hairs and lateral root initials.

Previous analyses have shown that *EDS1* expression is induced upon pathogen challenge (Falk *et al.*, 1999; Feys *et al.*, 2001). Also, in the present study EDS1 protein levels increased upon inoculation with virulent *P. parasitica* (Figure 3.16). However, infection of 2-week-old *P_{EDS1}::GUS* lines with virulent and avirulent *P. parasitica* isolates did not reveal obviously enhanced GUS activity in cells adjacent to HR lesions in the incompatible interactions or in cells surrounding growing pathogen mycelium in compatible interactions. This may be due to the already high *P_{EDS1}*-driven *GUS* expression in unchallenged leaves of 2-week-old plants (Figure 3.3). In contrast to the *P_{EDS1}::GUS* lines, no *GUS* expression in unchallenged tissues of the *SAG101* enhancer trap line Sel139 was detected (Figure 3.15). Enhanced expression of the *GUS* reporter gene in Sel139 upon virulent and avirulent *P. parasitica* infection demonstrated strong pathogen inducibility of the *SAG101* promoter in cells that were directly in contact with the pathogen or in close proximity to those cells (Figure 3.15).

So far little is known about the expression profiles of other defence regulatory compounds in diverse plant tissues. *NPR1*, a key regulator of SAR that functions downstream of SA is expressed throughout the plant at low levels (Durrant and Dong, 2004). *NPR1* is also required for another induced resistance response that is triggered by non-pathogenic root-colonising bacteria, known as induced systemic resistance (ISR) and confers resistance to bacteria and fungi in aerial plant tissues (Pieterse *et al.*, 1998; Iavicoli *et al.*, 2003; Durrant and Dong, 2004). Whether the strong presence of EDS1 and PAD4 in roots correlates with an involvement in ISR signalling is not yet known. Another example of a disease resistance component that is expressed throughout the plant is SGT1 (suppressor of the G2 allele of *SKP1*) (S. Betsuyaku and J. Parker, unpublished data). SGT1 has features of animal HSP90 co-chaperones and appears to be required as an assembly factor for R protein complex accumulation (Shirasu and Schulze-Lefert, 2003). Unlike EDS1 and PAD4, that are essential for resistance specified by the TIR-NB-LRR class of R proteins, SGT1 is required for resistance mediated by R proteins of both the TIR-NB-LRR and the CC-NB-LRR class (Austin *et al.*, 2002; Muskett *et al.*, 2002; Tör *et al.*, 2002; Muskett and Parker, 2003) and also for non-host resistance in *N. benthamiana* (Peart *et al.*, 2002b).

In summary, the data presented in section 3.1 demonstrate the presence of EDS1 and PAD4 proteins in all of the plant tissues, consistent with their important function in plant disease resistance signalling both in local responses and systemic tissues and the ability of diverse plant pathogens to cause disease in different tissues. Constitutive expression of EDS1 and PAD4 ready to process a signal after pathogen recognition might thereby account for rapid defence signal relay. The transcription of *SAG101* in all tissues implies that the SAG101 protein is present within these unchallenged tissues and might signal in cooperation with EDS1 and PAD4 throughout the plant, as was demonstrated in this study in infection assays of leaf tissues (see also 4.3.2).

4.2 Subcellular localisation of EDS1, PAD4 and SAG101 and analysis of their *in vivo* interactions via fluorescence resonance energy transfer (FRET)

Our current understanding of signal transduction processes is based on the idea that signalling proteins may translocate and/or undergo reversible binding interactions as key steps of the signal transmission process. Until this study it was not known where within the cell EDS1 and PAD4 fulfil their functions as essential disease resistance signalling components and whether SAG101 is involved in this signalling process. In order to unravel the signalling functions of EDS1, PAD4 and SAG101 it was therefore important to determine their localisations in the cell and the nature of associations with each other.

4.2.1 EDS1 and PAD4 co-localise in the cytosol and the nucleus whereas SAG101 is exclusively nuclear

EDS1 and PAD4 are predicted to be soluble from their amino acid sequences as they lack an obvious signal peptide or transmembrane region (Falk *et al.*, 1999; Jirage *et al.*, 1999). They were also shown to be present in soluble protein extracts (Feys *et al.*, 2001). Immunoblot analyses of soluble and microsomal membrane fractions of leaf tissues performed in this study demonstrated that EDS1 and PAD4 are soluble proteins in unchallenged cells (see 3.2.1 and Figure 3.9). Thus, if these proteins possess any lipase or lipid binding activity it is likely to be in the soluble compartment of the cell. However, it will be important to test if any changes in their subcellular distribution occur upon pathogen infection.

For detailed analysis of EDS1, PAD4 and SAG101 subcellular localisations a single cell particle bombardment assay was utilised (see 2.2.14.2). Detached *Arabidopsis eds1-1/pad4-5* leaves were co-transfected with DNA constructs containing *EDS1* driven by the CaMV double 35S promoter (P_{35SS}) and fused to a C-terminal YFP tag (P_{35SS}*::EDS1::YFP*) (see 2.2.13.11 and Figure 3.5) and either P_{35SS}*::PAD4::CFP* or P_{35SS}*::SAG101::CFP*. Intracellular fluorescence analysed by confocal laser scanning microscopy (CLSM) revealed that EDS1 and PAD4 co-localised both in the cytosol and inside the nucleus whereas SAG101 was only detected in the nuclear compartment (Figure 3.6). Similar partitioning of these proteins in cellular fractionation experiments of wild-type or Myc-PAD4 leaf tissues (see 3.2.1 and Figure 3.7) suggested that the transiently overexpressed proteins were correctly localised and that the fluorescence observed was not due to overexpression or bombardment artefacts but reflects their physiological localisation in pathogen-unchallenged tissues. Additionally, expression of all full length fusionprotein constructs was verified by transient *Agrobacterium*-mediated expression in *N. benthamiana* leaves. In these tests, no free CFP or YFP was detectable by immunoblot analyses (data not shown), demonstrating that nuclear fluorescence was not due to passive diffusion of free CFP of YFP into the nucleus.

The same subcellular distributions of EDS1-YFP, PAD4-CFP and SAG101-CFP were obtained when the fusionprotein constructs were not co-bombarded but expressed individually in single epidermal cells of *Arabidopsis eds1-1/pad4-5* leaves, demonstrating, that PAD4 and SAG101, at least when transiently overexpressed, do not depend on the presence of EDS1 to enter the nucleus. Moreover, EDS1-YFP fluorescence was still observed inside nuclei after bombardment into *sag101* or *pad4/sag101* cells, indicating that EDS1 also does not dependent on SAG101 or PAD4 to enter the nucleus.

Inspection of the amino acid sequences of EDS1, PAD4 and SAG101 revealed motifs that were consistent with their observed subcellular localisations (see 3.2 and Figure 3.4). SAG101 was found to possess a potential monopartite nuclear localisation signal (NLS) whereas EDS1 contains two possible bipartite NLSs (Falk *et al.*, 1999). Although PAD4 does not contain an obvious NLS, it was found that PAD4 harbours a putative nuclear export signal (NES) that was also found in EDS1 but is absent in SAG101 and might account for the subcellular distributions of these three proteins (la Cour *et al.*, 2004).

The ability of proteins to enter the nucleus without possessing a predicted NLS has been demonstrated. Recently, it was reported that rice (*Oryza sativa*) MOC1 is located in the nucleus without containing a conventional NLS and thus might possess an unidentified NLS or might be imported into the nucleus through a NLS independent mechanism (Li *et al.*, 2003). Similarly, another protein from rice, *Os*LSD1, a functional homolog of *Arabidopsis* LSD1, was shown to localise in the nucleus although no NLS could be predicted in its protein sequence (Wang *et al.*, 2005). Interestingly, *Arabidopsis LSD1* encodes a zinc finger protein that negatively regulates a cell death pathway by a repressive function on an SA-dependent feedback-loop controlled by EDS1 and PAD4 (see also 1.2) (Dietrich *et al.*, 1997; Rustérucci *et al.*, 2001; Mateo *et al.*, 2004). Whether there is a direct interplay of EDS1, or PAD4 and LSD1 inside the nucleus has not been investigated.

The fact that both EDS1 and PAD4 were found to localise in the cytosol and the nucleus and that both proteins contain putative NESs, suggested that shuttling of EDS1 and/or PAD4 between these two compartments might be important for defence signal relay (see also Model in Figure 4.1). Mobility between the cytosol and nucleus is an essential feature of another plant defence regulator, NPR1, an ankyrin-repeat protein controlling basal and systemic resistance downstream of SA (Cao *et al.*, 1997; Zhang *et al.*, 1999; Kinkema *et al.*, 2000; Mou *et al.*, 2003; Dong, 2004). NPR1, like EDS1 contains a bipartite NLS (Kinkema *et al.*, 2000). In the absence of SA, NPR1 accumulates in an oligomeric complex in the cytosol through intermolecular disulfide bridges (Mou *et al.*, 2003). SA causes a cellular redox change which ultimately reduces NPR1, causing it to form monomers that can translocate to the nucleus and activate defence gene expression. One further recent finding is notable in this regard. MOS3, a putative nucleoporin 96 that localises to the nuclear envelope, was shown to be an essential signalling component of basal resistance and a constitutively activated variant of the TIR-NB-LRR type R protein SNC1 (Zhang and Li, 2005). Constitutive disease resistance conferred by the *snc1* (*suppressor of npr1-1, constitutive 1*) gain-of-function mutation not only requires MOS3 as a signalling compound but also depends on the signalling properties of EDS1 and PAD4 (Li *et al.*, 2001; Zhang *et al.*, 2003). Their subcellular localisations together with the fact that EDS1, PAD4 and MOS3 signal in basal defences and the same *R* gene-triggered resistance pathway suggest that nuclear-cytoplasmic trafficking plays a vital role in both *R* gene-mediated and basal plant disease resistance (see also Figure 4.1). Identification of MOS3 as a component shared between *R* gene signalling and basal resistance (Zhang and Li, 2005), that is also the case for EDS1, PAD4 and SAG101 (Aarts *et al.*, 1998; Feys *et al.*, 2001; Xiao *et al.*, 2005; Feys *et al.*, submitted) further suggests that significant overlap exists between the signal transduction pathways of *R* gene-mediated and basal resistance responses.

In order to gain insights into possible subcellular localisation dynamics of EDS1 upon triggering of resistance responses via pathogen inoculations or application of diverse stimuli such as redox stress (Rustérucci *et al.*, 2001; Mateo *et al.*, 2004), stable transgenic EDS1 fluorescent protein (fp)-tagged lines have been generated in the *eds1-1* mutant background (see 3.2.1). Fluorescence microscopy of these lines expressing EDS1-CFP or EDS1-YFP under control of P_{35SS} or the native L*er EDS1* promoter (P_{EDS1}) revealed the same cellular distribution as seen in the single cell bombardment assay although fluorescence of P_{EDS1} driven lines was weak (Figure 3.8). The C-terminal fp-tags did not interfere with EDS1 function in these stable transgenic plants as they fully complemented the *eds1-1* mutant phenotype upon infection with incompatible *P. parasitica* (data not shown). Overexpression of EDS1 in transgenic plants did not have apparent detrimental effects on the plant, as could for example also be shown for overexpression of *NPR1* (Cao *et al.*, 1998; Friedrich *et al.*, 2001). Immunoblot analyses confirmed that fluorescence observed inside nuclei was not due to a passive diffusion of free CFP or YFP, as only full length fusion proteins were detectable (data not shown). A C-terminal CFP- or YFP-tag also did not interfere with PAD4 function in stable transgenic plants of *pad4-5* expressing the fusion proteins under control of P_{35SS} or P_{PAD4}. The generation of stable transgenic SAG101 lines with the CFP and YFP fusion protein constructs used for the single cell bombardment assay (see also 3.2.1) is in progress.

I wished to investigate whether fp-tagged EDS1 changes in cellular localisation upon triggering EDS1 dependent responses. Initial experiments, in which EDS1 fp-tagged lines were infiltrated with *Pseudomonas syringae* pv. *tomato* (*Pst*) DC3000 expressing *avrRps4* to trigger EDS1-dependent resistance responses so far did not reveal obvious changes in the localisation of EDS1 compared to 10 mM $MgCl_2$ control-infiltrated lines (data not shown). As mentioned above, it is possible that EDS1 shuttles between the cytosol and the nucleus as the protein contains both, an NLS and NES (Figure 3.4). It is thus conceivable that the subcellular distribution of EDS1 does not change obviously upon triggering of the defence pathway. However, it is possible that an “activated” version of EDS1, possibly through conformational changes upon changes in the cellular redox state, as demonstrated for NPR1 (Mou *et al.*, 2003), or a phosphorylation event, activates defence responses upon entering a different cell compartment. Binding of a lipid or lipid derived molecule upon triggering of the pathway might also account for activation of EDS1 which could then passage its ligand into a different compartment to activate defences. Alternatively, it is tempting to speculate that an activated EDS1 version could be translocated to the nucleus merely to remove it from the cytoplasm and thereby prevent it functioning there. Retention of EDS1 in the nuclear compartment might be facilitated in response to a signal that mediates a conformational change in EDS1 and masks the NES or through NES-masking by direct binding of another protein in the NES region. Inhibition of nuclear export by NES-masking through direct protein interaction has recently been shown for BRCA1 (breast cancer type 1 susceptibility protein) and BARD1 (BRCA1-associated RING domain protein 1) (Fabbro *et al.*, 2002; Rodriguez *et al.*, 2004) in human cells. BARD1 is a nucleo-cytoplasmic shuttling protein that contains an NES which facilitates its nuclear export. The BARD1 NES is located within the BRCA1-binding domain, resulting in nuclear anchorage of BARD1 upon heterodimersation with BRCA1. Interestingly, BARD1 and BRCA1 stabilise each other and similar to BARD1, BRCA1 also shuttles between the cytosol and the nucleus when not bound to BARD1 (Rodriguez and Henderson, 2000; Fabbro *et al.*, 2002). As binding of BRCA1 to BARD1 also masks the NES of BRCA1 the two proteins regulate the subcellular localisation of one another through reciprocal masking of their respective NES, thereby trapping the heterodimer in the nucleus. Nuclear retention of BARD1 reduces its apoptotic function in the cytoplasm and is important for cell survival (Rodriguez *et al.*, 2004). The authors further predicted that nuclear localisation of BARD1 could directly inhibit an apoptosis-stimulating factor which is activated upon export of BARD1 and that specific cellular signals might trigger dissociation of the BRCA1-BARD1 complex and thereby lead to a nuclear export-associated pathway for cell death (Rodriguez *et al.*, 2004). Whether a related regulatory mechanism is true for EDS1 and PAD4 that also might shuttle between the cytosol and the nucleus, is not known.

Shuttling between the cytoplasm and the nucleus has also been described for an mammalian isoform of Phosphatidylinositol-specific phospholipase C (PI-PLC), PI-PLCδ_1. PI-PLC hydrolyse phosphatidylinositol-4,5-bisphosphate generating inositol-1,4,5-

trisphosphate and diacylglycerol, both of which act as second messengers. In mammalian cells, inositol-1,4,5-trisphosphate was shown to participate in intracellular Ca^{2+} mobilisation whereas diacylglycerol attracts and activates certain protein kinase C (PKC) isoforms (Neri *et al.*, 1998; Yamaga *et al.*, 1999; Irvine, 2003). The predominant cytosolic localisation of PI-PLCδ_1 was shown to be the result of a functional NES. By using leptomycin B (LMB), a specific inhibitor of NES-dependent nuclear export, or disruption of the putative NES, the authors were able to demonstrate nuclear accumulation of GFP-tagged PI-PLCδ_1 in transfected Madin-Darby canine kidney cells (Yamaga *et al.*, 1999). LMB has been shown to bind directly and irreversibly to the export receptor CRM1 (exportin1; XPO1) for leucine-rich NESs to inhibit NES-mediated active nuclear export (Kudo *et al.*, 1999).

In one approach to reveal whether EDS1 might shuttle between the cytosol and nucleus, I generated protoplasts from the stable transgenic plants expressing fp-tagged EDS1 under control of P_{35SS} and the P_{EDS1} (see above, 3.2.1 and Figure 3.8). Experiments that are in progress utilise this protoplast system for application of the nuclear export inhibitor LMB (see above). If EDS1 constantly shuttles between these two compartments, the prediction would be that fp-tagged EDS1 would accumulate inside nuclei upon LMB application. Furthermore, protoplasts possess the advantage that pharmacological stimuli such as redox signals that EDS1 transduces (Rustérucci *et al.*, 2001; Mateo *et al.*, 2004; Wiermer *et al.*, in press), could be applied simultaneously to a large number of cells to trigger EDS1-dependent responses.

In order to monitor EDS1 in a perpetual activated state, the EDS1 fp-tagged stable transgenic plants were crossed to *snc1/eds1-2* double mutant plants and are currently in process of selection. The constitutive disease resistance and stunted morphology of *snc1* mutant plants are suppressed by *eds1* and *pad4* (Li *et al.*, 2001; Zhang *et al.*, 2003). I therefore predicted that crossing wild-type EDS1 containing the fp-tag into *snc1/eds1-2* would result in constitutive *snc1*-mediated defence responses that depend on “activated” EDS1. “Activated” fp-tagged EDS1 could then be analysed for its subcellular distribution and furthermore, protoplasts of those lines could be generated and monitored for nucleo-cytoplasmic shuttling of “activated” EDS1 through application of LMB to the protoplast medium (see above).

The EDS1 fp-tagged lines will further be crossed to PAD4 fp-tagged lines (N. Medina-Escobar and J. Parker, unpublished data) in order to monitor protein-protein interactions between these proteins upon pathogen infection via FRET-APB. Although no FRET signals were obtained for the interaction between fluorescently tagged EDS1 and PAD4 in pathogen unchallenged tissues (Figure 3.14 and discussed under 4.2.2), pathogen infection might increase the association between these two proteins and allow monitoring of changes in their association dynamics. Although an increase in co-immunoprecipitatable amount of EDS1 and PAD4 upon pathogen infection has been demonstrated (Feys *et al.*, 2001) it is not known in which cellular compartment(s) this increased interaction takes place.

4.2.2 EDS1 forms molecularly and spatially distinct associations

At the start of this study B. Feys could demonstrate that SAG101 is an EDS1-associated protein in soluble protein extracts of healthy (pathogen-unchallenged) leaf tissues (see also 3.2.2). However, the molecular and spatial nature of this association was not known. In this study I was able to demonstrate that SAG101 interacts directly with EDS1 *in planta* and that this interaction occurs in the nucleus (Figures 3.11 and 3.12). Consistently, a stronger signal for EDS1-YFP fluorescence was observed inside the nucleus and much weaker signals were obtained in the cytosol when EDS1-YFP was co-expressed with SAG101-CFP, suggesting that EDS1 might be preferentially held inside the nucleus by SAG101 (Figure 3.6). With regard to the nuclear localisation of SAG101 and its strong accumulation upon pathogen infection (see also 4.3.1 and Figure 3.15) I reasoned that EDS1, which might shuttle between the cytosol and the nucleus (see 4.2.1), could be trapped by SAG101 inside the nucleus and thus provide a mechanism by which the EDS1 pathway might be regulated (see also Figure 4.1). Nuclear retention of EDS1 might be facilitated by NES-masking through direct protein-protein interaction, as was demonstrated for the nucleo-cytoplasmic shuttling proteins BARD1 and BRCA1 (see 4.2.1).

Also, results presented in this study demonstrated the capability of EDS1 to dimerise *in planta*, as was suggested by yeast two-hybrid experiments (Feys *et al.*, 2001). FRET-APB experiments spatially resolved that EDS1-EDS1 interaction in unchallenged leaf tissues takes place in the cytosol but is absent inside the nucleus (Figure 3.13). This could be due to the presence of SAG101 in the nucleus which might compete with EDS1 dimers for binding (see above and Figure 4.1) or be a consequence of differential recruitment to the nucleus due to differences in accessibility of nuclear localisation signals. The absence of detectable EDS1 homomeric dimers in the nucleus further implies a difference in EDS1 interaction dynamics between these two cellular compartments, indicating that signal relay through the EDS1 regulatory pathway depends on its ability to form molecularly and spatially distinct associations (see also Figure 4.1).

The fact that the known *in planta* interaction between EDS1 and PAD4 (Feys *et al.*, 2001) was not reproducible by FRET-APB under the tested conditions could be due to a weak or transient interaction between these two proteins in unchallenged tissues. This would be consistent with recent Gal4-system based yeast two-hybrid data using EDS1 as bait. Through quantification of β-galactosidase activity in a liquid culture assay it appeared that strong interaction was found for EDS1-SAG101 and for EDS1-EDS1 but very weak interaction was found for EDS1-PAD4 (S. Malonek and J. Parker, unpublished results). The failure to detect interaction between EDS1-CFP and PAD4-YFP via FRET-APB in the cytosol or in the nucleus could also be due to the molecular orientations of the C-terminal fp-tags which might preclude transfer of fluorescence energy between this donor-acceptor pair. It is also conceivable that the EDS1-PAD4 interaction was not detectable because only a minor pool of EDS1 interacts with PAD4 as demonstrated by B. Feys, who was further able to resolve distinct EDS1-, PAD4- and SAG101-containing protein complexes by looking at their size exclusion chromatography profiles in leaf soluble extracts of pathogen-unchallenged plants (Feys *et al.*, submitted). The entire cellular pool of PAD4 associated with only a small proportion of total EDS1 in a ~200 kDa complex, which could be composed of EDS1 homodimers identified by FRET analysis (Figure 3.13) or EDS1 in combination with as yet unidentified component(s) (see also Figure 4.1). The EDS1-PAD4 complex did not appear to contain SAG101 because there was no migration-shift towards a lower molecular weight pool in a *sag101* mutant line. This was supported by the finding that EDS1, but not SAG101 protein, could be co-immunoprecipitated with Myc-PAD4 from soluble cell extracts (M. Wiermer and J. Parker, unpublished data). The bulk of EDS1 migrated at a size of ~120 kDa, consistent with the presence of EDS1 homo- and/or heterodimers. A “tail” of EDS1 migrating more slowly may thereby represent a small pool of monomeric EDS1. In contrast to PAD4, SAG101 protein migrated with the principle 120 kDa pool of EDS1, suggesting that most SAG101 associates with EDS1 in a complex that does not contain PAD4. Residual EDS1 in the ~120 kDa range in a *sag101* mutant might reflect the presence of EDS1 homodimers (see also Figure 4.1). Although PAD4 associated with only a minor fraction of the total EDS1 pool in the ~200 kDa fraction, mutations in *pad4* caused a significant reduction of EDS1 in the ~120 kDa complexes, suggesting a degree of co-regulation between individual EDS1 complexes that might be important for signal relay (Feys *et al.*, submitted).

The formation of separate EDS1-SAG101 and EDS1-PAD4 complexes in unchallenged leaf tissues was further supported by the fact that EDS1, PAD4 and SAG101 have mutually stabilising effects on their interacting partners (see 3.3.2.3, Figure 3.20 and Feys *et al.* (submitted)). SAG101 and PAD4 contributed additively to EDS1 accumulation (Figures 3.20 and 3.22) which by itself was stringently required for accumulation of both of its interaction partners SAG101 and PAD4 (Feys *et al.*, submitted). The requirement for EDS1 to stabilise both SAG101 and PAD4 implies that EDS1 may act as a type of adapter or scaffold for these two components to assure appropriate information flow through the EDS1 pathway (Smith and Scott, 2002; Morrison and Davis, 2003; Park *et al.*, 2003; Ziogas *et al.*, 2005). It was found that KSR (kinase suppressor of Ras), a molecular scaffold that binds Raf , MEK (MAPKK) and ERK (MAPK) and regulates signalling through the Raf/MEK/ERK kinase cascade (MAPK pathway), continuously undergoes nucleo-cytoplasmic shuttling (Brennan *et al.*, 2002) as was suggested for EDS1 and PAD4 (see 4.2.1 and Figure 4.1). Nucleo-cytoplasmic distribution of KSR is dynamically regulated by phosphorylation and through its direct interacting partner, MEK, that also shuttles continuously in and out of the nucleus (Adachi *et al.*, 2000). These results demonstrat that regulating the subcellular distribution of signalling components is one way a scaffold can control signalling through an intracellular pathway (Brennan *et al.*, 2002).

Thus, molecularly and spatially distinct EDS1, PAD4 and SAG101 associations have been discovered (Feys *et al.*, submitted) that point to a complex cellular dynamic between EDS1 and its signalling partners (Figure 4.1). However, the biochemical modes of action of these three proteins in resistance responses remain unclear. Stable transgenic *Arabidopsis* lines expressing EDS1 and PAD4 variants with exchanges of the predicted lipase catalytic residues were not compromised in resistance (B. Feys and J. Parker, unpublished data). The apparent dispensability of these catalytic amino acids in EDS1, PAD4 and their absence in wild-type SAG101 (Feys *et al.*, 2001; He and Gan, 2002) but retention of the lipase domains in all plant orthologues examined so far suggests that they may fulfil a structural rather than enzymatic role as discovered in some other signalling proteins (Llompart *et al.*, 2003; Wang *et al.*, 2003; Lu *et al.*, 2004). However, there are examples of dimerisation of lipases or esterases in various systems. In mammals the dimer of the cytosolic hormone-sensitive lipase (HSL) shows 40-fold greater activity than the monomer (Shen *et al.*, 2000) whereas lipoprotein lipase (LPL) is active as a dimer and not as monomer (Bergö *et al.*, 1996; Lookene *et al.*, 2004). Independent of its catalytical activity LPL has a further biologically relevant binding capacity by linking lipoproteins to the cell surface (Pentikäinen *et al.*, 2000). By analogy, the signalling functions of EDS1 and PAD4 could involve binding of a lipid molecule or its passage rather than its enzymatical processing. An increasing body of evidence points to the impact of various lipid derived molecules, lipid binding activities and lipases on plant cellular and systemic disease resistance signalling (Munnik *et al.*, 2000; Munnik, 2001; de Torres Zabela *et al.*, 2002; Maldonado *et al.*, 2002; Farmer *et al.*, 2003; Nandi *et al.*, 2003; Kachroo *et al.*, 2004; Nandi *et al.*, 2004; Shah, 2004; Forouhar *et al.*, 2005). In order to analyse possible ligand-binding of EDS1, stable transgenic *Arabidopsis* lines have been generated that express EDS1 with the eight amino acid affinity purification StrepII-tag under control of P_{EDS1} or P_{35SS}. *In planta* purification of StrepII-tagged EDS1 under native conditions from unchallenged and pathogen infected tissues might allow the identification of bound ligands via mass-spectrometry (E. Gobbato, M. Wiermer and J. Parker, experiments in progress).

Whatever the precise nature of EDS1-directed defence signal-transmission, the data presented in this work demonstrate the existence of molecularly and spatially distinct EDS1 associations in the cytoplasm and the nucleus. Evidence for co-regulation between individual EDS1 complexes further suggests that dynamic interactions of EDS1 and its signalling partners may also be important for defence signal relay (Feys *et al.*, submitted). The existence of a pre-existing pool of EDS1 and PAD4 in both compartments could favour a more rapid association to target molecules upon signal induction without the translocation-delay across the nuclear envelope and thus would be ideally suited for rapid signal transmission (Nigg, 1997; Gama-Carvalho and Carmo-Fonseca, 2001).

4.3 Investigating the role of SAG101 in *Arabidopsis* innate immunity

The finding that SAG101 physically interacts with EDS1 inside the plant nucleus and the sequence homology of SAG101 to the defence regulatory proteins EDS1 and PAD4 (Figure 3.4) prompted me to investigate a possible role of SAG101 in plant innate immunity.

4.3.1 EDS1, PAD4 and SAG101 accumulate upon pathogen infection

A first indication of involvement of SAG101 in plant innate immunity resulted from infections of the Col-*gl1 SAG101* enhancer trap line Sel139 containing a *GUS* reporter gene placed 3′ of the *SAG101* open reading frame (Figure 3.15 A, B) (He and Gan, 2002). This line displayed *GUS* reporter gene induction upon infection with virulent and avirulent *P. parasitica* isolates in cells around growing mycelium or HR lesions, respectively. Immunoblot analyses further revealed that SAG101 protein levels were elevated upon infection with virulent *P. parasitica* isolates (Figure 3.15 C), confirming the strong pathogen inducibility of the *SAG101* promoter. Enhanced expression of *SAG101* upon virulent and avirulent *P. parasitica* infection was suggestive of involvement of SAG101 in both *R* gene-mediated and basal plant defences. This assumption was verified by experiments demonstrating that SAG101 together with PAD4 contributes intrinsic signalling activities to the EDS1 signalling pathway (see 4.3.2).

The fact that SAG101 could not be detected in total protein extracts of non-infected Myc-PAD4 or Ws-0 plants under the experimental conditions was mentioned before (see 4.1) and was most likely due to the weak affinity of the SAG101 antibody towards its antigen. Nevertheless, SAG101 was shown to be present in unchallenged mature leaves of Myc-PAD4 and Ws-0 plants (Feys *et al.*, submitted). I could detect SAG101 in total protein extracts after infection with compatible *P. parasitica*. This demonstrated strong accumulation of SAG101 upon virulent *P. parasitica* infection and argued for its low abundance in pathogen-unchallenged leaf tissues.

An increase in EDS1 and PAD4 abundance was also seen in the same protein extracts of tissues infected with virulent *P. parasitica* when compared to unchallenged tissue extracts (Figure 3.16). This correlated with an increase in co-immunoprecipitable amounts of EDS1 and PAD4 after infection with virulent pathogens as demonstrated by Feys *et al.*, (2001).

Nevertheless, a clear increase in EDS1 and PAD4 protein levels in a compatible plant-pathogen interaction (Figure 3.16) has not been demonstrated before (for comparison see Feys *et al*., (2001)). Accumulation of EDS1 and PAD4 upon infection with virulent *P. parasitica* correlates with their important signalling function in basal disease resistance (Glazebrook *et al.*, 1996; Parker *et al.*, 1996; Aarts *et al.*, 1998; Feys *et al.*, 2001). The fact that *SAG101* expression is induced by compatible and incompatible *P. parasitica* isolates (Figure 3.15) is consistent with a requirement for SAG101 in plant defence (see 4.3.2).

4.3.2 SAG101 contributes to the EDS1 defence signalling pathway

In order to investigate the role of SAG101 in plant defence, two independent lines from the SLAT collection (Tissier *et al.*, 1999) in accession Col-0 that were homozygous for d*Spm* transposon insertions within the *SAG101* gene (referred to as *sag101-1* and *sag101-2*) were isolated by B. Feys (Feys *et al.*, submitted).

The *sag101-1* and *sag101-2* mutants were analysed for their disease resistance phenotype upon inoculation with virulent and avirulent isolates of *P. parasitica* or *Pst* DC3000. Resistance mediated by the TIR-type NB-LRR *R* genes *RPP2* (Figures 3.17 and 3.18) and *RPP4* (data not shown) against incompatible *P. parasitica* isolates and *RPS4* against *Pst* DC3000 expressing *avrRps4* (Figure 3.26) was unaffected in both *sag101* single mutant lines compared to the wild-type parental line, Col-0. Basal resistance responses in *sag101* single mutants also remained intact as these lines did not support sporulation of virulent *P. parasitica* (Figure 3.19) or bacterial growth of virulent *Pst* DC3000 (Figure 3.25) above levels seen in Col-0. This indicates that SAG101 function is either not needed for these resistance responses or is redundant with other *Arabidopsis* genes.

The pathogen responses of the *sag101* single mutants were in contrast to *pad4-1* that displayed weakened *RPP2*-, *RPP4*- (data not shown) and *RPS4*-mediated resistance, manifested as trailing plant cell necrosis (Figure 3.17) with significant sporulation of *P. parasitica* (Figure 3.18) and enhanced bacterial growth (Figure 3.26), respectively. Analysis of the *sag101* mutants in combination with *pad4* revealed that *SAG101* possesses a defence regulatory function that is partially redundant with *PAD4* in both TIR-NB-LRR type *R* gene-mediated and basal resistance. Moreover, the sum of PAD4 and SAG101 activities were found to be at least equivalent to EDS1 since *pad4*/*sag101* mutants were completely disabled in *RPP*-mediated resistance to *P. parasitica* (Figure 3.18 and data not shown) and *RPS4* resistance to *Pst* DC3000 expressing *avrRps4* (Figure 3.26). Indeed, the *pad4*/*sag101* combination appeared to create a "super-susceptible" background to the virulent *P. parasitica* isolate Noco2 (Figure 3.19) since the double mutant exhibited a greater loss of basal resistance than *pad4-1*. In other *Arabidopsis* accessions (Ws-0 and L*er*) *pad4* disables basal resistance and blocks ROI-derived signal potentiation as fully as *eds1* (see *eds1-2* and *pad4-2* in Figure 3.18 and Figure 3.25), suggesting equal contributions of EDS1 and PAD4 to these processes (Rustérucci *et al.*, 2001; Mateo *et al.*, 2004). The reason why the enhanced disease susceptibility phenotype of *pad4-1* upon infection with compatible *P. parasitica* Noco2 was not equivalent to *pad4-1/sag101* or *eds1* mutations in other accessions, as seen for infections with virulent *Pst* DC3000 (Figure 3.25) remains unclear. This might be a Col-0 accession specific phenomenon in basal resistance responses towards infection with virulent *P. parasitica* isolates. Infections of *pad4-1* mutant plants with other Col-0 compatible *P. parasitica* isolates (e.g. Emco5) should reveal whether this is a general phenomenon.

The infection phenotypes of *pad4-1/sag101* plants demonstrated that the combined activities of PAD4 and SAG101 are essential for full resistance and programmed cell death triggered by TIR-type NB-LRR proteins and expression of basal defences against virulent *P. parasitica*. This together with the findings that EDS1 associates with SAG101 inside the nucleus (see 3.2.2) and is stringently required for accumulation of SAG101 (Feys *et al.*, submitted) (see also 4.2.2) demonstrated that SAG101 contributes a significant activity to the EDS1-regulated resistance pathway. Resistance conferred by the CC-NB-LRR type *R* gene, *RPM1*, to *Pst* DC3000 expressing *avrRpm1* remained intact in *eds1* and *pad4-1/sag101* double mutant plants and is consistent with the notion that PAD4 and SAG101 contribute signalling activities to the EDS1 local resistance pathway that in general is necessary for TIR-NB-LRR but not CC-NB-LRR R proteins (Aarts *et al.*, 1998).

PAD4 and SAG101 stabilised EDS1 in an incremental fashion (Figure 3.20) consistent with the presence of distinct EDS1-PAD4 and EDS1-SAG101 associations in pathogen unchallenged cells (see 4.2.2 and Figure 4.1). EDS1 protein levels were depleted to ~60 % in *sag101*, 25 % in *pad4-1* and ~10 % in *pad4-1/sag101* compared to Col-0 wild-type levels. Also, EDS1 is stringently required to stabilise both PAD4 and SAG101 (Feys *et al.*, submitted). Two possible roles could be considered for PAD4 and SAG101. In one model, they structurally stabilise EDS1 that is the principle signalling moiety. Reducing EDS1 below a certain threshold (which would have to be below ~60 % seen in *sag101*) would therefore account for gradually increased disease susceptibility of *pad4-1* and *pad4-1/sag101* in TIR-NB-LRR type *R* gene-conditioned and basal resistance against virulent *P. parasitica*. In another model PAD4 and SAG101 contribute intrinsic signalling activity to the EDS1 complexes they reside in, implying that EDS1 may act as a scaffold for these two components to guarantee integrity of the signalling complexes and facilitate appropriate signal relay (see 4.2.2) (Smith and Scott, 2002; Morrison and Davis, 2003; Park *et al.*, 2003; Ziogas *et al.*, 2005). The reason for favouring the latter model resulted from infection phenotypes of the Col-*eds1*RNAi line (Feys *et al.*, submitted) in which two closely linked and highly sequence related *EDS1* genes, *EDS1A* and *EDS1B*, were effectively silenced (Figure 3.21). In Col-*eds1*RNAi, EDS1 protein levels were profoundly more depleted than in *pad4-1/sag101* to almost undetectable levels (Figure 3.22). However, *RPP2*- (Figure 3.22) and *RPP4*-mediated resistance (data not shown) were not as fully compromised as removing both PAD4 and SAG101 in *pad4-1/sag101*. These data demonstrate that PAD4 and SAG101 possess a defence regulatory function beyond stabilising EDS1 that is necessary for transduction of signals triggered by activated TIR-NB-LRR proteins leading to programmed cell death. Low amounts of EDS1 in Col-*eds1*RNAi (Figure 3.22) may be sufficient to transduce a signal from TIR-NB-LRR proteins to PAD4 and SAG101, that coupled to EDS1, amplify the defence response (Figure 3.23). Such amplification involving upregulation of *EDS1* and partners (Zhou *et al.*, 1998; Jirage *et al.*, 1999; Feys *et al.*, 2001; Xiao *et al.*, 2003; Chandra-Shekara *et al.*, 2004) may be critical for full expression of basal resistance and is supported by the finding that EDS1, PAD4 and SAG101 protein levels increased upon infection with virulent *P. parasitica* (Figures 3.15 and 3.16). The fact that the Col-*eds1*RNAi line displayed a similar degree of susceptibility as *pad4-1*/*sag101* to the virulent *P. parasitica* isolate Noco2 and *Pst* DC3000 (Figures 3.24 and 3.25) could be rationalised by a need to maintain a certain EDS1 threshold or inducibility of *EDS1* expression for full expression of basal resistance. Also, analysis of the T-DNA insertion lines in *EDS1A* and *EDS1B* point towards the importance of *EDS1* induction upon pathogen infection. Both copies of *EDS1* have been shown to complement the *eds1-2* mutant phenotype (J. Bautor, A. de Cruz-Cabral and J. Parker, unpublished data) (see also 3.3.2.4). *EDS1B* T-DNA insertion mutants that accumulate EDS1A protein to wild-type Col-0 levels (Figures 3.21 and 3.22) behaved like parental Col-0 in response to virulent and avirulent *P. parasitica* (Figure 3.23 and 3.24) and *Pst* (Figures 3.25 – 3.27). Despite the fact that *EDS1A* T-DNA insertion mutants do not express *EDS1A* and are strongly depleted in *EDS1B* transcripts to levels seen in Col-*eds1*RNAi (Figure 3.21), *EDS1A* insertion plants displayed stronger resistance than Col-*eds1*RNAi (Figures 3.23 – 3.24 and 3.25 – 3.26). This might be rationalised by the fact that *EDS1B* expression in the *EDS1A* insertion line is still pathogen inducible whereas both *EDS1* copies in Col-*eds1*RNAi are effectively silenced even after pathogen induction.

The finding that PAD4 and SAG101 possess a defence regulatory function beyond stabilising EDS1 was further supported by pathology phenotyping of *pad4-1/sag101* double mutant plants in response to the non-host powdery mildew pathogens *Erysiphe pisi* and *Blumeria graminis* f. sp. *hordei* (J. Dittgen, V. Lipka and P. Schulze-Lefert, unpublished) that normally infect barley and pea, respectively, and largely fail to penetrate *Arabidopsis* epidermal cells unless surface resistance is disabled (Collins *et al.*, 2003). In wild type *Arabidopsis* occasional spore germlings breach the surface layer but these rapidly induce epidermal cell death and grow no further (J. Dittgen, V. Lipka and P. Schulze-Lefert, unpublished). The *pad4*/*sag101* double mutant lines, significantly more than *eds1*, were found to permit sufficient invasive growth of the non-host powdery mildew isolates to enable pathogen sporulation. Therefore, the combined activities of PAD4 and SAG101 constitute a major basal resistance layer of *Arabidopsis* innate immunity to both host-adapted and non-host pathogens (J. Dittgen, V. Lipka and P. Schulze-Lefert, unpublished). These new findings add to those of previous studies that establish both common underlying processes and distinctions between host and non-host resistance responses involving the EDS1 pathway (Parker *et al.*, 1996; Yun *et al.*, 2003; Zimmerli *et al.*, 2004).

Results presented in this study demonstrated that SAG101 contributes to the EDS1 defence signalling pathway. Genetically, *SAG101* and *PAD4* are partially redundant. Loss of *SAG101* can be compensated for by the presence of *PAD4* in both TIR-NB-LRR type *R* gene-triggered and basal resistance (Figure 3.18 + 3.19 and 3.25 + 3.26). *SAG101* is not as efficient in compensating for the absence of *PAD4*, implying a unique PAD4 capability. This PAD4 activity, I reasoned, must be in combination with EDS1, since PAD4 depends on EDS1 for accumulation and all of the detectable PAD4 protein pool is associated with EDS1, at least in unchallenged cells (Feys *et al.*, submitted). Restriction of SAG101 to the nucleus may account for its inability to fully complement loss of PAD4 that localises to the cytosol and the nucleus (Figure 3.6). If this is the case, it follows that a cytosolic EDS1-PAD4 complex, and/or passaging of EDS1 and PAD4 between these two compartments may be important for signal relay as was suggested under 4.2.1. A model for the subcellular localisations and interaction of EDS1, PAD4 and SAG101 inside *Arabidopsis* cells is given in Figure 4.1

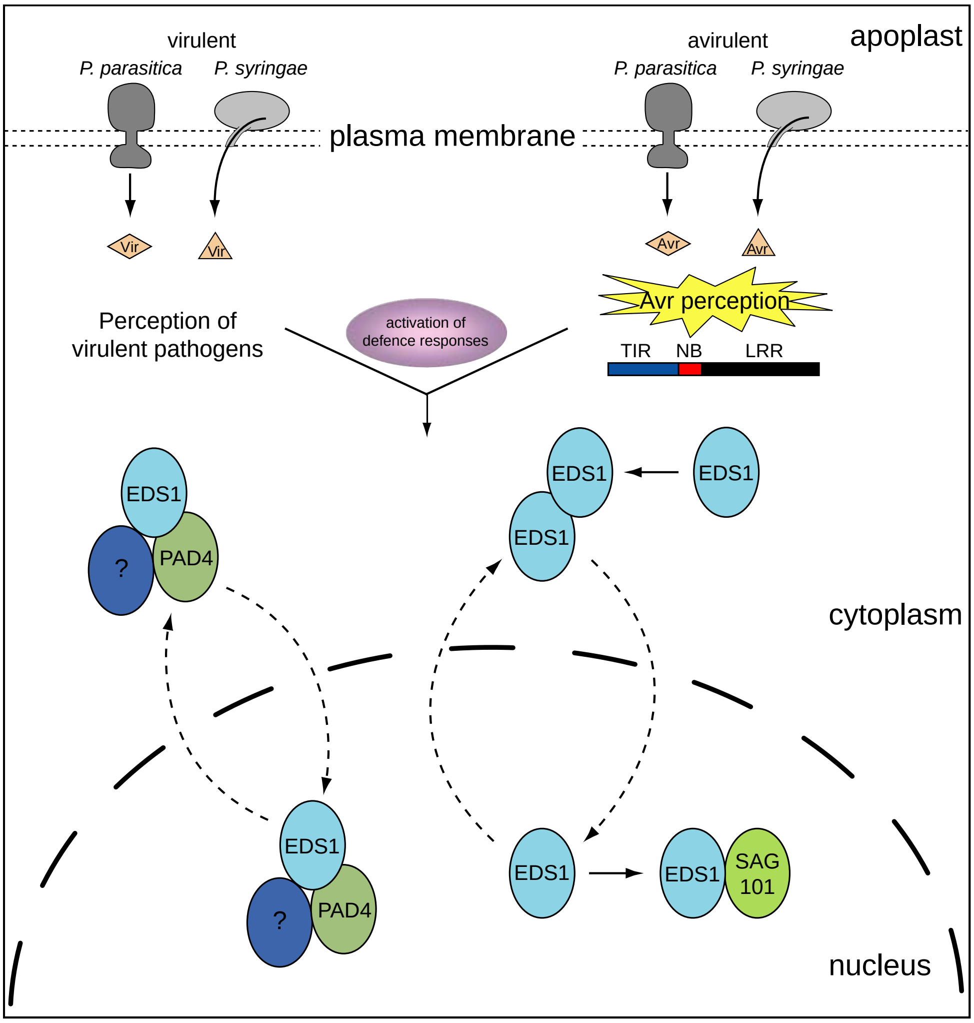

Fig. 4.1. Model for interaction dynamics of EDS1, PAD4 and SAG101 inside *Arabidopsis* cells. The subcellular localisations and interactions of EDS1, PAD4 and SAG101 depicted in this figure were found in healthy (pathogen-unchallenged) cells. Single cell bombardment assays of *Arabidopsis* leaves (Figure 3.6) and immunoblot analyses (Figure 3.7) revealed that EDS1 and PAD4 co-localise in the cytosol and the nucleus, whereas SAG101 is exclusively nuclear. A stronger presence of EDS1 was found in the nucleus when co-bombarded with SAG101 implying that SAG101 may hold EDS1 inside the nucleus. FRET studies resolved molecularly and spatially distinct EDS1 complexes. EDS1-SAG101 interaction was detected in the nucleus (Figure 3.11 and 3.12) whereas EDS1 homomeric dimers were detected in the cytoplasm but not in the nucleus (Figure 3.13). Feys *et al.* (submitted) could further demonstrate that the entire cellular pool of PAD4 associates with a small proportion of total EDS1 in a complex that could be composed of EDS1 homomeric dimers or EDS1 in combination with an as yet unidentified component(s). EDS1 and PAD4 localisation in the cytosol and the nucleus could be indicative of the presence of an EDS1-PAD4 complex in both compartments. A possible nuclear localisation signal in EDS1 and a putative nuclear export signal in both EDS1 and PAD4 suggests that these two proteins are shuttling between the cytoplasm and the nucleus (indicated by the dashed arrows). EDS1, PAD4 and SAG101 have mutually stabilising effects on their interacting partners. SAG101 and PAD4 contributed additively to EDS1 accumulation (Figures 3.20 and 3.22) which by itself was stringently required for accumulation of SAG101 and PAD4 (Feys *et al.*, submitted). The requirement for EDS1 to stabilise both SAG101 and PAD4 implies that EDS1 may act as a scaffold for these two components to assure appropriate information flow through the EDS1 pathway. The upper part of this figure illustrates that EDS1, PAD4 and SAG101 are essential signalling components of both TIR-NB-LRR protein triggered resistance to avirulent pathogens and basal resistance to virulent pathogens. In both responses SAG101 possesses a defence regulatory function that is partially redundant with PAD4. Loss of SAG101 can be compensated for by the presence of PAD4 but not *vice versa*. Restriction of SAG101 to the nucleus may account for its inability to fully complement the loss of PAD4. These data demonstrate that EDS1, PAD4 and SAG101, in concert, are important regulators of innate immunity and point to a complex nucleo-cytoplasmic dynamic between EDS1 and its interacting partners. Changes in the nature and/or distribution of these complexes triggered by a pathogen stimulus may be critical for defence signal relay. Vir and Avr: pathogen effectors. For further details see text.

4.4 Perspectives

The findings presented in this study and Feys *et al.* (submitted) revealed the existence of molecularly and spatially distinct EDS1 associations in the cytoplasm and the nucleus of pathogen-unchallenged *Arabidopsis* leaf tissues. Evidence for co-regulation between individual EDS1 complexes suggests a complex cellular dynamic between EDS1 and its signalling partners PAD4 and SAG101. Therefore changes in the nature and/or distribution of these signalling complexes triggered by a pathogen stimulus may be critical for defence signal relay.

Experiments in progress should resolve possible changes in spatial interaction dynamics between EDS1, PAD4 and SAG101 by their ability to co-immunoprecipitate from subcellular fractions upon triggering of the defence pathway. Stable transgenic *Arabidopsis* lines expressing fluorescent protein (fp)-tagged versions of EDS1, PAD4 and SAG101 might provide a powerful tool to analyse the dynamics of their localisations and associations upon triggering the EDS1 pathway by diverse stimuli (e.g. pathogen infections or application of redox stress). Experiments are also underway that utilise a protoplast system to trigger simultaneously a large number of cells through application of pharmacological compounds to the medium. Protoplasts have been generated from lines expressing fp-tagged EDS1 and addition of the nuclear export inhibitor LMB should reveal whether EDS1 is a nucleo-cytoplasmic shuttling protein. Further, to analyse if trapping of EDS1 inside the nucleus is sufficient to induce resistance responses, fp-tagged EDS1 variants of which the NES has been disrupted via site-directed mutagenesis will be stably transformed into *eds1* mutant backgrounds. The effect of retaining EDS1 in the cytosol on plant disease resistance will be accomplished by mutating the putative NLS of EDS1 and by fusing EDS1 to the glucocorticoid receptor (GR) which would allow release of the EDS1-GR fusion protein into the nucleus by addition of the steroid hormone dexamethasone (DEX). Fp-tagged EDS1 lines have also been crossed into a *snc1* mutant background which might allow us to monitor EDS1 in a constitutively activated state.

Finally, stable transgenic *Arabidopsis* lines have been generated that express StrepII-tagged EDS1 under control of P_{EDS1} or P_{35SS}. *In planta* purification of native EDS1-StrepII from healthy and pathogen-challenged leaf material might allow us to identify bound ligands or posttranscriptional modifications via mass-spectrometry that could be important for EDS1-directed signal transmission. The results obtained from these experiments will be vital to understand signal relay through the EDS1 pathway.

5 Literature

Aarts, N., Metz, M., Holub, E., Staskawicz, B.J., Daniels, M.J., and Parker, J.E. (1998). Different requirements for *EDS1* and *NDR1* by disease resistance genes define at least two *R* gene-mediated signaling pathways in *Arabidopsis*. Proc Natl Acad Sci U S A **95,** 10306-10311.

Abramovitch, R.B., and Martin, G.B. (2004). Strategies used by bacterial pathogens to suppress plant defenses. Curr Opin Plant Biol **7,** 356-364.

Adachi, M., Fukuda, M., and Nishida, E. (2000). Nuclear export of MAP kinase (ERK) involves a MAP kinase kinase (MEK)-dependent active transport mechanism. J Cell Biol **148,** 849-856.

Akira, S., and Takeda, K. (2004). Toll-like receptor signalling. Nat Rev Immunol **4,** 499-511.

Alonso, J.M., Stepanova, A.N., Leisse, T.J., Kim, C.J., Chen, H., Shinn, P., Stevenson, D.K., Zimmerman, J., Barajas, P., Cheuk, R., Gadrinab, C., Heller, C., Jeske, A., Koesema, E., Meyers, C.C., Parker, H., Prednis, L., Ansari, Y., Choy, N., Deen, H., Geralt, M., Hazari, N., Hom, E., Karnes, M., Mulholland, C., Ndubaku, R., Schmidt, I., Guzman, P., Aguilar-Henonin, L., Schmid, M., Weigel, D., Carter, D.E., Marchand, T., Risseeuw, E., Brogden, D., Zeko, A., Crosby, W.L., Berry, C.C., and Ecker, J.R. (2003). Genome-wide insertional mutagenesis of *Arabidopsis thaliana*. Science **301,** 653-657.

Athman, R., and Philpott, D. (2004). Innate immunity via Toll-like receptors and Nod proteins. Curr Opin Microbiol **7,** 25-32.

Austin, M.J., Muskett, P., Kahn, K., Feys, B.J., Jones, J.D., and Parker, J.E. (2002). Regulatory role of *SGT1* in early *R* gene-mediated plant defenses. Science **295,** 2077-2080.

Axtell, M.J., and Staskawicz, B.J. (2003). Initiation of *RPS2*-specified disease resistance in *Arabidopsis* is coupled to the AvrRpt2-directed elimination of RIN4. Cell **112,** 369-377.

Belkhadir, Y., Subramaniam, R., and Dangl, J.L. (2004). Plant disease resistance protein signaling: NBS-LRR proteins and their partners. Curr Opin Plant Biol **7,** 391-399.

Bergö, M., Olivecrona, G., and Olivecrona, T. (1996). Forms of lipoprotein lipase in rat tissues: in adipose tissue the proportion of inactive lipase increases on fasting. Biochem J **313 (Pt 3),** 893-898.

Brennan, J.A., Volle, D.J., Chaika, O.V., and Lewis, R.E. (2002). Phosphorylation regulates the nucleocytoplasmic distribution of kinase suppressor of Ras. J Biol Chem **277,** 5369-5377.

Cao, H., Li, X., and Dong, X. (1998). Generation of broad-spectrum disease resistance by overexpression of an essential regulatory gene in systemic acquired resistance. Proc Natl Acad Sci U S A **95,** 6531-6536.

Cao, H., Bowling, S.A., Gordon, A.S., and Dong, X.N. (1994). Characterization of an Arabidopsis Mutant That Is Nonresponsive to Inducers of Systemic Acquired-Resistance. Plant Cell **6,** 1583-1592.

Cao, H., Glazebrook, J., Clarke, J.D., Volko, S., and Dong, X. (1997). The Arabidopsis *NPR1* gene that controls systemic acquired resistance encodes a novel protein containing ankyrin repeats. Cell **88,** 57-63.

Chamaillard, M., Girardin, S.E., Viala, J., and Philpott, D.J. (2003a). Nods, Nalps and Naip: intracellular regulators of bacterial-induced inflammation. Cell Microbiol **5,** 581-592.

Chamaillard, M., Hashimoto, M., Horie, Y., Masumoto, J., Qiu, S., Saab, L., Ogura, Y., Kawasaki, A., Fukase, K., Kusumoto, S., Valvano, M.A., Foster, S.J., Mak, T.W., Nunez, G., and Inohara, N. (2003b). An essential role for NOD1 in host recognition of bacterial peptidoglycan containing diaminopimelic acid. Nature Immunology **4,** 702-707.

Chandra-Shekara, A.C., Navarre, D., Kachroo, A., Kang, H.G., Klessig, D., and Kachroo, P. (2004). Signaling requirements and role of salicylic acid in *HRT*- and *rrt*-mediated resistance to turnip crinkle virus in Arabidopsis. Plant J **40,** 647-659.

Chen, Z., Kloek, A.P., Boch, J., Katagiri, F., and Kunkel, B.N. (2000). The *Pseudomonas syringae avrRpt2* gene product promotes pathogen virulence from inside plant cells. Mol Plant Microbe Interact **13,** 1312-1321.

Chen, Z.Y., Kloek, A.P., Cuzick, A., Moeder, W., Tang, D.Z., Innes, R.W., Klessig, D.F., McDowell, J.M., and Kunkel, B.N. (2004). The *Pseudomonas syringae* type III effector AvrRpt2 functions downstream or independently of SA to promote virulence on *Arabidopsis thaliana*. Plant J **37,** 494-504.

Clarke, J.D., Aarts, N., Feys, B.J., Dong, X.N., and Parker, J.E. (2001). Constitutive disease resistance requires *EDS1* in the *Arabidopsis* mutants *cpr1* and *cpr6* and is partially *EDS1*-dependent in *cpr5*. Plant J **26,** 409-420.

Clough, S.J., and Bent, A.F. (1998). Floral dip: a simplified method for *Agrobacterium*-mediated transformation of *Arabidopsis thaliana*. Plant J **16,** 735-743.

Collins, N.C., Thordal-Christensen, H., Lipka, V., Bau, S., Kombrink, E., Qiu, J.L., Huckelhoven, R., Stein, M., Freialdenhoven, A., Somerville, S.C., and Schulze-Lefert, P. (2003). SNARE-protein-mediated disease resistance at the plant cell wall. Nature **425,** 973-977.

Dangl, J.L., and Jones, J.D.G. (2001). Plant pathogens and integrated defence responses to infection. Nature **411,** 826-833.

de Torres Zabela, M., Fernandez-Delmond, I., Niittyla, T., Sanchez, P., and Grant, M. (2002). Differential expression of genes encoding *Arabidopsis* phospholipases after challenge with virulent or avirulent *Pseudomonas* isolates. Mol Plant Microbe Interact **15,** 808-816.

Deslandes, L., Olivier, J., Peeters, N., Feng, D.X., Khounlotham, M., Boucher, C., Somssich, L., Genin, S., and Marco, Y. (2003). Physical interaction between RRS1-R, a protein conferring resistance to bacterial wilt, and PopP2, a type III effector targeted to the plant nucleus. Proc Natl Acad Sci USA **100,** 8024-8029.

Dietrich, R.A., Richberg, M.H., Schmidt, R., Dean, C., and Dangl, J.L. (1997). A novel zinc finger protein is encoded by the Arabidopsis *LSD1* gene and functions as a negative regulator of plant cell death. Cell **88,** 685-694.

Dong, X.N. (2004). NPR1, all things considered. Current Opinion in Plant Biology **7,** 547-552.

Durrant, W.E., and Dong, X. (2004). Systemic acquired resistance. Annu Rev Phytopathol **42,** 185-209.

Fabbro, M., Rodriguez, J.A., Baer, R., and Henderson, B.R. (2002). BARD1 induces BRCA1 intranuclear foci formation by increasing RING-dependent BRCA1 nuclear import and inhibiting BRCA1 nuclear export. J Biol Chem **277,** 21315-21324.

Falk, A., Feys, B.J., Frost, L.N., Jones, J.D.G., Daniels, M.J., and Parker, J.E. (1999). *EDS1*, an essential component of *R* gene-mediated disease resistance in *Arabidopsis* has homology to eukaryotic lipases. Proc Natl Acad Sci USA **96,** 3292-3297.

Farmer, E.E., Almeras, E., and Krishnamurthy, V. (2003). Jasmonates and related oxylipins in plant responses to pathogenesis and herbivory. Curr Opin Plant Biol **6,** 372-378.

Felix, G., Duran, J.D., Volko, S., and Boller, T. (1999). Plants have a sensitive perception system for the most conserved domain of bacterial flagellin. Plant J **18,** 265-276.

Feys, B.J., and Parker, J.E. (2000). Interplay of signaling pathways in plant disease resistance. Trends Genet **16,** 449-455.

Feys, B.J., Moisan, L.J., Newman, M.A., and Parker, J.E. (2001). Direct interaction between the *Arabidopsis* disease resistance signaling proteins, EDS1 and PAD4. EMBO J **20,** 5400-5411.

Feys, B.J., Wiermer, M., Bhat, R.A., Moisan, L.J., Medina-Escobar, N., Neu, C., Cabral, A., and Parker, J.E. (2005). *Arabidopsis* SENESCENCE-ASSOCIATED GENE101 Stabilizes and Signals within an ENHANCED DISEASE SUSCEPTIBILITY1 Complex in Plant Innate Immunity (submitted).

Flor, H.H. (1971). Current Status of Gene-for-Gene Concept. Annu Rev Phytopathol **9,** 275-&.

Forouhar, F., Yang, Y., Kumar, D., Chen, Y., Fridman, E., Park, S.W., Chiang, Y., Acton, T.B., Montelione, G.T., Pichersky, E., Klessig, D.F., and Tong, L. (2005). Structural and biochemical studies identify tobacco SABP2 as a methyl salicylate esterase and implicate it in plant innate immunity. Proc Natl Acad Sci U S A **102,** 1773-1778.

Friedrich, L., Lawton, K., Dietrich, R., Willits, M., Cade, R., and Ryals, J. (2001). *NIM1* overexpression in Arabidopsis potentiates plant disease resistance and results in enhanced effectiveness of fungicides. Mol Plant Microbe Interact **14,** 1114-1124.

Gadella, T.W.J., van der Krogt, G.N.M., and Bisseling, T. (1999). GFP-based FRET microscopy in living plant cells. Trends Plant Sci **4,** 287-291.

Gama-Carvalho, M., and Carmo-Fonseca, M. (2001). The rules and roles of nucleocytoplasmic shuttling proteins. Febs Lett **498,** 157-163.

Girardin, S.E., Sansonetti, P.J., and Philpott, D.J. (2002). Intracellular vs extracellular recognition of pathogens - common concepts in mammals and flies. Trends Microbiol **10,** 193-199.

Glazebrook, J. (2004). Contrasting Mechanisms of Defense Against Biotrophic and Necrotrophic Pathogens. Annu Rev Phytopathol.

Glazebrook, J., Rogers, E.E., and Ausubel, F.M. (1996). Isolation of Arabidopsis mutants with enhanced disease susceptibility by direct screening. Genetics **143,** 973-982.

Glazebrook, J., Zook, M., Mert, F., Kagan, I., Rogers, E.E., Crute, I.R., Holub, E.B., Hammerschmidt, R., and Ausubel, F.M. (1997). Phytoalexin-deficient mutants of *Arabidopsis* reveal that *PAD4* encodes a regulatory factor and that four *PAD* genes contribute to downy mildew resistance. Genetics **146,** 381-392.

Gómez-Gómez, L., and Boller, T. (2002). Flagellin perception: a paradigm for innate immunity. Trends Plant Sci **7,** 251-256.

Grant, M.R., Godiard, L., Straube, E., Ashfield, T., Lewald, J., Sattler, A., Innes, R.W., and Dangl, J.L. (1995). Structure of the *Arabidopsis RPM1* gene enabling dual specificity disease resistance. Science **269,** 843-846.

Gupta, V., Willits, M.G., and Glazebrook, J. (2000). *Arabidopsis thaliana EDS4* contributes to salicylic acid (SA)-dependent expression of defense responses: evidence for inhibition of jasmonic acid signaling by SA. Mol Plant Microbe Interact **13,** 503-511.

Hammond-Kosack, K.E., and Parker, J.E. (2003). Deciphering plant-pathogen communication: fresh perspectives for molecular resistance breeding. Curr Opin Biotech **14,** 177-193.

He, Y.H., and Gan, S.S. (2002). A gene encoding an acyl hydrolase is involved in leaf senescence in Arabidopsis. Plant Cell **14,** 805-815.

Heath, M.C. (2000). Nonhost resistance and nonspecific plant defenses. Curr Opin Plant Biol **3,** 315-319.

Hinsch, M., and Staskawicz, B. (1996). Identification of a new *Arabidopsis* disease resistance locus, *RPS4*, and cloning of the corresponding avirulence gene, *avrRps4*, from *Pseudomonas syringae* pv. *pisi*. Mol Plant Microbe Interact **9,** 55-61.

Holt, B.F., Hubert, D.A., and Dangl, J.L. (2003). Resistance gene signaling in plants - complex similarities to animal innate immunity. Curr Opin Immunol **15,** 20-25.

Holub, E.B., Beynon, L.J., and Crute, I.R. (1994). Phenotypic and Genotypic Characterization of Interactions between Isolates of *Peronospora parasitica* and Accessions of *Arabidopsis thaliana*. Mol Plant Microbe Interact **7,** 223-239.

Hu, G., deHart, A.K.A., Li, Y., Ustach, C., Handley, V., Navarre, R., Hwang, C.-F., Aegerter, B.J., Williamson, V.M., and Baker, B. (2005). *EDS1* in tomato is required for resistance mediated by TIR-class *R* genes and the receptor-like *R* gene *Ve*. Plant J **42,** 376-391.

Hua, J., Grisafi, P., Cheng, S.H., and Fink, G.R. (2001). Plant growth homeostasis is controlled by the *Arabidopsis BON1* and *BAP1* genes. Genes Dev **15,** 2263-2272.

Huitema, E., Vleeshouwers, V.G.A.A., Francis, D.M., and Kamoun, S. (2003). Active defence responses associated with non-host resistance of *Arabidopsis thaliana* to the oomycete pathogen *Phytophthora infestans*. Mol Plant Pathol **4,** 487-500.

Iavicoli, A., Boutet, E., Buchala, A., and Metraux, J.P. (2003). Induced systemic resistance in *Arabidopsis thaliana* in response to root inoculation with *Pseudomonas fluorescens* CHA0. Mol Plant Microbe Interact **16,** 851-858.

Innes, R.W., Bisgrove, S.R., Smith, N.M., Bent, A.F., Staskawicz, B.J., and Liu, Y.C. (1993). Identification of a disease resistance locus in *Arabidopsis* that is functionally homologous to the *RPG1* locus of soybean. Plant J **4,** 813-820.

Irvine, R.F. (2003). Nuclear lipid signalling. Nat Rev Mol Cell Bio **4,** 349-360.

Jambunathan, N., Siani, J.M., and McNellis, T.W. (2001). A humidity-sensitive Arabidopsis copine mutant exhibits precocious cell death and increased disease resistance. Plant Cell **13,** 2225-2240.

Jia, Y., McAdams, S.A., Bryan, G.T., Hershey, H.P., and Valent, B. (2000). Direct interaction of resistance gene and avirulence gene products confers rice blast resistance. EMBO J **19,** 4004-4014.

Jirage, D., Tootle, T.L., Reuber, T.L., Frost, L.N., Feys, B.J., Parker, J.E., Ausubel, F.M., and Glazebrook, J. (1999). *Arabidopsis thaliana* PAD4 encodes a lipase-like gene that is important for salicylic acid signaling. Proc Natl Acad Sci USA **96,** 13583-13588.

Kachroo, A., Venugopal, S.C., Lapchyk, L., Falcone, D., Hildebrand, D., and Kachroo, P. (2004). Oleic acid levels regulated by glycerolipid metabolism modulate defense gene expression in *Arabidopsis*. Proc Natl Acad Sci U S A **101,** 5152-5157.

Kamoun, S. (2001). Nonhost resistance to *Phytophthora*: novel prospects for a classical problem. Curr Opin Plant Biol **4,** 295-300.

Karpova, T.S., Baumann, C.T., He, L., Wu, X., Grammer, A., Lipsky, P., Hager, G.L., and McNally, J.G. (2003). Fluorescence resonance energy transfer from cyan to yellow fluorescent protein detected by acceptor photobleaching using confocal microscopy and a single laser. J Microsc-Oxford **209,** 56-70.

Kearney, B., and Staskawicz, B.J. (1990). Widespread distribution and fitness contribution of *Xanthomonas campestris* avirulence gene *avrBs2*. Nature **346,** 385-386.

Kinkema, M., Fan, W.H., and Dong, X.N. (2000). Nuclear localization of NPR1 is required for activation of *PR* gene expression. Plant Cell **12,** 2339-2350.

Kobayashi, Y., Kobayashi, I., Funaki, Y., Fujimoto, S., Takemoto, T., and Kunoh, H. (1997). Dynamic reorganization of microfilaments and microtubules is necessary for the expression of non-host resistance in barley coleoptile cells. Plant J **11,** 525-537.

Koch, E., and Slusarenko, A. (1990). *Arabidopsis* Is Susceptible to Infection by a Downy Mildew Fungus. Plant Cell **2,** 437-445.

Koncz, C., and Schell, J. (1986). The Promoter of T_L-DNA Gene 5 Controls the Tissue-Specific Expression of Chimeric Genes Carried by a Novel Type of *Agrobacterium* Binary Vector. Mol. Gen. Genet. **204,** 383-396.

Kudo, N., Matsumori, N., Taoka, H., Fujiwara, D., Schreiner, E.P., Wolff, B., Yoshida, M., and Horinouchi, S. (1999). Leptomycin B inactivates CRM1/exportin 1 by covalent modification at a cysteine residue in the central conserved region. Proc Natl Acad Sci U S A **96,** 9112-9117.

Kumar, D., and Klessig, D.F. (2003). High-affinity salicylic acid-binding protein 2 is required for plant innate immunity and has salicylic acid-stimulated lipase activity. Proc Natl Acad Sci USA **100,** 16101-16106.

Kunkel, B.N., and Brooks, D.M. (2002). Cross talk between signaling pathways in pathogen defense. Curr Opin Plant Biol **5,** 325-331.

la Cour, T., Kiemer, L., Molgaard, A., Gupta, R., Skriver, K., and Brunak, S. (2004). Analysis and prediction of leucine-rich nuclear export signals. Protein Eng Des Sel **17,** 527-536.

Li, X., Clarke, J.D., Zhang, Y.L., and Dong, X.N. (2001). Activation of an EDS1-mediated *R*-gene pathway in the *snc1* mutant leads to constitutive, NPR1-independent pathogen resistance. Mol Plant Microbe Interact **14,** 1131-1139.

Li, X., Qian, Q., Fu, Z., Wang, Y., Xiong, G., Zeng, D., Wang, X., Liu, X., Teng, S., Hiroshi, F., Yuan, M., Luo, D., Han, B., and Li, J. (2003). Control of tillering in rice. Nature **422,** 618-621.

Liu, Y.L., Schiff, M., Marathe, R., and Dinesh-Kumar, S.P. (2002). Tobacco *Rar1*, *EDS1* and *NPR1/NIM1* like genes are required for *N*-mediated resistance to tobacco mosaic virus. Plant J **30,** 415-429.

Llompart, B., Castells, E., Rio, A., Roca, R., Ferrando, A., Stiefel, V., Puigdomenech, P., and Casacuberta, J.M. (2003). The direct activation of MIK, a germinal center kinase (GCK)-like kinase, by MARK, a maize atypical receptor kinase, suggests a new mechanism for signaling through kinase-dead receptors. J Biol Chem **278,** 48105-48111.

Lookene, A., Zhang, L., Hultin, M., and Olivecrona, G. (2004). Rapid subunit exchange in dimeric lipoprotein lipase and properties of the inactive monomer. J Biol Chem **279,** 49964-49972.

Lu, W., Yamamoto, V., Ortega, B., and Baltimore, D. (2004). Mammalian Ryk is a Wnt coreceptor required for stimulation of neurite outgrowth. Cell **119,** 97-108.

Mackey, D., Holt, B.F., Wiig, A., and Dangl, J.L. (2002). RIN4 interacts with *Pseudomonas syringae* type III effector molecules and is required for RPM1-mediated resistance in *Arabidopsis*. Cell **108,** 743-754.

Mackey, D., Belkhadir, Y., Alonso, J.M., Ecker, J.R., and Dangl, J.L. (2003). *Arabidopsis* RIN4 is a target of the type III virulence effector AvrRpt2 and modulates RPS2-mediated resistance. Cell **112,** 379-389.

Maldonado, A.M., Doerner, P., Dixon, R.A., Lamb, C.J., and Cameron, R.K. (2002). A putative lipid transfer protein involved in systemic resistance signalling in *Arabidopsis*. Nature **419,** 399-403.

Mateo, A., Muhlenbock, P., Rusterucci, C., Chang, C.C., Miszalski, Z., Karpinska, B., Parker, J.E., Mullineaux, P.M., and Karpinski, S. (2004). *LESION SIMULATING DISEASE 1* is required for acclimation to conditions that promote excess excitation energy. Plant Physiol **136,** 2818-2830.

McLusky, S.R., Bennett, M.H., Beale, M.H., Lewis, M.J., Gaskin, P., and Mansfield, J.W. (1999). Cell wall alterations and localized accumulation of feruloyl-3'-methoxytyramine in onion epidermis at sites of attempted penetration by *Botrytis allii* are associated with actin polarisation, peroxidase activity and suppression of flavonoid biosynthesis. Plant J **17,** 523-534.

Menke, F.L.H., van Pelt, J.A., Pieterse, C.M.J., and Klessig, D.F. (2004). Silencing of the mitogen-activated protein kinase MPK6 compromises disease resistance in Arabidopsis. Plant Cell **16,** 897-907.

Meyers, B.C., Kozik, A., Griego, A., Kuang, H.H., and Michelmore, R.W. (2003). Genome-wide analysis of NBS-LRR-encoding genes in Arabidopsis. Plant Cell **15,** 809-834.

Morrison, D.K., and Davis, R.J. (2003). Regulation of MAP kinase signaling modules by scaffold proteins in mammals. Annu Rev Cell Dev Biol **19,** 91-118.

Mou, Z., Fan, W.H., and Dong, X.N. (2003). Inducers of plant systemic acquired resistance regulate NPR1 function through redox changes. Cell **113,** 935-944.

Munnik, T. (2001). Phosphatidic acid: an emerging plant lipid second messenger. Trends Plant Sci **6,** 227-233.

Munnik, T., Meijer, H.J., Ter Riet, B., Hirt, H., Frank, W., Bartels, D., and Musgrave, A. (2000). Hyperosmotic stress stimulates phospholipase D activity and elevates the levels of phosphatidic acid and diacylglycerol pyrophosphate. Plant J **22,** 147-154.

Muskett, P., and Parker, J. (2003). Role of *SGT1* in the regulation of plant *R* gene signalling. Microbes Infect **5,** 969-976.

Muskett, P.R., Kahn, K., Austin, M.J., Moisan, L.J., Sadanandom, A., Shirasu, K., Jones, J.D., and Parker, J.E. (2002). Arabidopsis *RAR1* exerts rate-limiting control of *R* gene-mediated defenses against multiple pathogens. Plant Cell **14,** 979-992.

Mysore, K.S., and Ryu, C.M. (2004). Nonhost resistance: how much do we know? Trends Plant Sci **9,** 97-104.

Nandi, A., Welti, R., and Shah, J. (2004). The *Arabidopsis thaliana* dihydroxyacetone phosphate reductase gene *SUPPRESSSOR OF FATTY ACID DESATURASE DEFICIENCY1* is required for glycerolipid metabolism and for the activation of systemic acquired resistance. Plant Cell **16,** 465-477.

Nandi, A., Krothapalli, K., Buseman, C.M., Li, M.Y., Welti, R., Enyedi, A., and Shah, J. (2003). Arabidopsis *sfd* mutants affect plastidic lipid composition and suppress dwarfing, cell death, and the enhanced disease resistance phenotypes resulting from the deficiency of a fatty acid desaturase. Plant Cell **15,** 3051-3051.

Neri, L.M., Borgatti, P., Capitani, S., and Martelli, A.M. (1998). Nuclear diacylglycerol produced by phosphoinositide-specific phospholipase C is responsible for nuclear translocation of protein kinase C-α. J Biol Chem **273,** 29738-29744.

Nigg, E.A. (1997). Nucleocytoplasmic transport: signals, mechanisms and regulation. Nature **386,** 779-787.

Nimchuk, Z., Eulgem, T., Holt, B.E., and Dangl, J.L. (2003). Recognition and response in the plant immune system. Annu Rev Genet **37,** 579-609.

Nürnberger, T., Brunner, F., Kemmerling, B., and Piater, L. (2004). Innate immunity in plants and animals: striking similarities and obvious differences. Immunol Rev **198,** 249-266.

Park, S.H., Zarrinpar, A., and Lim, W.A. (2003). Rewiring MAP kinase pathways using alternative scaffold assembly mechanisms. Science **299,** 1061-1064.

Parker, J.E., Holub, E.B., Frost, L.N., Falk, A., Gunn, N.D., and Daniels, M.J. (1996). Characterization of *eds1*, a mutation in Arabidopsis suppressing resistance to *Peronospora parasitica* specified by several different *RPP* genes. Plant Cell **8,** 2033-2046.

Parker, J.E., Szabò, V., Staskawicz, B.J., Lister, C., Dean, C., Daniels, M.J., and Jones, J.D.G. (1993). Phenotypic Characterization and Molecular Mapping of the *Arabidopsis thaliana* Locus *RPP5*, Determining Disease Resistance to *Peronospora parasitica*. Plant J **4,** 821-831.

Peart, J.R., Cook, G., Feys, B.J., Parker, J.E., and Baulcombe, D.C. (2002a). An *EDS1* orthologue is required for *N*-mediated resistance against tobacco mosaic virus. Plant J **29,** 569-579.

Peart, J.R., Lu, R., Sadanandom, A., Malcuit, I., Moffett, P., Brice, D.C., Schauser, L., Jaggard, D.A.W., Xiao, S.Y., Coleman, M.J., Dow, M., Jones, J.D.G., Shirasu, K., and Baulcombe, D.C. (2002b). Ubiquitin ligase-associated protein SGT1 is required for host and nonhost disease resistance in plants. Proc Natl Acad Sci USA **99,** 10865-10869.

Pentikäinen, M.O., Öörni, K., and Kovanen, P.T. (2000). Lipoprotein lipase (LPL) strongly links native and oxidized low density lipoprotein particles to decorin-coated collagen. Roles for both dimeric and monomeric forms of LPL. J Biol Chem **275,** 5694-5701.

Petersen, M., Brodersen, P., Naested, H., Andreasson, E., Lindhart, U., Johansen, B., Nielsen, H.B., Lacy, M., Austin, M.J., Parker, J.E., Sharma, S.B., Klessig, D.F., Martienssen, R., Mattsson, O., Jensen, A.B., and Mundy, J. (2000). *Arabidopsis* MAP kinase 4 negatively regulates systemic acquired resistance. Cell **103,** 1111-1120.

Pieterse, C.M., van Wees, S.C., van Pelt, J.A., Knoester, M., Laan, R., Gerrits, H., Weisbeek, P.J., and van Loon, L.C. (1998). A novel signaling pathway controlling induced systemic resistance in Arabidopsis. Plant Cell **10,** 1571-1580.

Reuber, T.L., Plotnikova, J.M., Dewdney, J., Rogers, E.E., Wood, W., and Ausubel, F.M. (1998). Correlation of defense gene induction defects with powdery mildew susceptibility in *Arabidopsis* enhanced disease susceptibility mutants. Plant J **16,** 473-485.

Ritter, C., and Dangl, J.L. (1995). The *avrRpm1* gene of *Pseudomonas syringae* pv. *maculicola* is required for virulence on *Arabidopsis*. Mol Plant Microbe Interact **8,** 444-453.

Rodriguez, J.A., and Henderson, B.R. (2000). Identification of a functional nuclear export sequence in BRCA1. J Biol Chem **275,** 38589-38596.

Rodriguez, J.A., Schüchner, S., Au, W.W., Fabbro, M., and Henderson, B.R. (2004). Nuclear-cytoplasmic shuttling of BARD1 contributes to its proapoptotic activity and is regulated by dimerization with BRCA1. Oncogene **23,** 1809-1820.

Rustérucci, C., Aviv, D.H., Holt, B.F., Dangl, J.L., and Parker, J.E. (2001). The disease resistance signaling components *EDS1* and *PAD4* are essential regulators of the cell death pathway controlled by *LSD1* in Arabidopsis. Plant Cell **13,** 2211-2224.

Sanger, F., Nicklen, S., and Coulson, A.R. (1977). DNA Sequencing with Chain-Terminating Inhibitors. Proc Natl Acad Sci USA **74,** 5463-5467.

Schmelzer, E. (2002). Cell polarization, a crucial process in fungal defence. Trends Plant Sci **7,** 411-415.

Schulze-Lefert, P. (2004). Knocking on heaven's wall: pathogenesis of and resistance to biotrophic fungi at the cell wall. Curr Opin Plant Biol **7,** 377-383.

Shah, H., Gadella, T.W.J., van Erp, H., Hecht, V., and de Vries, S.C. (2001). Subcellular localization and oligomerization of the *Arabidopsis thaliana* somatic embryogenesis receptor kinase 1 protein. J Mol Biol **309,** 641-655.

Shah, J. (2004). Lipids, Lipases, and Lipid-Modifying Enzymes in Plant Disease Resistance. Annu Rev Phytopathol.

Shao, F., Golstein, C., Ade, J., Stoutemyer, M., Dixon, J.E., and Innes, R.W. (2003). Cleavage of *Arabidopsis* PBS1 by a bacterial type III effector. Science **301,** 1230-1233.

Shen, W.J., Patel, S., Hong, R., and Kraemer, F.B. (2000). Hormone-sensitive lipase functions as an oligomer. Biochemistry **39,** 2392-2398.

Shirano, Y., Kachroo, P., Shah, J., and Klessig, D.F. (2002). A gain-of-function mutation in an Arabidopsis Toll Interleukin-1 Receptor-Nucleotide Binding Site-Leucine-Rich Repeat type R gene triggers defense responses and results in enhanced disease resistance. Plant Cell **14,** 3149-3162.

Shirasu, K., and Schulze-Lefert, P. (2003). Complex formation, promiscuity and multi-functionality: protein interactions in disease-resistance pathways. Trends Plant Sci **8,** 252-258.

Smith, F.D., and Scott, J.D. (2002). Signaling complexes: junctions on the intracellular information super highway. Curr Biol **12,** R32-40.

Thomma, B., Eggermont, K., Penninckx, I., Mauch-Mani, B., Vogelsang, R., Cammue, B.P.A., and Broekaert, W.F. (1998). Separate jasmonate-dependent and salicylate-dependent defense-response pathways in *Arabidopsis* are essential for resistance to distinct microbial pathogens. Proc Natl Acad Sci U S A **95,** 15107-15111.

Thordal-Christensen, H. (2003). Fresh insights into processes of nonhost resistance. Curr Opin Plant Biol **6,** 351-357.

Tissier, A.F., Marillonnet, S., Klimyuk, V., Patel, K., Torres, M.A., Murphy, G., and Jones, J.D.G. (1999). Multiple independent defective *Suppressor-mutator* transposon insertions in Arabidopsis: A tool for functional genomics. Plant Cell **11,** 1841-1852.

Tör, M., Gordon, P., Cuzick, A., Eulgem, T., Sinapidou, E., Mert-Türk, F., Can, C., Dangl, J.L., and Holub, E.B. (2002). Arabidopsis SGT1b is required for defense signaling conferred by several downy mildew resistance genes. Plant Cell **14,** 993-1003.

Underhill, D.M., and Ozinsky, A. (2002). Toll-like receptors: key mediators of microbe detection. Curr Opin Immunol **14,** 103-110.

Van der Biezen, E.A., and Jones, J.D. (1998). Plant disease-resistance proteins and the gene-for-gene concept. Trends Biochem Sci **23,** 454-456.

Viala, J., Chaput, C., Boneca, I.G., Cardona, A., Girardin, S.E., Moran, A.P., Athman, R., Memet, S., Huerre, M.R., Coyle, A.J., DiStefano, P.S., Sansonetti, P.J., Labigne, A., Bertin, J., Philpott, D.J., and Ferrero, R.L. (2004). Nod1 responds to peptidoglycan delivered by the *Helicobacter pylori cag* pathogenicity island. Nat Immunol **5,** 1166-1174.

Wang, L., Pei, Z., Tian, Y., and He, C. (2005). OsLSD1, a rice zinc finger protein, regulates programmed cell death and callus differentiation. Mol Plant Microbe Interact **18,** 375-384.

Wang, W., Hall, A.E., O'Malley, R., and Bleecker, A.B. (2003). Canonical histidine kinase activity of the transmitter domain of the ETR1 ethylene receptor from Arabidopsis is not required for signal transmission. Proc Natl Acad Sci U S A **100,** 352-357.

Wiermer, M., Feys, B.J., and Parker, J.E. (2005). Plant immunity: the EDS1 regulatory node. Curr Opin Plant Biol **8**. (in press).

Witte, C.P., Noël, L.D., Gielbert, J., Parker, J.E., and Romeis, T. (2004). Rapid one-step protein purification from plant material using the eight-amino acid StrepII epitope. Plant Molecular Biology **55,** 135-147.

Xia, Y.J., Nikolau, B.J., and Schnable, P.S. (1997). Developmental and hormonal regulation of the Arabidopsis *CER2* gene that codes for a nuclear-localized protein required for the normal accumulation of cuticular waxes. Plant Physiology **115,** 925-937.

Xiao, S., Calis, O., Patrick, E., Zhang, G., Charoenwattana, P., Muskett, P., Parker, J.E., and Turner, J.G. (2005). The atypical resistance gene, *RPW8*, recruits components of basal defence for powdery mildew resistance in Arabidopsis. Plant J **42,** 95-110.

Xiao, S.Y., Brown, S., Patrick, E., Brearley, C., and Turner, J.G. (2003). Enhanced transcription of the Arabidopsis disease resistance genes *RPW8.1* and *RPW8.2* via a salicylic acid-dependent amplification circuit is required for hypersensitive cell death. Plant Cell **15,** 33-45.

Xiao, S.Y., Ellwood, S., Calis, O., Patrick, E., Li, T.X., Coleman, M., and Turner, J.G. (2001). Broad-spectrum mildew resistance in *Arabidopsis thaliana* mediated by *RPW8*. Science **291,** 118-120.

Yamaga, M., Fujii, M., Kamata, H., Hirata, H., and Yagisawa, H. (1999). Phospholipase C-δ1 contains a functional nuclear export signal sequence. J Biol Chem **274,** 28537-28541.

Yang, S.H., and Hua, J. (2004). A haplotype-specific *Resistance* gene regulated by *BONZAI1* mediates temperature-dependent growth control in Arabidopsis. Plant Cell **16,** 1060-1071.

Yun, B.W., Atkinson, H.A., Gaborit, C., Greenland, A., Read, N.D., Pallas, J.A., and Loake, G.J. (2003). Loss of actin cytoskeletal function and EDS1 activity, in combination, severely compromises non-host resistance in *Arabidopsis* against wheat powdery mildew. Plant J **34,** 768-777.

Zhang, Y., and Li, X. (2005). A Putative Nucleoporin 96 Is Required for Both Basal Defense and Constitutive Resistance Responses Mediated by *suppressor of npr1-1*, *constitutive 1*. Plant Cell **17,** 1306-1316.

Zhang, Y., Fan, W., Kinkema, M., Li, X., and Dong, X. (1999). Interaction of NPR1 with basic leucine zipper protein transcription factors that bind sequences required for salicylic acid induction of the *PR-1* gene. Proc Natl Acad Sci U S A **96,** 6523-6528.

Zhang, Y.L., Goritschnig, S., Dong, X.N., and Li, X. (2003). A gain-of-function mutation in a plant disease resistance gene leads to constitutive activation of downstream signal transduction pathways in *suppressor of npr1-1*, *constitutive 1*. Plant Cell **15,** 2636-2646.

Zhou, F., Menke, F.L., Yoshioka, K., Moder, W., Shirano, Y., and Klessig, D.F. (2004). High humidity suppresses *ssi4*-mediated cell death and disease resistance upstream of MAP kinase activation, H_2O_2 production and defense gene expression. Plant J **39,** 920-932.

Zhou, N., Tootle, T.L., Tsui, F., Klessig, D.F., and Glazebrook, J. (1998). *PAD4* functions upstream from salicylic acid to control defense responses in Arabidopsis. Plant Cell **10,** 1021-1030.

Zimmerli, L., Stein, M., Lipka, V., Schulze-Lefert, P., and Somerville, S. (2004). Host and non-host pathogens elicit different jasmonate/ethylene responses in *Arabidopsis*. Plant J **40,** 633-646.

Zimmermann, P., Hirsch-Hoffmann, M., Hennig, L., and Gruissem, W. (2004). GENEVESTIGATOR. Arabidopsis microarray database and analysis toolbox. Plant Physiology **136,** 2621-2632.

Ziogas, A., Moelling, K., and Radziwill, G. (2005). CNK1 is a scaffold protein that regulates Src-mediated Raf-1 activation. J Biol Chem **in press**.

Zipfel, C., Robatzek, S., Navarro, L., Oakeley, E.J., Jones, J.D.G., Felix, G., and Boller, T. (2004). Bacterial disease resistance in *Arabidopsis* through flagellin perception. Nature **428,** 764-767.

Diese Arbeit wurde in der Arbeitsgruppe von Dr. Jane Parker am Max-Planck-Institut für Züchtungsforschung durchgeführt. Jane danke ich herzlich für die Möglichkeit zur Bearbeitung des interessanten Themas, ihre hundertprozentige Unterstützung während der gesamten Zeit sowie ihre ständige Diskussionsbereitschaft. Thanks a lot Jane!!!

Ebenso möchte ich meinem Doktorvater Prof. Dr. Paul Schulze-Lefert für so manch guten Ratschlag und die Möglichkeit zur Promotion am MPIZ danken.

Prof. Dr. M. Hülskamp danke ich für die freundliche Übernahme des Korreferats dieser Arbeit.

Prof. Dr. U.-I. Flügge danke ich für die Übernahme des Prüfungsvorsitzes.

Vielen Dank an die JP-Crew für die tolle Atmosphäre und ständige Hilfsbereitschaft, als da wären: Adriana, Dieter, Doris, Enrico, Guangyong, Jagreet, Jaqueline, Koh, Laurent, Lennart, Lucia, Michael, Nieves, Paul, Pino, Shige, Stefan und Steffen, sowie dem SL-Teil: Bart, Graeme und Lisa

Den „Romeis“ ein Dankeschön für die nette Laboratmosphäre und Hilfsbereitschaft.

Many thanks to Nieves for all her help and useful discussions.

Chibi-Marco und Dr. Bau sei gedankt für viel Spaß, Aufmunterung, so manch nette Kicker-Partie und die klasse Trips in die O-Zone.

Vielen Dank der Badminton-Bande für den sportlichen Ausgleich.

Many thanks to Riyaz for his help with all the FRET analyses and procession of data.

Für das Korrekturlesen dieser Arbeit sei nochmals Steffen „Frantisek“ gedankt.

Meinen Eltern danke ich von ganzem Herzen für all ihre Unterstützung.

Ein riesiges Dankeschön geht vor allem an Stine, die immer für mich da ist!!!

Ich versichere, dass ich die von mir vorgelegte Dissertation selbständig angefertigt, die benutzten Quellen und Hilfsmittel vollständig angegeben und die Stellen der Arbeit - einschließlich Tabellen, Karten und Abbildungen -, die anderen Werken im Wortlaut oder dem Sinn nach entnommen sind, in jedem Einzelfall als Entlehnung kenntlich gemacht habe; dass diese Dissertation noch keiner anderen Fakultät oder Universität zur Prüfung vorgelegen hat; dass sie - abgesehen von den auf Seite I angegebenen Teilpublikationen - noch nicht veröffentlicht worden ist sowie, dass ich eine solche Veröffentlichung vor Abschluss des Promotionsverfahrens nicht vornehmen werde. Die Bestimmungen dieser Promotionsordnung sind mir bekannt. Die von mir vorgelegte Dissertation ist von Prof. Dr. Paul Schulze-Lefert betreut worden.

Köln, 17. Mai 2005

(Marcel Wiermer)

Lebenslauf

Angaben zur Person

Name:	Marcel Wiermer
Geburtsdatum/-ort:	22. Januar 1976 in Greven
Nationalität:	deutsch
Familienstand:	ledig

Schulbildung

1982 – 1986	Johannes Grundschule, Altenberge
1986 – 1995	Städtisches Gymnasium Borghorst Abschluss: Abitur

Zivildienst

07/1995 – 09/1996	Institut für Pflanzenschutz, Saatgutuntersuchung und Bienenkunde der Landwirtschaftskammer Westfalen-Lippe

Studium

WS 96/97 – WS 01/02	Studium an der Westfälischen Wilhelms-Universität (WWU) Münster, Fachbereich Biologie
12/2000 – 10/2001	Diplomarbeit am Institut für Biochemie und Biotechnologie der Pflanzen unter Leitung von Prof. Dr. B. M. Moerschbacher: „Isolierung und Charakterisierung einer Invertase und ihres Gens aus *Puccinia graminis* f. sp. *tritict*“
16.11.2001	Diplomvergabe
Seit 02/2002	Bearbeitung des Dissertationsthemas am Max-Planck-Institut für Züchtungsforschung in Köln, Abteilung Molekulare Phytopathologie unter Leitung von Prof. Dr. P. Schulze-Lefert im Labor von Dr. J. E. Parker

Köln, 17. Mai 2005 ______________________________